AD-A076 485 GENERAL DYNAMICS SAN DIEGO CA CONVAIR DIV F/G 22/2
COMPOSITE MATERIAL APPLICATION TO THE MK12A RV MIDBAY SUBSTRUCT--ETC(U)
SEP 79 W GARCIA , J HERTZ , J PRUNTY DAAG46-76-C-0073
UNCLASSIFIED CASD/ASC-76-001A AMMRC-TR-79-51 NL

1 OF 2
AD
A076485

AMMRC TR 79-51

COMPOSITE MATERIAL APPLICATION TO THE MK12A RV MIDBAY SUBSTRUCTURE

AUGUST 1979

W. GARCIA
J. HERTZ
J. PRUNTY
H. McCUTCHEN

General Dynamics Corporation
Convair Division
Post Office Box 80847
San Diego, California 92138

FINAL REPORT

Contract Number DAAG46-76-C-0073

Approved for public release; distribution unlimited

Prepared for

ARMY MATERIALS AND MECHANICS RESEARCH CENTER
Watertown, Massachusetts 02172

The findings in this report are not to be construed as an official Department of the Army position, unless so designated by other authorized documents.

Mention of any trade names or manufacturers in this report shall not be construed as advertising nor as an official indorsement or approval of such products or companies by the United States Government.

DISPOSITION INSTRUCTIONS

Destroy this report when it is no longer needed.
Do not return it to the originator.

Unclassified

SECURITY CLASSIFICATION OF THIS PAGE (When Data Entered)

REPORT DOCUMENTATION PAGE		READ INSTRUCTIONS BEFORE COMPLETING FORM
1. REPORT NUMBER AMMRC TR 79-51	2. GOVT ACCESSION NO.	3. RECIPIENT'S CATALOG NUMBER
4. TITLE (and Subtitle) Composite Material Application to the MK12A RV Midbay Substructure		5. TYPE OF REPORT & PERIOD COVERED Final Report - Supplement Oct 1976 - July 1978 6. PERFORMING ORG. REPORT NUMBER CASD-ASC-76-001A
7. AUTHOR(s) W. Garcia, J. Prunty J. Hertz, H. McCutchen		8. CONTRACT OR GRANT NUMBER(s) DAAG46-76-C-0073
9. PERFORMING ORGANIZATION NAME AND ADDRESS General Dynamics Convair Division P. O. Box 80847 San Diego, CA 92138		10. PROGRAM ELEMENT, PROJECT, TASK AREA & WORK UNIT NUMBERS D/A Project: 1W162113A661 AMCMS Code: 612113.11.07000 Agency Accession:
11. CONTROLLING OFFICE NAME AND ADDRESS Army Materials and Mechanics Research Center Watertown, Massachusetts 02172		12. REPORT DATE September 1979 13. NUMBER OF PAGES 152
14. MONITORING AGENCY NAME & ADDRESS (if different from Controlling Office)		15. SECURITY CLASS. (of this report) Unclassified 15a. DECLASSIFICATION/DOWNGRADING SCHEDULE N/A

16. DISTRIBUTION STATEMENT (of this Report)

This document has been approved for public release and sale; its distribution is unlimited.

17. DISTRIBUTION STATEMENT (of the abstract entered in Block 20, if different from Report)

18. SUPPLEMENTARY NOTES

19. KEY WORDS (Continue on reverse side if necessary and identify by block number)

Composite materials
Composite structures
Fiber composites
Graphite composites
Missile airframes

20. ABSTRACT (Continue on reverse side if necessary and identify by block number)

The work reported herein represents a feasibility study to reduce weight of the MK12A reentry vehicle midbay structure by replacing the aluminum structure with graphite composite materials. Following conceptual design of the MK12A midbay structure utilizing advanced composite materials, the effort was redirected to the Advanced Ballistic Reentry Vehicle (ABRV). Specimens and subcomponent elements representative of the ABRV configuration were provided for nuclear vulnerability and hardness testing at the Air Force Weapons Laboratory.

DD FORM 1 JAN 73 1473 EDITION OF 1 NOV 65 IS OBSOLETE

Unclassified

147 650

SECURITY CLASSIFICATION OF THIS PAGE (When Data Entered)

FOREWORD

This final report describes conceptual design studies for a MK 12A Midbay Substructure and specimen/subcomponent configurations utilizing advanced composite materials for nuclear vulnerability and hardening (NV&H) tests by the Air Force Weapons Laboratory. The work was sponsored by the Arm Materials and Mechanics Research Center, Watertown, Massachusetts, in conjunction with the Air Force Space and Missile Systems Organization (SAMSO), the Air Force Flight Dynamics Laboratory (AFFDL), and the Air Force Materials Laboratory (AFML). The AMMRC Technical Supervisor was Mr. Lewis R. Aronin.

Technical contributions in the study were provided by the Composite Structures, Thermodynamics and Material Technology, engineering functions of General Dynamics, Convair, under the management of R. C. Harbison, Manager of Structural Design.

TABLE OF CONTENTS

Section			Page
1	INTRODUCTION		1
2	DESIGN STUDIES		3
	2.1	INTRODUCTION	3
	2.2	DESIGN	3
	2.2.1	Conceptual Design	3
	2.2.1.1	Alternative Detail Configuration	3
	2.2.1.2	Initial Configuration	18
	2.2.1.3	Final Configuration	27
	2.2.1.4	Compliance with Design Requirements	33
	2.2.2	Fiber/Resin System Selection and Analysis	36
	2.2.2.1	Fungus	38
	2.2.2.2	Permeability	39
	2.2.3	Structural Analysis	40
	2.2.3.1	Materials Properties	40
	2.2.3.2	Applied Loads	41
	2.2.3.3	Mark 12A Laminate Definition	44
	2.2.3.4	Station 25.55 Ring	46
	2.2.3.5	Station 32.18 Ring	47
	2.2.3.6	Shell Stability Analysis	52
	2.2.4	Thermal Analysis	53
	2.2.4.1	Analysis Objectives	53
	2.2.4.2	Thermal Models	63
	2.2.4.3	Analysis Assumptions	55
	2.2.4.4	Materials Properties	55
	2.2.4.5	Analysis Results	61
	2.2.5	Mass Properties	62
3	SPECIMEN AND SUBCOMPONENT TESTING		65
	3.1	INTRODUCTION	65
	3.2	SPECIMEN CONFIGURATIONS	65
	3.3	SPECIMEN TESTING	66
	3.4	INTERLAMINAR TENSION AND SHORT BEAM SCREENING TEST	68
	3.5	SUBCOMPONENT TESTS	72
	3.5.1	Lap Shear Results	74
	3.5.2	Simulated Ring Test	74
	3.5.3	Gore Concentrations Test Results	74

TABLE OF CONTENTS (concluded)

Section			Page
	3.5.4	Longitudinal Ply Termination Stress Concentration	74
	3.5.5	Flexure at Doubler Tests	74
	3.6	NUCLEAR VULNERABILITY AND HARDNESS TEST SPECIMENS	83
	3.6.1	Material Systems	83
	3.6.2	Specimens and Subcomponent Design	83
	3.6.3	Ultrasonic Tests	93
4	MANUFACTURING PROCESSES		97
	4.1	INTRODUCTION	97
	4.2	SHELL STRUCTURE	97
	4.3	DOUBLER AND PADS	97
	4.4	COMPOSITE RING	97
	4.5	LAYUP AND CONSOLIDATION OF PREPREG	97
	4.6	CURING	98
	4.7	RV SUBSTRUCTURE ASSEMBLY	98
5	CONCLUSIONS AND RECOMMENDATIONS		101
	5.1	CONCLUSIONS	101
	5.2	RECOMMENDATIONS	102
6	REFERENCES		103
APPENDIX A		Station 32 and Station 42 Computer Program Input Listings	A-1
APPENDIX B		Manufacturing Plan	B-1
APPENDIX C		Quality Assurance Plan	C-1
APPENDIX D		Cure Cycles	D-1
APPENDIX E		Test Data	E-1
APPENDIX F		Test Plan	F-1

LIST OF ILLUSTRATIONS

Figure		Page
2.1-1	Original Baseline Design	4
2.2.1-1	Forward Ring, Concept #1	7
2.2.1-2	Forward Ring, Concept #2	8
2.2.1-3a	Forward Ring, Concept #3	9
2.2.1-3b	Forward Ring, Concept #3	10
2.2.1-4	Forward Ring, Concept #4	12
2.2.1-5	Sta. 32.18 Ring, Concept #1	13
2.2.1-6	Sta. 32.18 Ring, Concept #1 (Revised)	14
2.2.1-7	Sta. 32.18 Ring, Concept #2	16
2.2.1-8	Aft Ring, Concept #1	17
2.2.1-9	Aft Ring, Concept #2	19
2.2.1-10	Antenna Housing, Metallic	20
2.2.1-11	Antenna Housing, Nonmetallic	21
2.2.1-12	Recommended Preliminary Design Configuration	22
2.2.1-13	Forward Ring Recommended Configuration	23
2.2.1-14	Sta. 32.18 Ring, Recommended Configuration	24
2.2.1-15	Aft Ring Recommended Configuration	25
2.2.1-16	Antenna Housing Recommended Configuration	26
2.2.1-17	Conductivity Requirements	28
2.2.1-18	Final Configuration	30
2.2.1-19	Preliminary Design Drawing	31
2.2.3-1	Shear Strength Vs. Bond Thickness	42
2.2.3-2	Stress in Single Lap Shear Joint	43
2.2.3-3	Finite Element Model of Sta. 25.55 Ring	48
2.2.3-4	Stresses in Sta. 25.55 Joint URNB 15KFT	49
2.2.3-5	Finite Element Model of Sta. 32.18 Ring	50

LIST OF ILLUSTRATIONS (continued)

Figure		Page
2.2.3-6	Station 32.18 Bondline Stresses	51
2.2.4-1	Mark 12A Midbay Graphite/Epoxy Structure — Concept #1, Baseline	54
2.2.4-2	Nodalized Thermal Model, Station 32 Ring Area — Concept #1, Baseline	56
2.2.4-3	Station 42 Predicted Temperatures (0.040 adhesive) Concept #1, Baseline	57
2.2.4-4	Station 42 Predicted Temperatures (No Adhesive) Concept #1, Baseline	58
2.2.4-5	Station 32 Thrust Ring Predicted Temperatures (0.040 adhesive) Concept #1, Baseline	59
2.2.4-6	Station 32 Thrust Ring Predicted Temperatures (No Adhesive) Concept #1, Baseline	60
3.5-1	Shear Strength Vs Bond Thickness	77
3.5-2	Shear Strength Vs Bond Thickness (with glass scrim)	78
3.5-3	Simulated Ring Test	79
3.5-4	Gore Concentration Test Results	80
3.5-5	Longitudinal Ply Termination Stress Concentration Tests	81
3.5-6	Flexure at Doubler Termination Test	82
3.6-1A	NV&H Test Specimen Configurations	85
3.6-1B	NV&H Test Specimen Configurations	87
3.6-1C	NV&H Test Specimen Configurations	89
3.6-2	Typical Cylinder Details	91
3.6-3	Typical Cylinder Assembly with Heat Shield applied	92
3.6-4	Cylinder Assembly Ultrasonic SCAN (Worst Case)	95

LIST OF TABLES

Table		Page
2.2.2-1	Results of Material Trade	37
2.2.3-1	G/E Material Properties	40
2.2.3-2	EA934 Properties	41
2.2.3-3	Applied Loads on Laminate at STA 32.18 Aft (Ultimate)	44
2.2.3-4	Laminate Properties used in Laminate Analysis	45
2.2.5-1	Weight and Balance Comparison	63
2.2.5-2	Material Matrix, Composite Midbay Substructure	64
3.3-1	Test Program	67
3.3-2	Average Tension Properties - G/PI Composites	69
3.3-3	Average Compression Properties - G/PI Composites	70
3.3-4	Average Properties - G/PI Composites	71
3.4-1	Screening Tests on Graphite/Resin Composites	73
3.5-1	Lap Shear Test Results - Composite to Aluminum	75
3.6-1	Summary of NV&H Test Specimens	84

SUMMARY

The conceptual design study for a MK12A midbay substructure utilizing advanced composite materials was initiated with the collection of composite material data to select fiber/resin system candidates for application to the substructure. During the study phase three graphite fiber reinforcements in conjunction with two classes of resins, i.e.; epoxies and addition polyimides, were considered. Properties of graphite-epoxies used in the study were based on a survey of large quantities of data available from previous programs. Three systems were selected as candidates. Five graphite-polyimides were selected from the data bank and supplemented with data from a comprehensive screening program. This included longitudinal tension, longitudinal compression, in-plane shear, and interlaminar tension testing at room temperature, 350°F and 600°F. During the study, revised temperature plots were received from G.E. Thermoanalysis utilizing the revised G. E. Data predicts a maximum composite front face temperature of 260°F, well within the capability of current 350°F curing epoxy systems. Therefore graphite/epoxy rather than graphite/polyimide is recommended for the Mark12A midbay structure.

With structural requirements and structural analysis as the driver, several concepts were considered during the initial study phase. The recommended concept with an estimated weight savings of 3.5 pounds features a one-piece shell skin of laminated graphite/epoxy with judicious use of aluminum and Lexan in suitable areas. The design satisfies the specified criteria and complies with all of the interface requirements in the GE-RESD document, "MK12A Graphite Composite Structure Design Requirements to Support Feasibility Studies."

The conclusion derived from the study phase is that the recommended approach is entirely feasible. Component fabrication and assembly methods proposed for this purpose use well proven techniques already demonstrated on production flight hardware for many of General Dynamics/Convair programs.

Following completion of the midbay substructure study, various configurations of flat specimens, rings, and cylinder assemblies were designed and fabricated for nuclear vulnerability and hardness tests by the Air Force Weapons Laboratory. Application of the carbon/phenolic heatshield material was an Air Force responsibility.

Test specimens, described in detail in Section 3, were divided into groups; A, B, and C. Group A, flat specimens, were fabricated utilizing ply and orientation layup recommended in the MK12 midbay substructure study. By AMMRC/AFFDL direction, Group B, rings and cylinders, and Group C, primarily flats, were configured to design considerations in the ABRV advanced composite program.

SECTION 1

INTRODUCTION

In recent years advanced composite systems have taken an increasingly important role in space programs structural applications due to weight savings and unmatched mechanical and physical properties. Early programs in advanced composite materials were aimed at aircraft structural applications to save weight and improve performance. Space programs such as Space Shuttle, NIMBUS-G, HEAO-B, and others are realizing the same benefits. Recent work carried out by AMMRC on the development of composite forebodies for ballistic missile defense advanced terminal interceptors has demonstrated a technology for fabricating missile structures. Clearly the technological base has been layed for a MK 12A reentry vehicles composite substructure.

The overall program objective of this feasibility study is to reduce weight by replacing the existing MK 12A aluminum midbay substructure with graphite composite materials. In order to meet this primary goal, the following guidelines were used in conducting this program.

1. Develop structural and thermal data on graphite/epoxy and graphite/polyimide systems.
2. Develop preliminary design data applicable to the MK12A midbay substructure.
3. Demonstrate the feasibility of applying composite materials to the MK12A midbay structure.
4. Consider feasibility evaluation data with respect to Special Effects supplied to Convair.
5. Place emphasis on reducing the weight of the midbay structure.
6. Fabricate and test graphite/polyimide flat panel specimens.
7. Test subelement specimens representative of critical joints.
8. Develop and test graphite/polyimide flat panel specimens.
9. Develop graphite/epoxy and graphite/polyimide specimens and subcomponent elements for nuclear vulnerability and hardening tests.

To determine the feasibility and impact of advanced composite material technology on the MK 12A midbay substructure, this study used a baseline design of an aluminum substructure provided by General Electric in a requirements document titled, "MK 12A Graphite Composite Structure Design Requirements to Support Feasibility Studies,"

dated 7 July 1976, and redesigned the structure to take advantage of composite materials. Based on Convair's advanced composite experience and the available literature, several resin systems and graphite fibers were selected for initial characterization. Through studies and technical evaluation, optimum material system(s) were selected for consideration in the conceptual design phase. Several concepts were developed and evaluated; and a summary of the technical data is presented in the main body of this report.

The report has been organized into the following major subsections.

1. Introduction
2. Design Studies
3. Specimen and Subcomponent Testing
4. Manufacturing Processes
5. Conclusions
6. References
7. Appendix

SECTION 2

DESIGN STUDIES

2.1 INTRODUCTION

This section discusses a baseline configuration for the midbay substructure and alternative concepts considered during the study phase; electrical properties considerations; fiber/resin system candidates, selection and analysis; and structural, thermodynamics, and mass properties analyses.

The program effort was planned in two phases: (1) conceptual design phase, and (2) development of specimens and subcomponent elements for NV & H Test. This section reports on the conceptual design phase and emphasizes advanced composite materials application to MK12A midbay substructure. Figure 2.1-1 shows the original baseline composite structure design.

2.2 DESIGN

2.2.1 CONCEPTUAL DESIGN.

2.2.1.1 Alternative Detail Configurations. Since the overall configuration and structural concept was established, consideration of alternative detail configurations was limited to the areas listed below.

1. The Shell Skin
2. Ring, Forward
3. Ring, Sta. 32.18
4. Ring, Aft
5. Payload Restraining Pads
6. Antenna Support

Since stringent design criteria were established and the objective was to satisfy these criteria and meet a challenging weight reduction goal, a cost versus weight trade study was not appropriate, particularly in view of the relatively small cost differential between the prime candidates.

The following sections describe the alternatives which were studied in each of these areas.

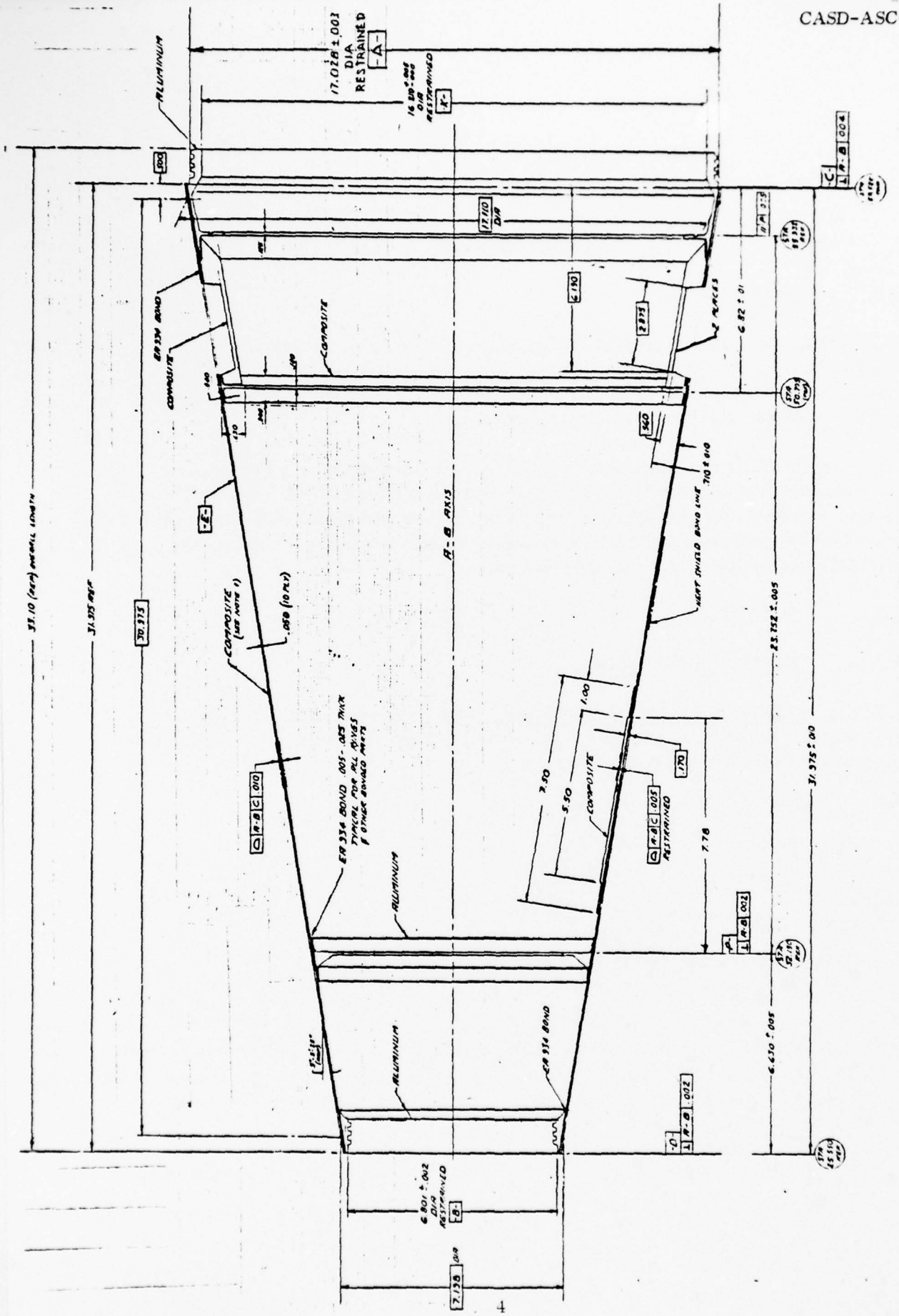

Figure 2.1-1. Original Baseline Design

The Shell Skin

The dominant criteria for the design of the shell skin are:

1. Limitation of strain to the heat shield strain capability.
2. Stability under the airload crushing condition.

The original baseline skin was tentatively defined as a uniform 10-ply, 0.05-inch thick graphite/epoxy laminate to approximate the performance of aluminum with respect to the above criteria.

During the subsequent study, the peak skin temperature was specified by General Electric to be 260F at impact in the ULRR case. In view of this, consideration of polyimide composites for the MK12A was abandoned. Three graphite/epoxy candidates were considered.

1. T300/5208
2. HM-S/934
3. GY-70/934

For the initial design, HM-S/934 was selected on the basis of yielding minimum weight for compatibility with the heat shield strain limitation. Consideration was given to changing to the higher modulus GY-70/934 for the aft end of the shell where stability is the more critical criterion. This possibility was not adopted at this stage and was subsequently eliminated as a result of the impact tests described in Reference 3.

Other changes to the baseline skin were made as a result of preliminary analysis. The most significant was the extension of the first step of the payload restraining pads forward to the Sta. 32.18 ring to reduce the skin strain in the area of peak load intensity immediately aft of the ring.

The initial design of the skin is described in more detail in Section 2.2.1.2, and the final design is described in Section 2.2.1.3.

Ring, Forward

The primary functions of this ring are to provide for attachment of the forward section of the MK12A and to distribute into the shell of the midbay the associated overall bending moment, shear and axial load.

For the purpose of this study, to avoid problems with the interfaces with the forward and aft sections of the MK12A, aluminum rings are retained at the forward and aft ends of the midbay. The possible alternatives which were given some consideration in the early phases of the study were the low density metals, beryllium and magnesium.

A laminated composite would not be a suitable material for application to these detail configurations in which severe notch effects on interlaminar stresses would be unavoidable. Consideration of beryllium and magnesium for the Sta. 32.18 payload suppport ring has reinforced the case against the use of these materials for the threaded rings. In the case of magnesium, the integrity of the anticorrosion treatment when the threaded rings are engaged, would be impossible to assure. Notch sensitive beryllium is unsuited to the threaded rings due to the necessarily small filet radii applicable to these parts. Furthermore, finite element modeling of a ring has revealed that the high modulus of beryllium induces unacceptably high stress concentration in the bond between the ring and the shell skin.

The following concepts have been investigated for the forward ring. All feature the attachment of the ring to the skin by EA934 adhesive bonding. The nominal design load intensity for the bond is 2583 pounds/inch ultimate at essentially room temperature in the 15,245 foot URNB condition. There is no problem with elevated temperature in the bond since the worst condition, at impact in the ULRR case, causes a bond line temperature of only 150F.

Concept #1 — This, the original baseline concept for the forward ring, is shown in Figure 2.2.1-1. It is the most simple approach to bonding the aluminum ring to the composite skin. This was rejected since precision machining of the forward edge is required after the installation of the ring to meet the close tolerance correlation between this edge and the thread location.

Concept #2 — This concept, shown in Figure 2.2.1-2, was a variant of Concept #1 which evolved into Concept #4 which is discussed later.

Concept #3 — Figure 2.2.1-3a and 2.2.1-3b depict this approach. The basic idea in this case was to minimize weight by replacing as much aluminum as possible with the lower density composite. This approach has been shown to be invalid since as Figure 2.2.1-3a clearly shows, adequate bond width for the 2583 pounds/inch nominal load intensity is not attainable within the original geometrical constraints of the ring. Figure 2.2.1-3b illustrates a first pass at increasing the bond width by increasing the overall width of the ring cross section. The weight advantage gained by replacing aluminum with lower density composite is negated by the increase in overall size. The weight of this version, as shown in the figure, is 0.73 pounds.

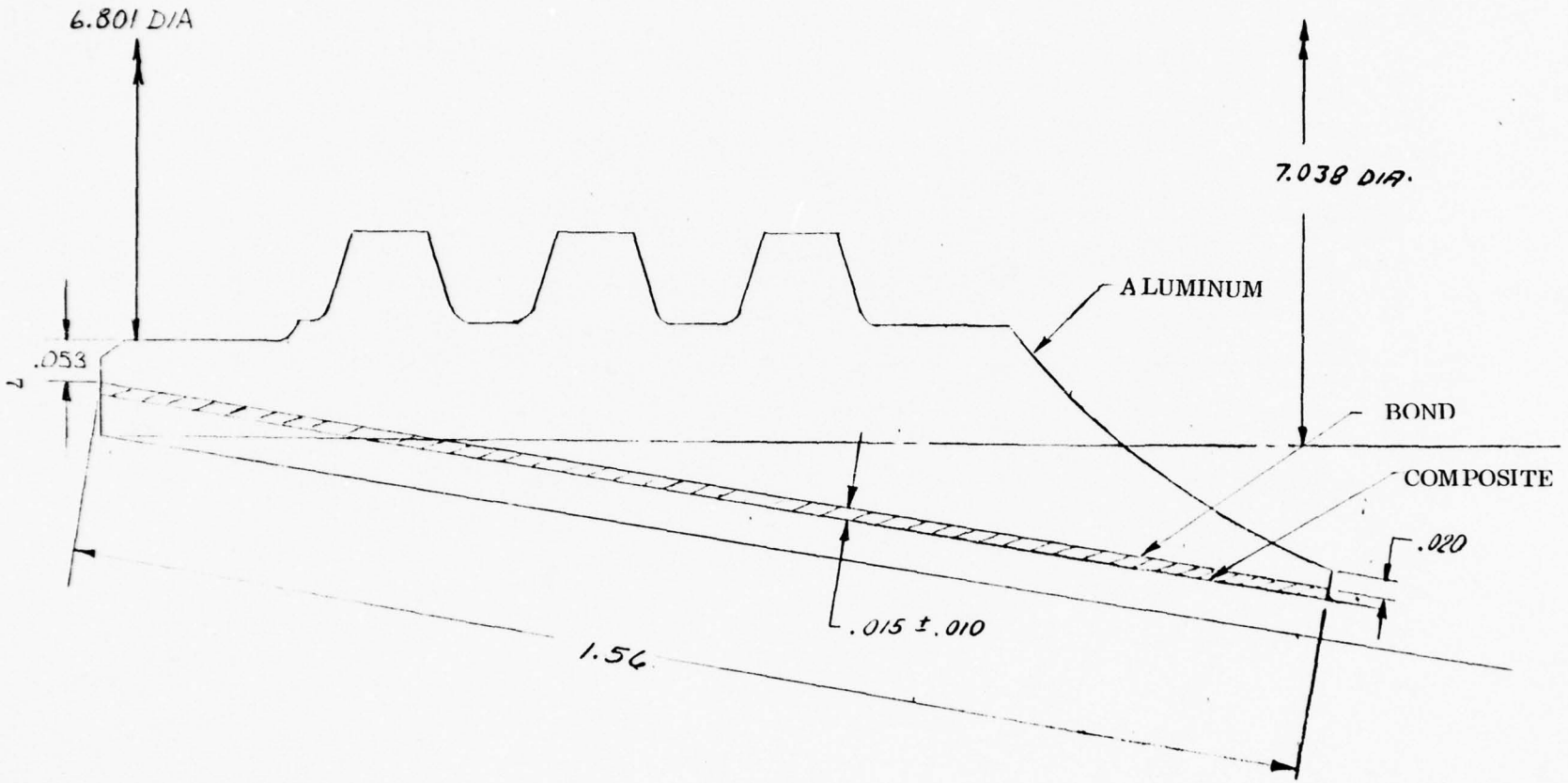

Figure 2.2.1-1. Forward Ring, Concept #1

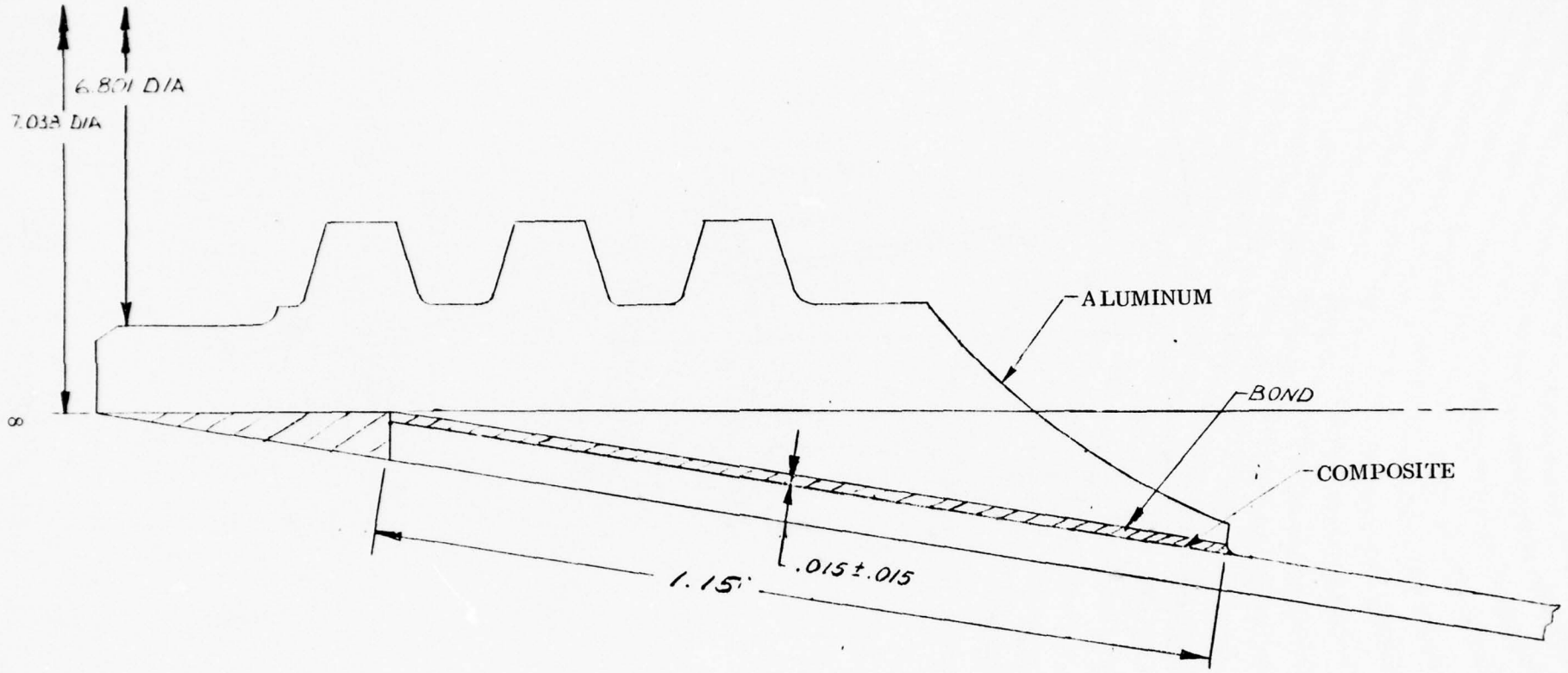

Figure 2.2.1-2. Forward Ring, Concept #2

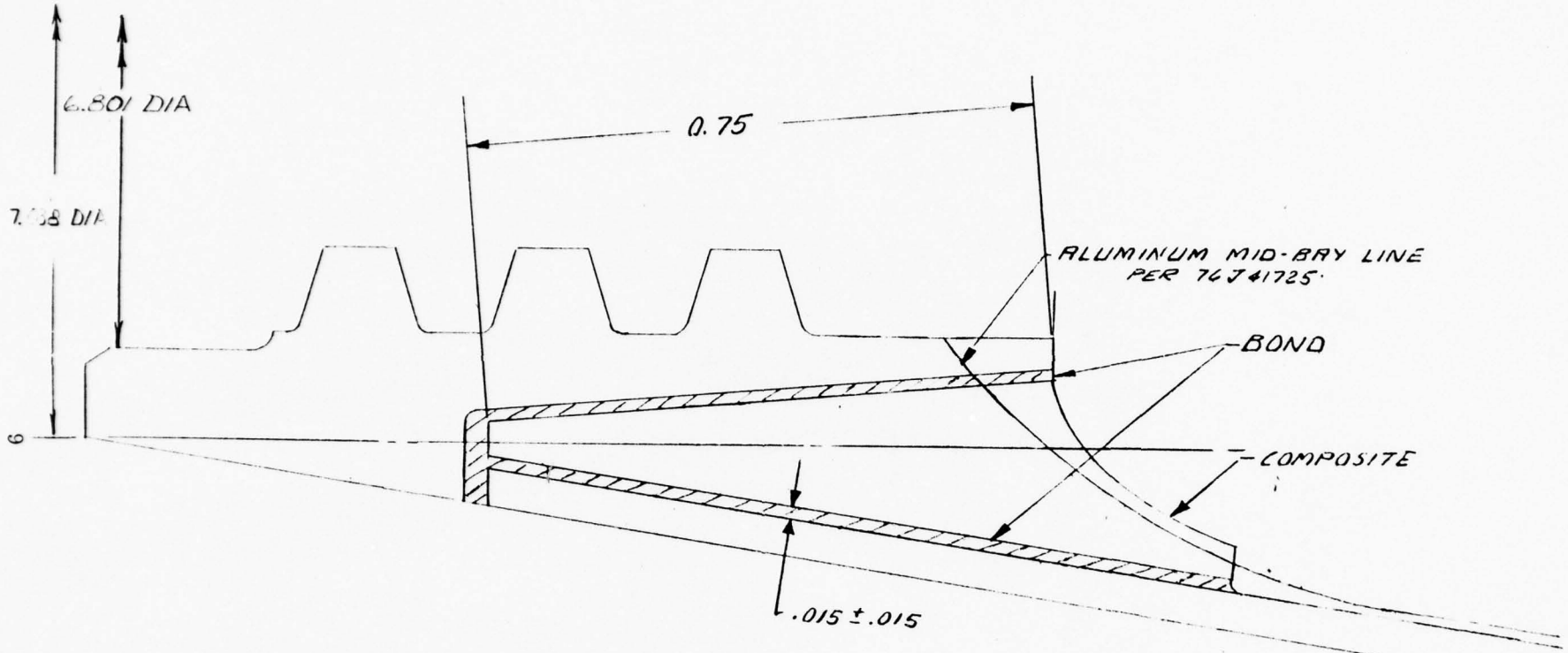

Figure 2.2.1-3a. Forward Ring, Concept #3

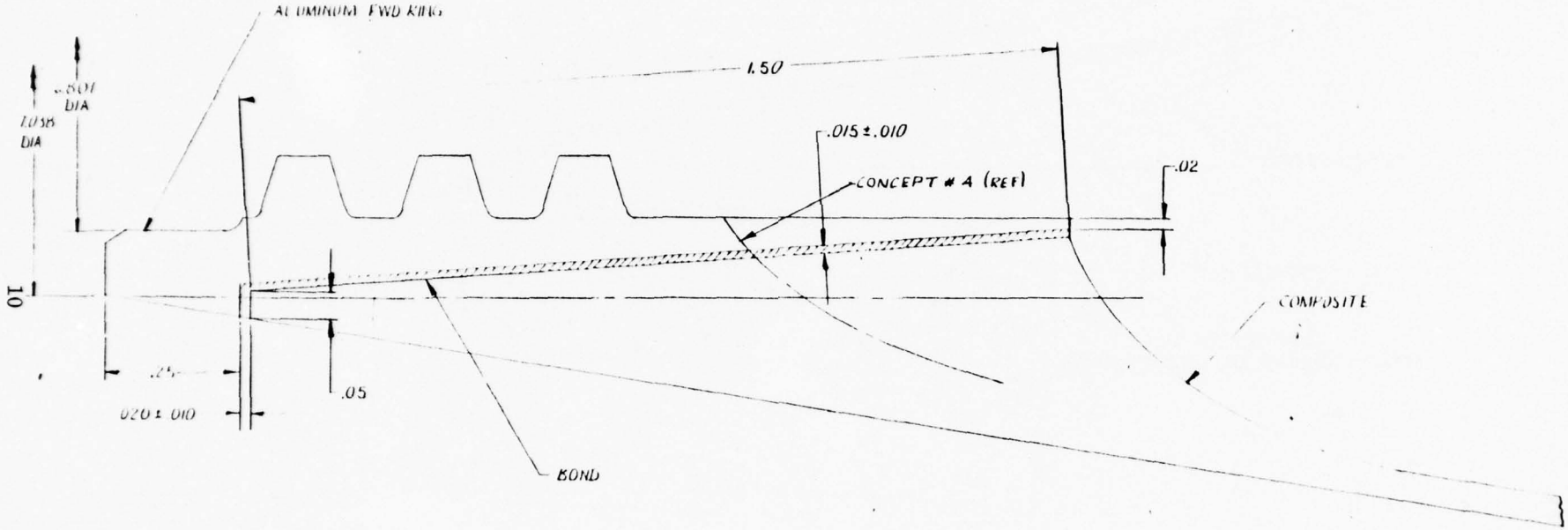

Figure 2.2.1-3b. Forward Ring, Concept #3

Concept #4 -- This concept, which is shown in Figure 2.2.1-4, was adopted for the initial configuration of the MK12A Midbay Composite Structure. It was selected on the basis of:

- Minimized weight
- Machining of the critical forward edge is done on the ring detail.

Several iterations of finite element modeling, as described in Section 2.2.3, were made on this ring configuration to determine the width and taper ratios required to obtain acceptable peak stresses in the bondline. The weight of this concept is .64 pounds, .09 pounds below that of Concept #3.

Ring, Sta. 32.18

The primary function of this ring is to provide the forward support for the payload. In the peak loading condition in the URNB case, a forward inertia load of 30,625 pounds ultimate is applied uniformly distributed around the ring. This is applied in conjunction with a 53750 in-lb moment and 6250 pounds shear. The ultimate load intensity induced by the axial load and moment in the ring/skin bondline is 1930 lbs/in. This condition is essentially at room temperature.

Two concepts have been considered for this ring.

- Concept #1 — A metallic concept
- Concept #2 — A composite concept

Concept #1 — The original baseline concept was a direct adaptation of the aluminum ring used in the all-aluminum midbay structure. This is depicted in Figure 2.2.1-5. Finite element modeling demonstrated the inadequacy of the small flanges with respect to the distribution of the bond shear stress. Several iterations of modeling evolved the geometry shown in Figure 2.2.1-6 for an aluminum ring. The cross section of the ring was increased in width from the baseline 1.50 inches to 2.34 inches with finely tapered flanges to reduce the peak stress in the bond line to an acceptable value. The resultant geometry, which is adopted for the initial structure configuration is shown in Figure 2.2.1-6.

The finite element model of this ring geometry was exercised on the basis of using beryllium. It was found that the modulus of this material, 42M psi versus 10M psi for aluminum, transferred a much higher proportion of the load to the edges of flanges with resulting unacceptable peak stresses in the bond line. Correction of this condition would require a greatly increased width of finely tapered flanges, resulting in a geometry which is considered unsuitable for this brittle material.

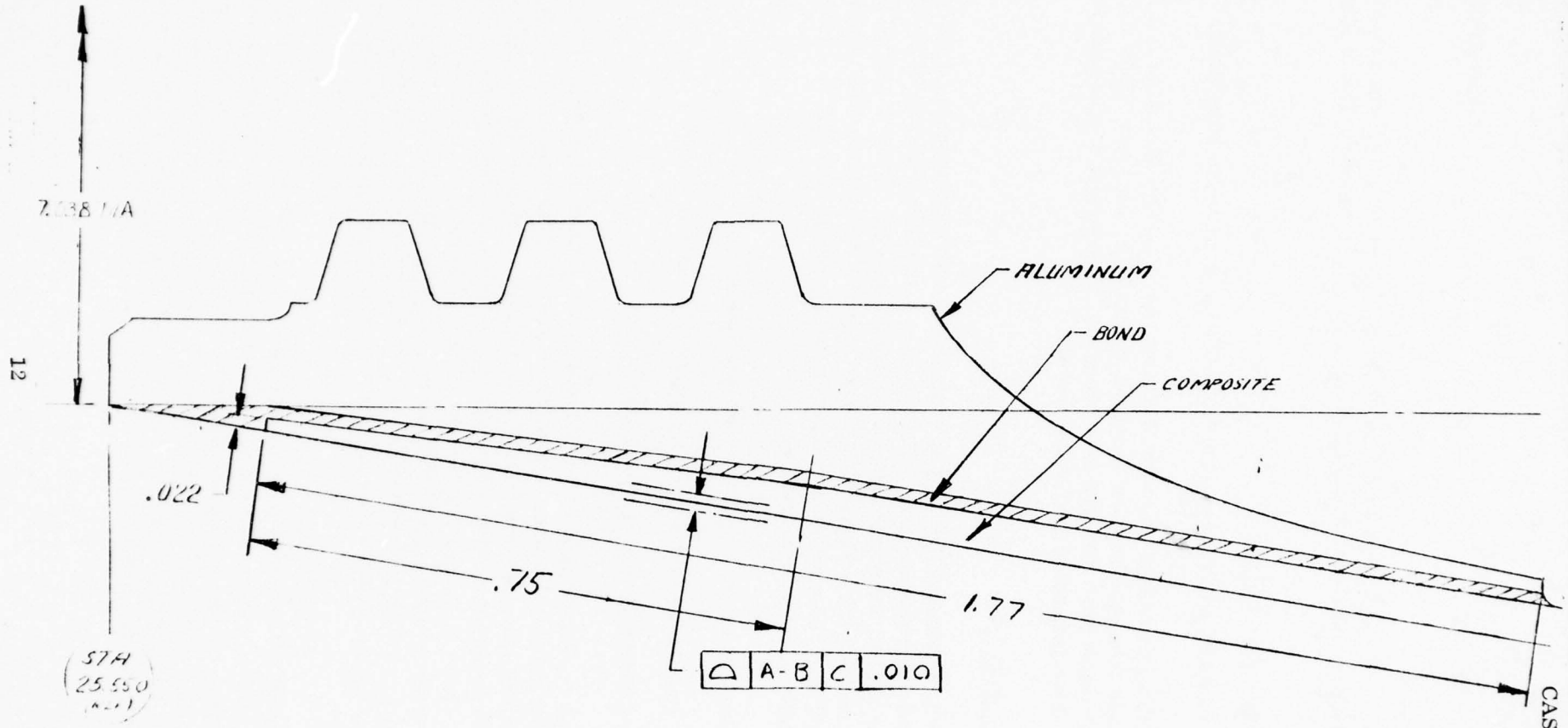

Figure 2.2.1-4. Forward Ring, Concept #4

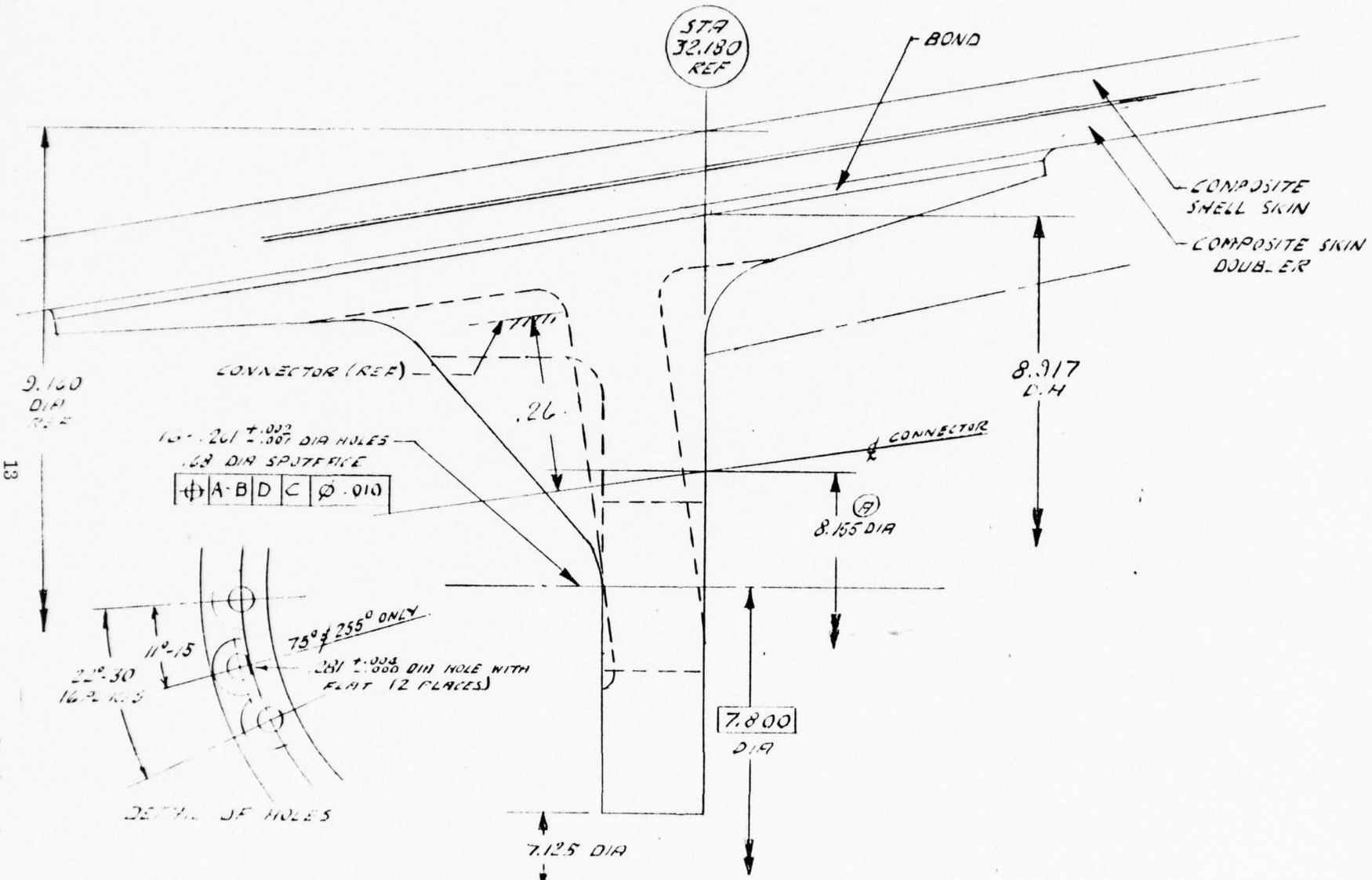

Figure 2.2.1-5. Sta. 32.18 Ring, Concept #1

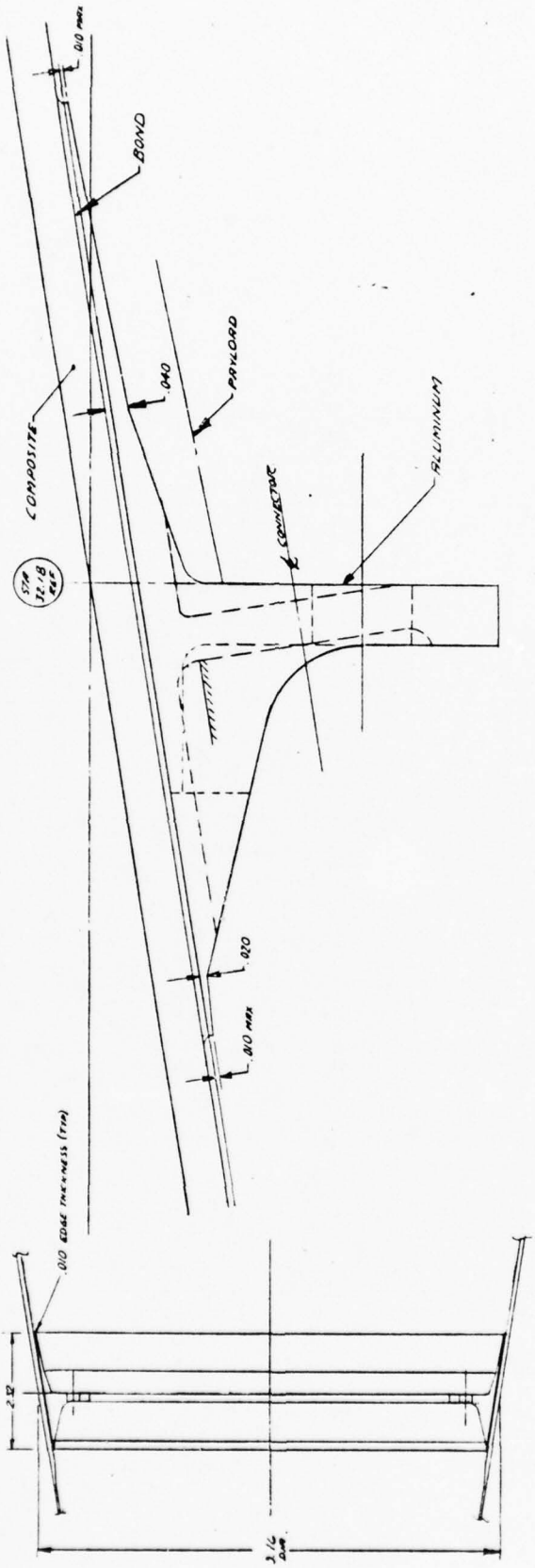

Figure 2.2.1-6. Sta. 32.18 Ring, Concept #1 (Revised)

Magnesium was also considered for this application. In addition to having a low density, 0.064 pci versus 0.101 pci for aluminum, the low modulus, 6.5M psi versus 10M psi for aluminum, in contrast to that for beryllium, would be advantageous in the design of the ring/skin bond. Magnesium was not adopted due to reliability considerations. This was in view of doubts with respect to maintenance of the corrosion protection system after manipulating box wrenches-in tightly confined counterbores during installation of the payload.

Concept #2 - The graphite/epoxy concept for this ring is shown in Figure 2.2.1-7. From the geometrical standpoint, this adopts the same approach as the metallic version described above. Some consideration was given to an arrangement of triangular fillets between the payload attachment bolts to back up the basic upstanding flange. This was not pursued since the complex layup of such an arrangement in the small, 0.9-inch high, cross section of the ring is considered to be impractical as a production process. Cocuring of a ring with the shell skin was also rejected due to the difficulty of attaining the ±.001-inch tolerance on the face of the ring.

Close grid finite element modeling is required to demonstrate the stress levels induced in the graphite/epoxy ring shown in Figure 2.2.1-7. Approximate analysis, however, shows that the current cross section, using the same geometry as the aluminum concept, would not be satisfactory. Analysis of the aluminum ring shows that 1200 lbs/in of the 1930 lbs/in bond load is transmitted via the aft flange of the ring. In the graphite/epoxy version, the thickness of the aft flange at the root is constrained by the proximity of the payload envelope to .088 inches thick. This would result in a tension stress of 13,600 psi at the root of the flange with correspondingly high interlaminar stress around the radius. Attempts to resolve this problem were not successful. Elimination of the aft flange would induce unacceptably high peak shear stress in the bond at the abrupt start of the ring cross section. Inducing sufficient load to go forward to relieve the aft flange, if practicable, would require at least a substantial increase in the forward section of the ring. This would offset the weight advantage obtained from the low density of graphite/epoxy. For this reason the aluminum concept was retained.

Ring, Aft

Concept #1 - Figure 2.2.1-8 shows the selected concept for this ring. Aluminum is retained as the material for the threaded ring for the reasons discussed in Section 2.2.1.1 (Ring Forward). The aft payload support ring at Station 55.932 is also aluminum and is integral with the threaded ring. As in the case of the forward threaded ring, the design incorporates the critical annular butt face in the detail of the ring, thereby eliminating close tolerance machining on the assembly of the midbay. The bondline load intensity of 510 lbs/in indicates that this is by far the least critical of the three loaded rings with respect to attachment to the skin. This concept was selected on the basis of minimum weight.

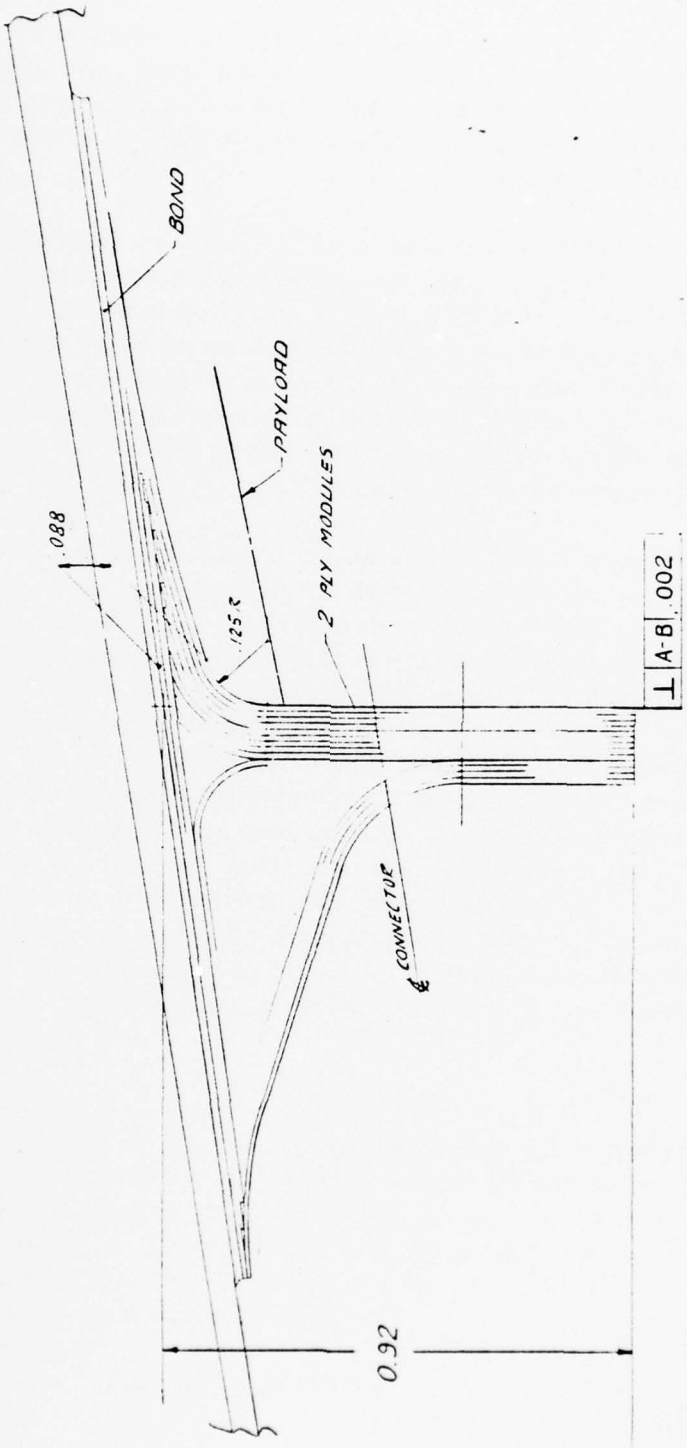

Figure 2.2.1-7. Sta. 32.18 Ring, Concept #2

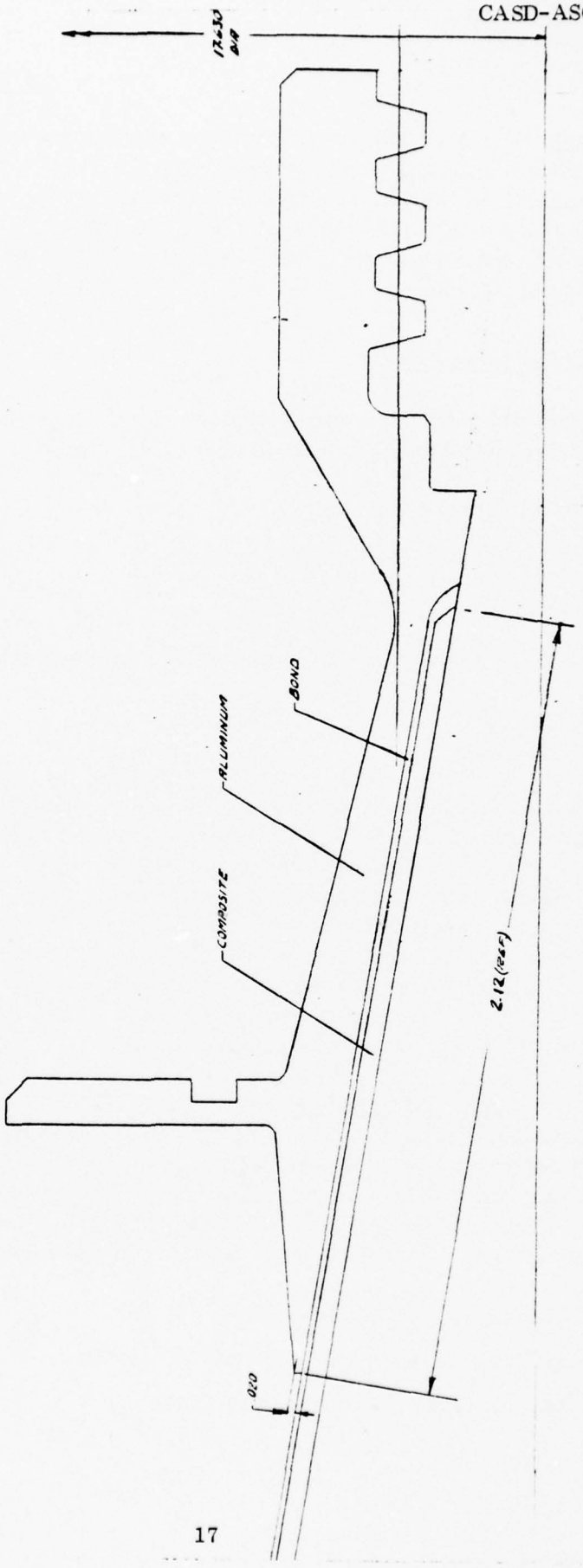

Figure 2.2.1-8. Aft Ring, Concept #1

Concept #2 – Figure 2.2.1-9 illustrates a concept in which an aluminum threaded ring is spliced into a graphite/epoxy payload ring. A problem is created with this concept by the annular sealing slot required in the upstanding leg of the payload ring. Thickening of the ring to alleviate this notch effect, in conjunction with the weight associated with splicing the payload ring, more than offsets the effect of transitioning to the lower density graphite/epoxy.

Payload Restraining Pad

Three material candidates were considered for the eight discrete pads which restrain the payload immediately aft of the Station 32.18 ring.

1. Graphite/epoxy laminate
2. Graphite/epoxy faced Kevlar
3. Lexan

The latter was selected for the initial study configuration on the basis of least weight.

Antenna Housings

Aluminum and magnesium were considered as candidates for a metallic version of this housing. Figure 2.2.1-10 illustrates a configuration suited to metallics. Figure 2.2.1-11 shows a configuration for a nonmetallic molded version. Molded graphite/epoxy, molded Kevlar/epoxy and Lexan were considered. Magnesium was the most attractive with respect to weight, with an estimated value of 0.43 pounds. This material, however is not recommended in view of the uncertainties with respect to maintaining the integrity of the corrosion protection system during subsequent machining and installation operations. Lexan, which yields an estimated weight of 0.49 pounds for these components was adopted for the initial study configuration.

2.2.1.2 Initial Configuration. Figure 2.2.1-12 depicts the configuration initially recommended, and Figures 2.2.1-13 through -16 show the associated details. The concept features a one piece shell skin of laminated graphite/epoxy with secondary bonded pads and doublers in the payload area. The stiffening ring at Station 50.505 utilizes ultra-high modulus GY-70/934 graphite/epoxy, the most efficient material for this application. A summary of the material application is as follows:

1. Shell Skin - Graphite/epoxy HM-S/934
2. Ring Sta. 50.505 - Graphite/epoxy GY-70/934
3. Ring, Forward - Aluminum 7050 T7351

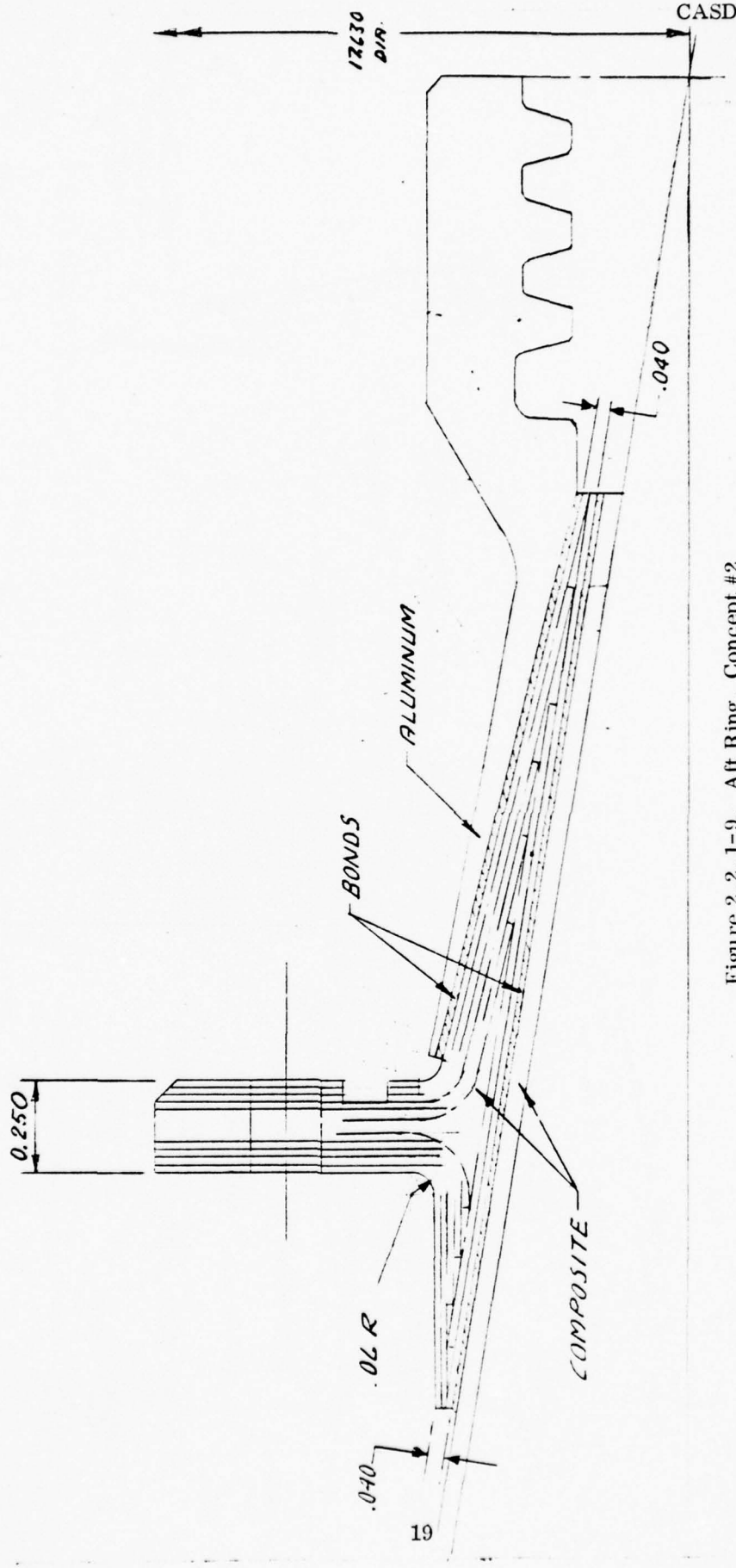

Figure 2.2.1-9. Aft Ring, Concept #2

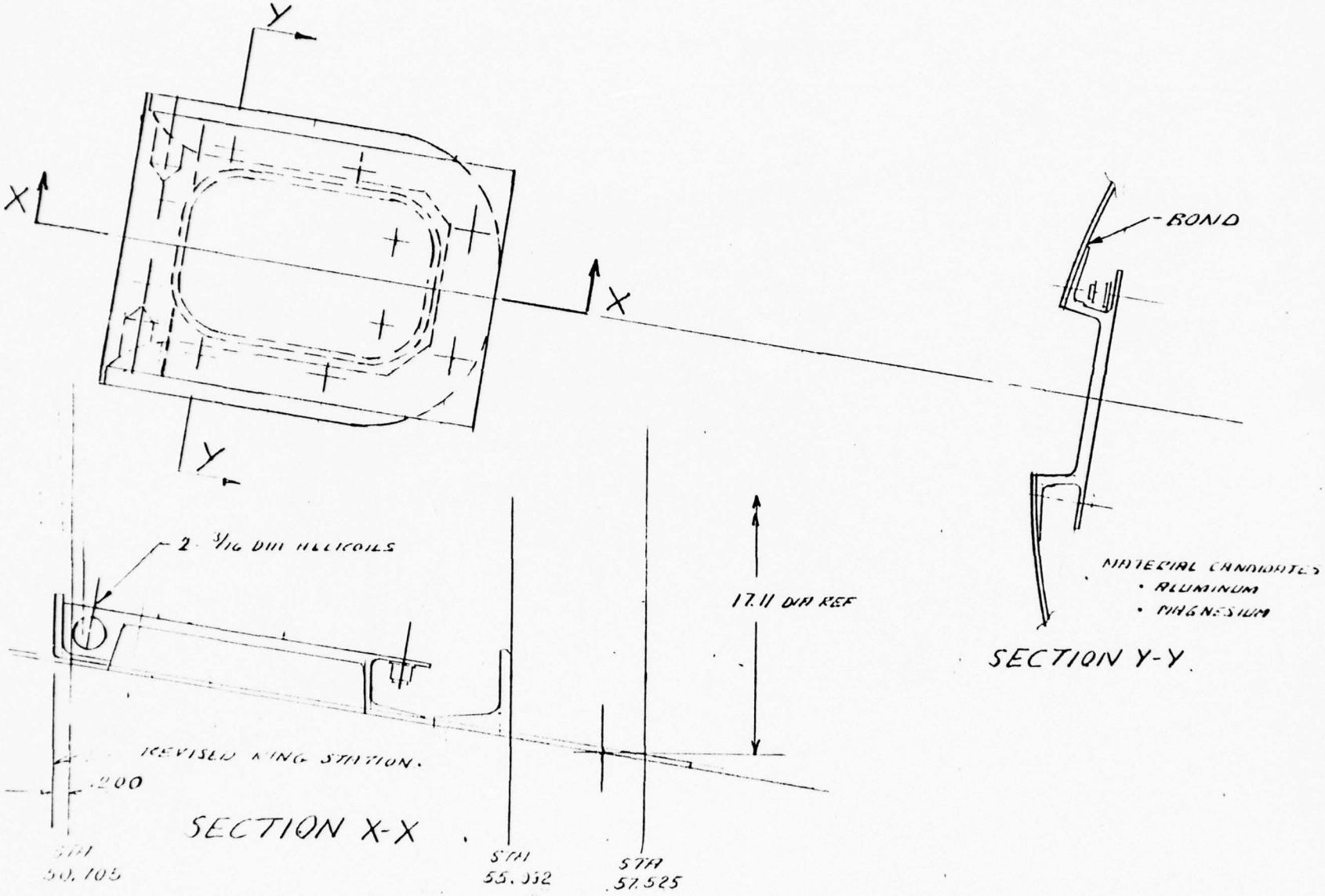

Figure 2.2.1-10. Antenna Housing, Metallic

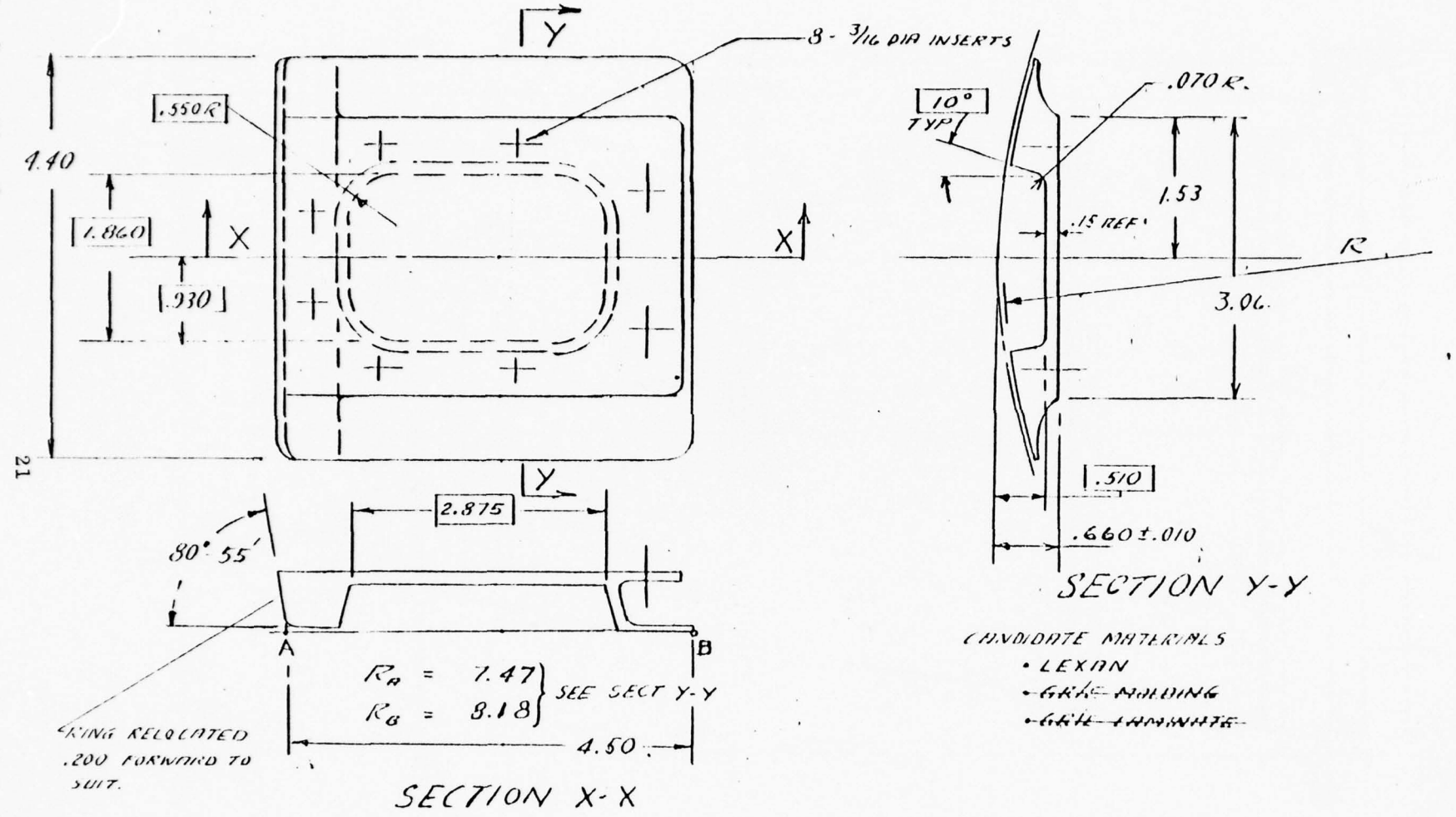

Figure 2.2.1-11. Antenna Housing, Nonmetallic

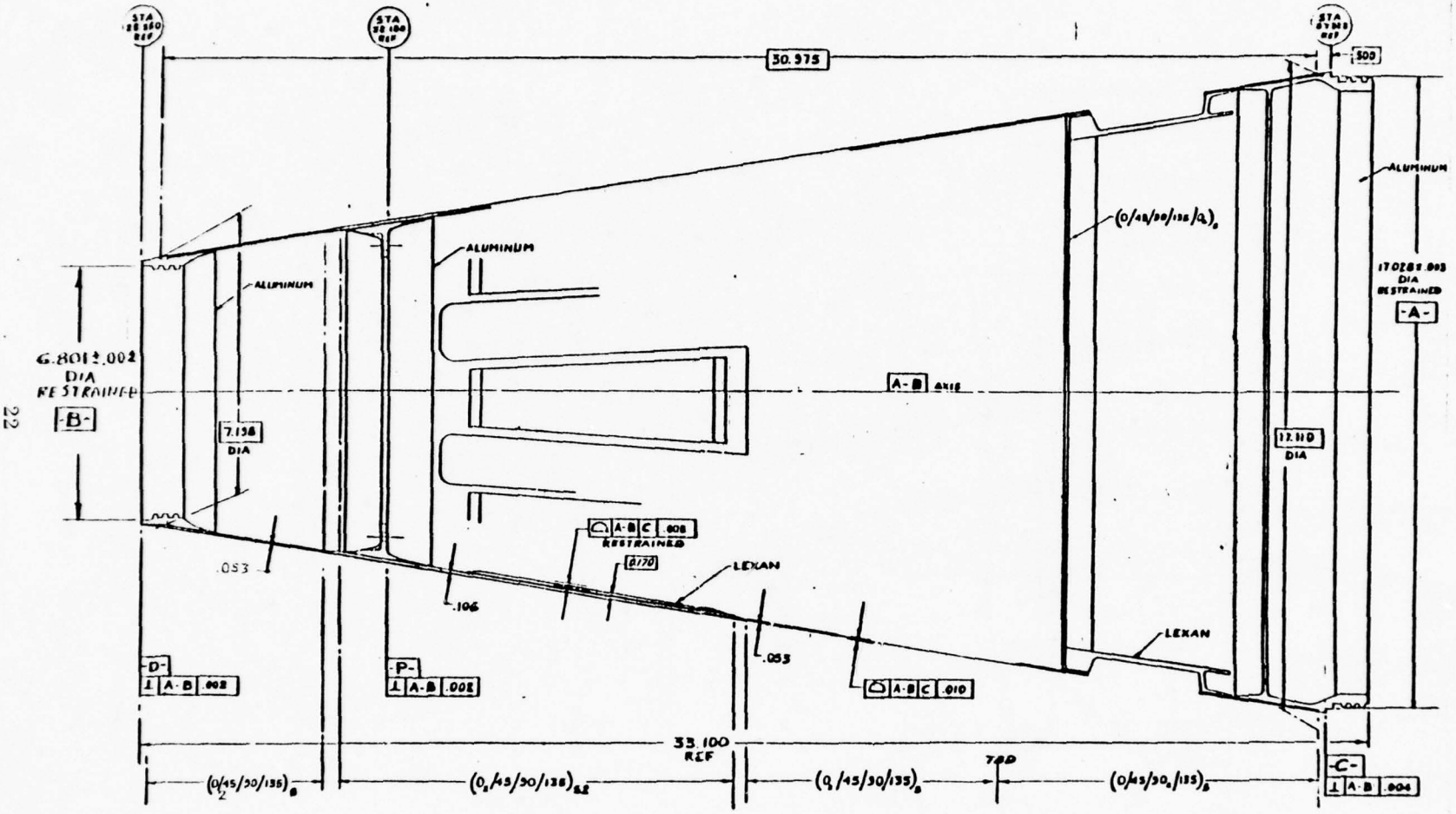

Figure 2.2.1-12. Recommended Preliminary Design Configuration

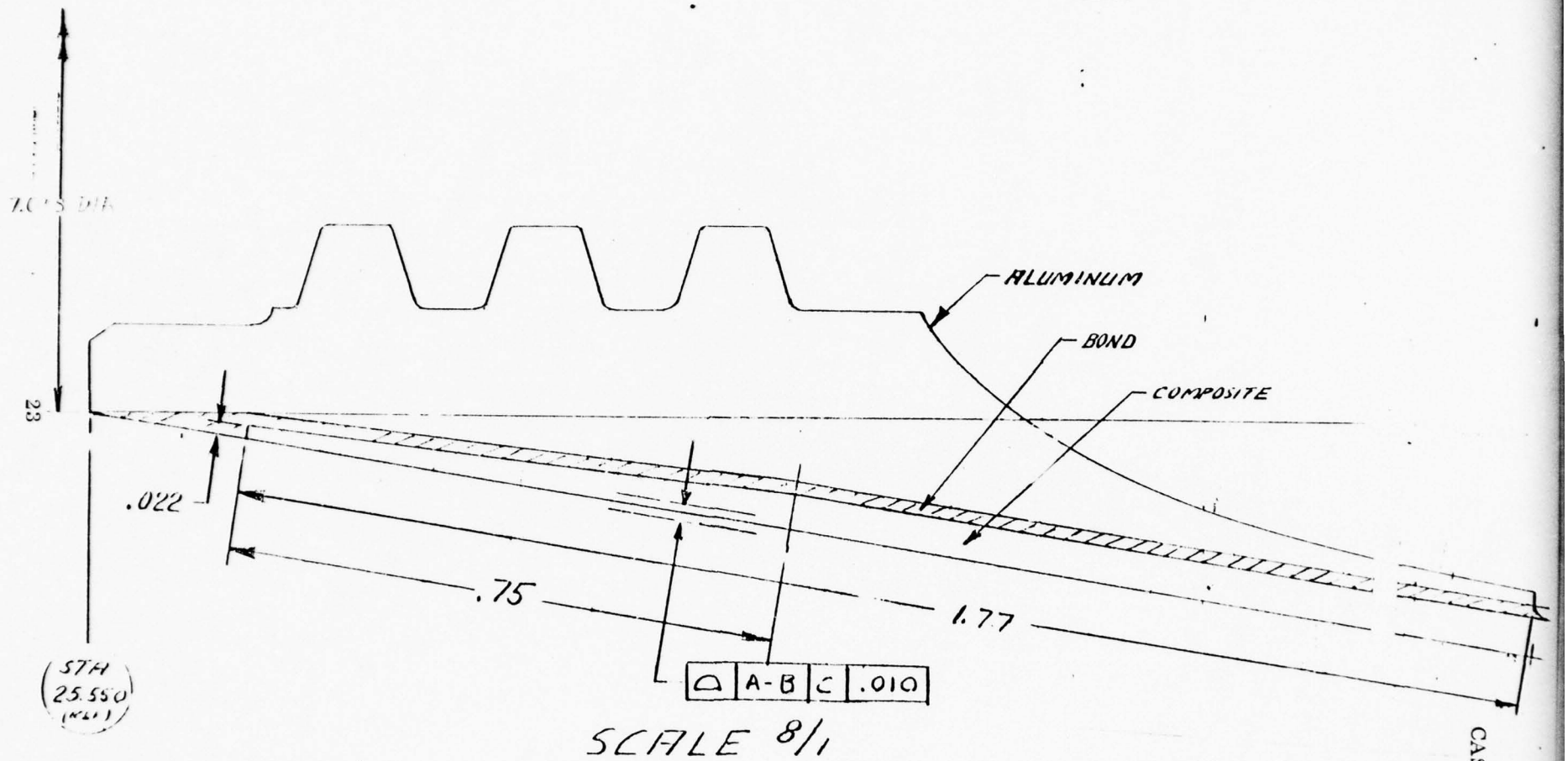

Figure 2.2.1-13. Forward Ring Recommended Configuration

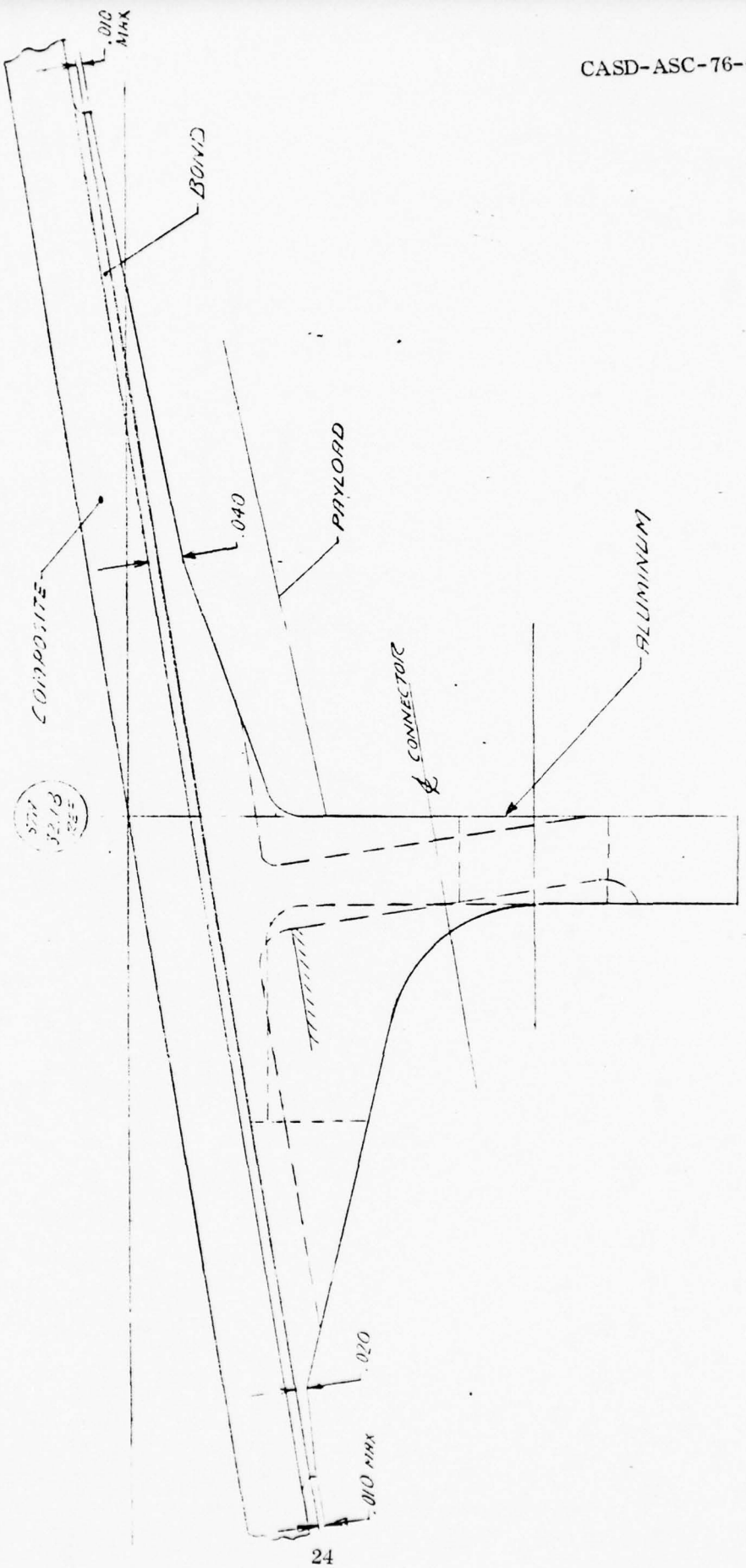

Figure 2.2.1-14. Sta. 32.18 Ring, Recommended Configuration

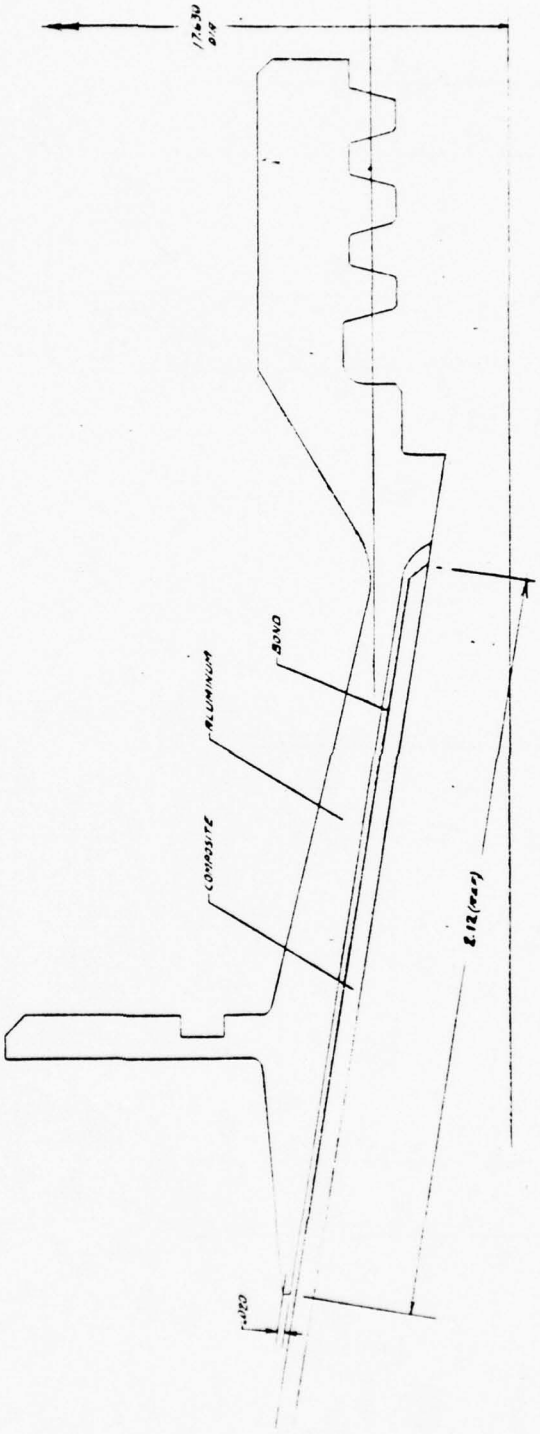

Figure 2.2.1-15. Aft Ring Recommended Configuration

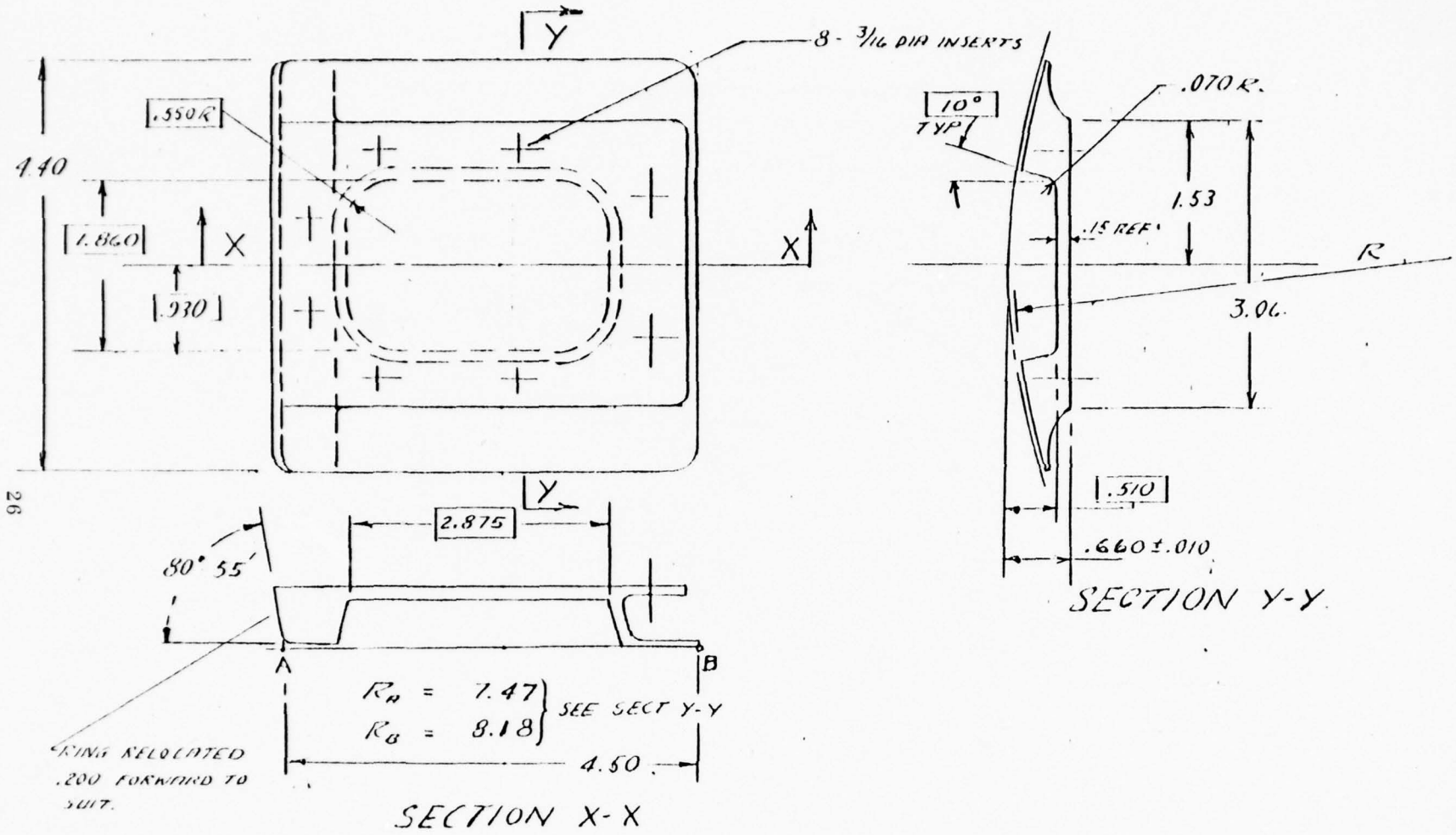

Figure 2.2.1-16. Antenna Housing Recommended Configuration

4. Ring, Sta. 32.18 - Aluminum 7050 T7351
5. Ring, Aft - Aluminum 7050 T7351
6. Payload Restraint Pads - Lexan
7. Antenna Housing - Lexan

With respect to joining methods, the design features in all bonded structure using EA934 room temperature cure adhesive for the graphite-epoxy/aluminum and graphite-epoxy/graphite bonds and for the EA9314 Lexan/graphite epoxy cases.

The design satisfied the specified criteria and complied with all of the interface requirements defined in the GE-RESPD document, "MK12A Graphite Composite Structure Design Requirements to Support Feasibility Studies."

The conclusion derived from the initial study phase is that the recommended approach is entirely feasible. Component fabrication and assembly methods proposed for this purpose use well proven techniques already demonstrated on production flight hardware.

2.2.1.3 Final Configuration Changes From the Initial Configuration. At the first design review, the results of plate slap tests on the candidate materials were presented. These data indicated the superiority of T-300/5208 compared to the HM-S/934 material which was used in the initial design. In consequence of this, a directive was given to redesign the mid-bay structure using T-300/5208.

Furthermore, data was presented which indicated the need to improve the electrical conductivity of the shell to comply with the requirements for resistance to Electro-Magnetic Pulses (EMP) and lightening strikes.

The task for the final preliminary design was therefore decreed to be the definition of a shell laminate using T-300/5208 graphite-epoxy and incorporating some device to increase the conductivity to the required level. The structural analysis for shell strength and stability associated with this effort is reported in Section 2.2.3.

The first consideration in the design and analytical task was to determine the method of compliance with the electrical conductivity requirements. Figure 2.2.1-17 shows the data presented at the first design review. This shows the attenuation requirements for the EMP and lightening strike cases, with plots of the performance of various materials and gages in terms of the numerical reciprocal of resistivity per meter. A survey of available data, most notably recent test data from General Dynamics, Fort Worth Division, indicated that for graphite-epoxy in cross-plied laminates of the MK12A shell thickness, the value of ν/M would be of the order of the lower curve, actually $2.04 \times 10^{4} \nu/M$. This value is obviously not adequate for compliance with the

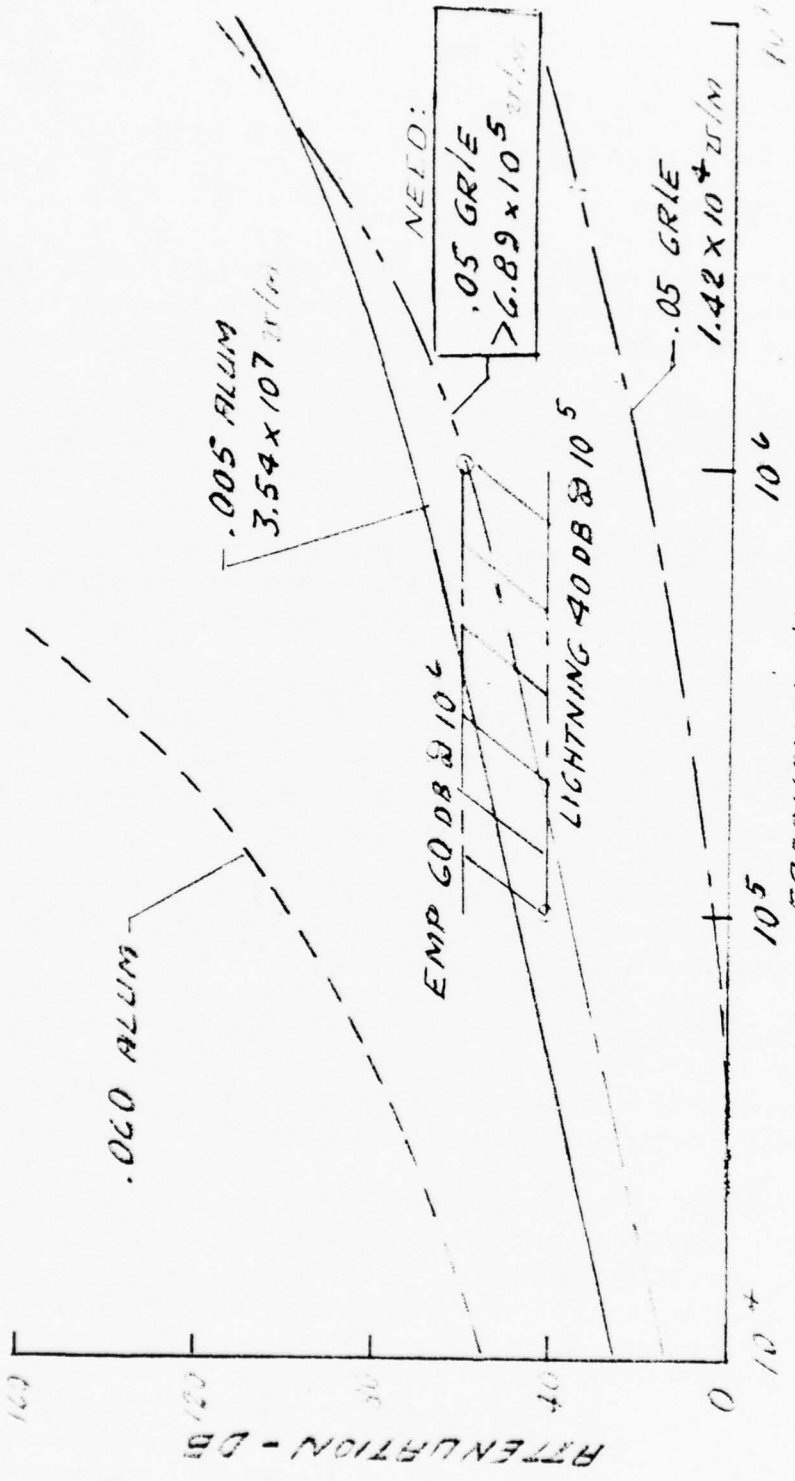

Figure 2.2.1-17. Conductivity Requirements

specified EMP and lightening strike requirements. For the purpose of preliminary design, a somewhat conservative approach was adopted without attempting the refined analysis which would be necessary for final optimization. This approach consisted of accepting the effectiveness of a 0.005 inch thick aluminum foil shown in Figure 2.2.1-17. A layer of aluminum of this thickness was incorporated into the laminate design to extend over the full outer surface of the mid-bay structural shell. The adopted method of attachment involves secondary bonding with a 0.005 inch thick fiberglass scrim interposed between the aluminum and the graphite-epoxy to prevent galvanic corrosion. This proposed method of attachment is probably also conservative, since subsequent tests in other programs have demonstrated the feasibility of co-curing the aluminum to the laminate, thereby saving 0.54 lbs. of bond. Galvanic corrosion of the co-cured aluminum can probably be prevented by the inhibition of moisture or the expulsion of moisture as required in any case prior to the sealing of the payload cavity. This use of aluminum foil for conformance with the specified EMP conductivity requirement is favorable with respect to compatibility with the requirement for impermeability of the structural shell.

Description of the Final Configuration

Figure 2.2.1-18 presents a schematic of the final configuration and Figure 2.2.1-19 depicts the detailed preliminary design drawing.

The structural shell uses a basic T-300/5208 laminate, 0.055 inches thick, and of $(0_2/\pm45/90)_S$, 10 ply configuration. (The ply orientation notation does not reflect the actual stacking sequence, which is $(0/+45/90/-45/0)_S$. This also applies to the notations given below). On the outside of the shell is a 0.005 inch thick layer of aluminum, secondary bonded to the laminate with a 0.005 inch thick separator scrim, giving a total bond line thickness of 0.013 inches. At the payload support pads, and extending forward under the Sta. 32.180 thrust ring, is an internal scalloped reinforcement 0.055 inches thick of $(0_7/90_3)$ orientation. Each payload pad is built up further by a $(0_5/90_2)$ (90_N) series of plies to permit final machining to the overall 0.170 inch basic thickness, and to the internal total profile tolerance of ±.0025 inches.

The internal rings and pads are secondary bonded to the shell with EA934 room temperature curing adhesive. The adequacy of this type of ring to shell bond has been demonstrated by the tests reported in Section 2.2.3.

A definition of the final preliminary design configuration is:

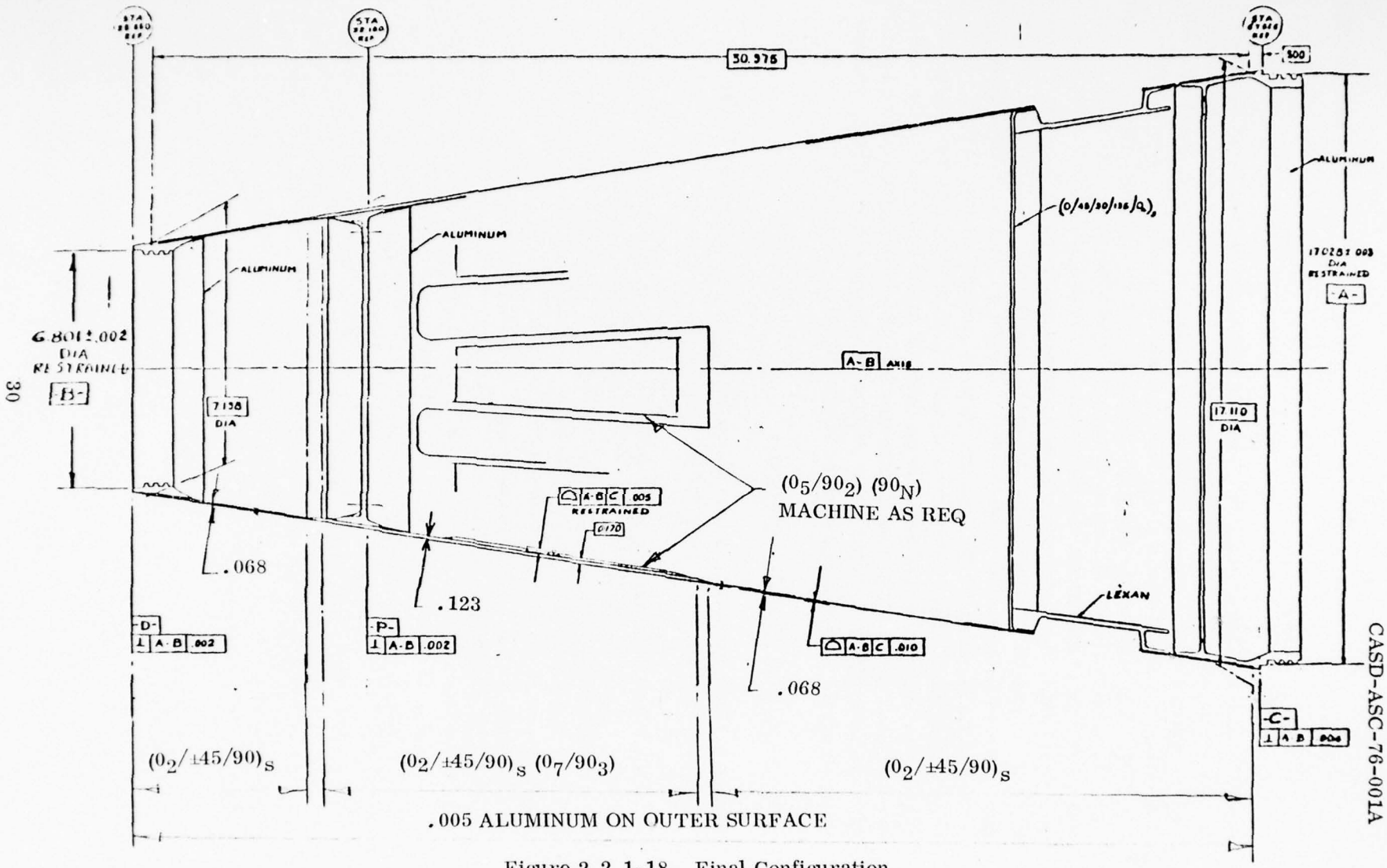

CASD-ASC-76-001A

Figure 2.2.1-18. Final Configuration

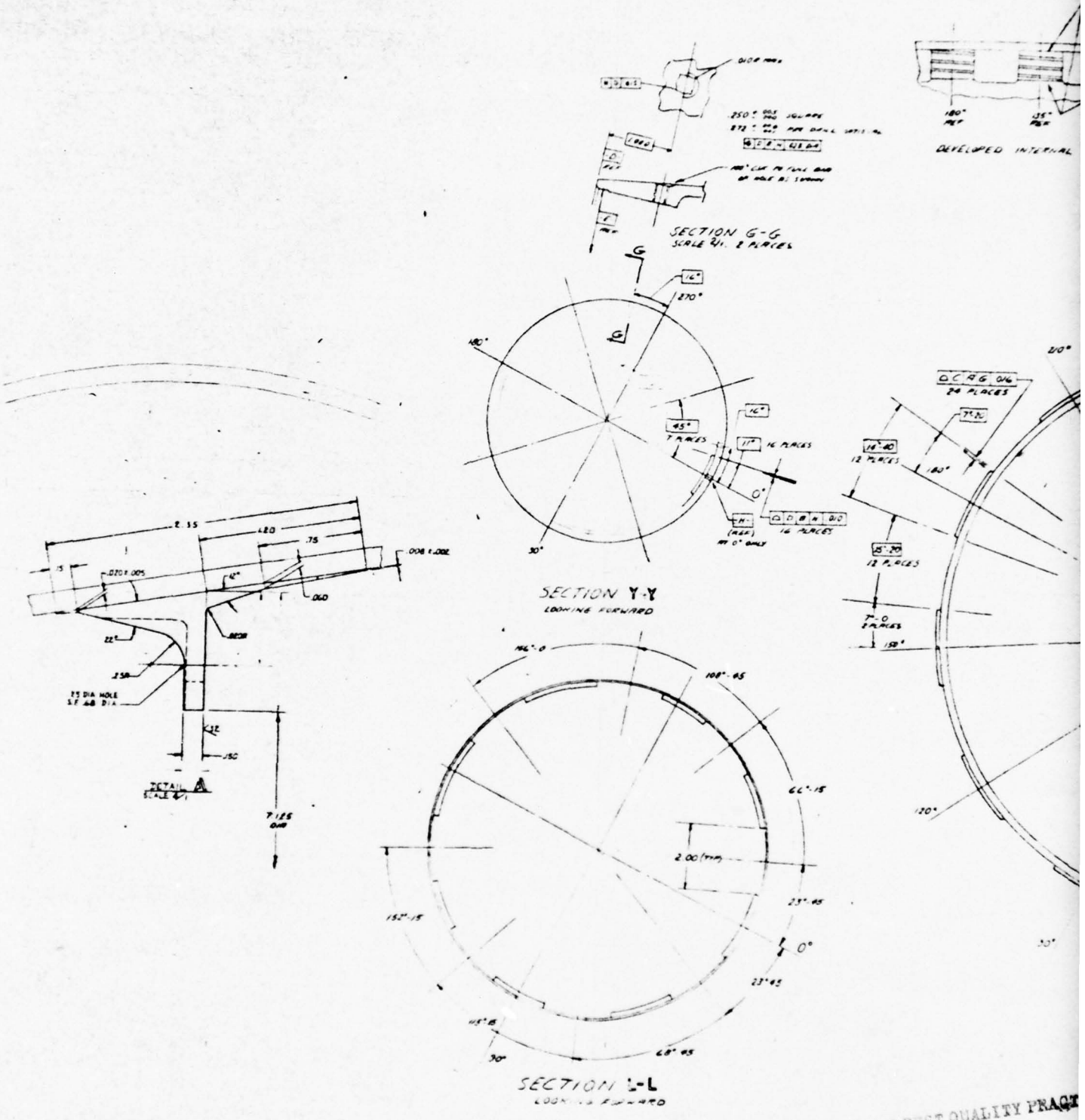

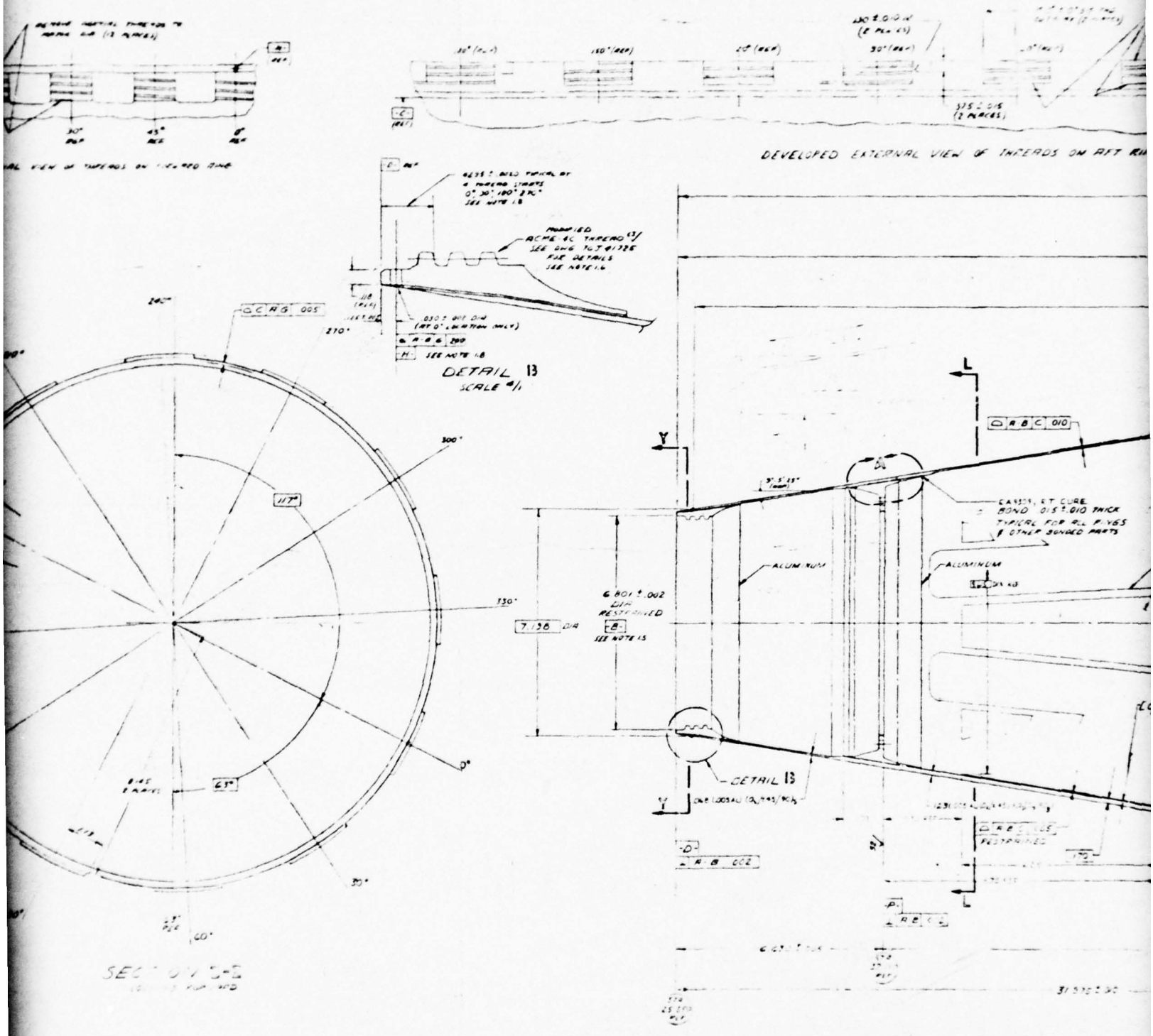

Figure 2.2.1-19. Preliminary Design Drawing

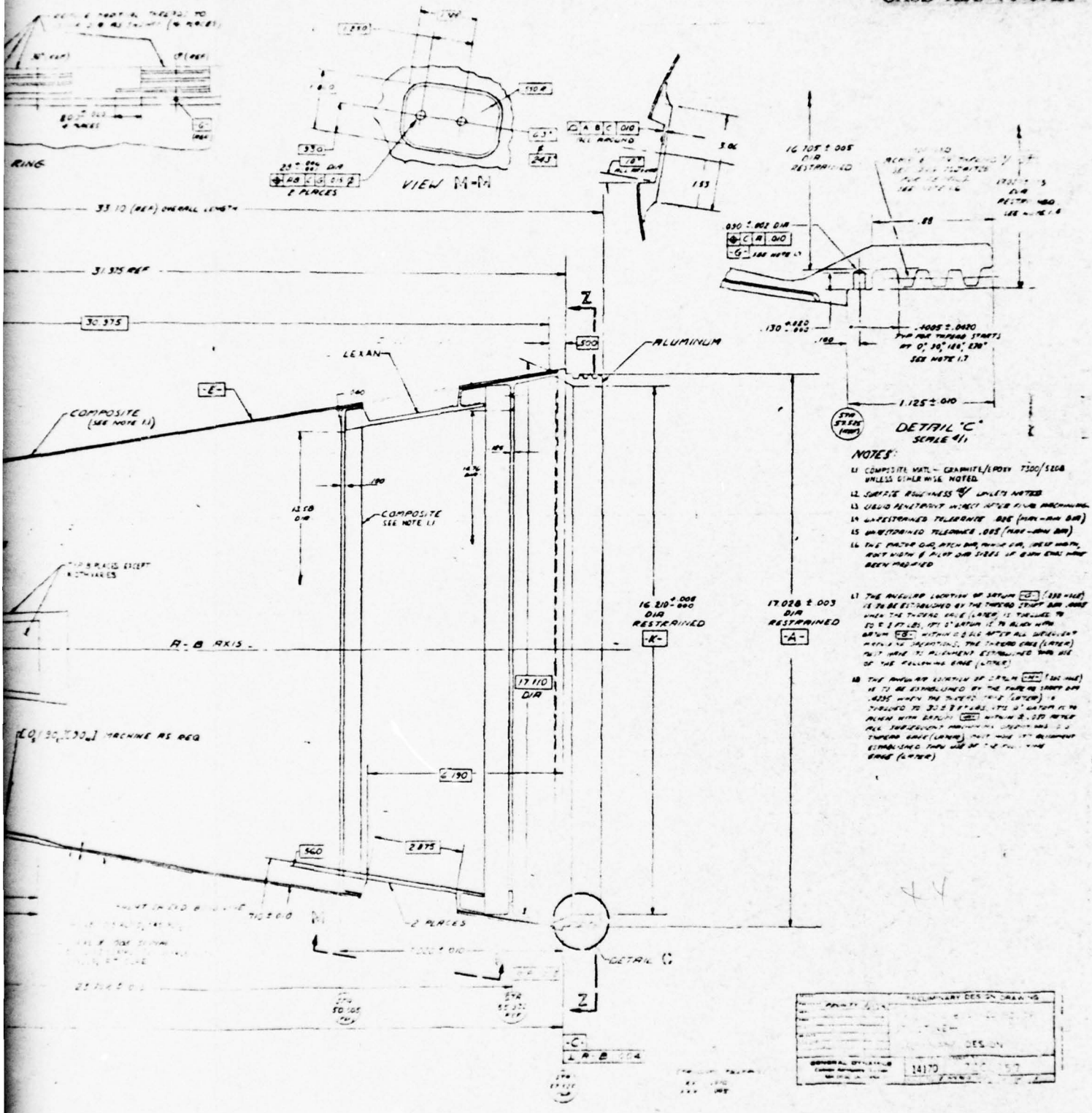

NOTES:

1.1 COMPOSITE MATL – GRAPHITE/EPOXY T300/5208 UNLESS OTHERWISE NOTED.

1.2 SURFACE ROUGHNESS 63 UNLESS NOTED

1.3 USE DYE PENETRANT INSPECT AFTER FINAL MACHINING

1.4 UNRESTRAINED TELERANCE .005 (MAX – MIN DIM)

1.5 UNRESTRAINED TELERANCE .005 (MAX – MIN DIM)

1.6 THE PITCH DIA, PITCH DIA, MINOR DIA, THREAD WIDTH, AND WIDTH @ FLAT ON TIPS OF BOTH ENDS HAVE BEEN MODIFIED

1.7 THE ANGULAR LOCATION OF DATUM -C- (.030 HOLE) IS TO BE ESTABLISHED BY THE THREAD START DIM (.1005 WHEN THE THREAD END (LATER) IS TOOLED TO 30.375 ± .125. IT'S LOCATION IS TO BE 0.0° ± 90° FROM DATUM -B- WITHIN 0.010 AFTER ALL INTERFACE MATING INSPECTIONS. THE THREAD END (LATER) MAY HAVE TO BE MACHINED ESTABLISHING THAT USE OF THE FOLLOWING EQUATION:

1.8 THE ANGULAR LOCATION OF DATUM -C- (.030 HOLE) IS TO BE ESTABLISHED BY THE THREAD START DIM (.1005 WHEN THE THREAD END (LATER) IS TOOLED TO 30.375 ± .125. IT'S LOCATION IS TO BE ALIGN WITH DATUM -B- WITHIN 0.010 AFTER ALL INTERFACE MATING INSPECTIONS. THE THREAD END (LATER) MAY HAVE TO BE MACHINED ESTABLISHING THAT USE OF THE FOLLOWING EQUATION:

COMPONENT	MATERIAL	FIGURE
Shell	Alum./T-300/5208	2.2.1-18
Ring, Sta. 50.505	T-300/5208	2.2.1-19
Ring, Forward	Alum. 7075-T7351	2.2.1-13
Ring, Sta. 32.18	Alum. 7075-T7351	2.2.1-14
Ring, Aft	Alum. 7075-T7351	2.2.1-15
Pads, Payload Restraint	T-300/5208	2.2.1-18
Housing, Antenna	Lexan	2.2.1-16

This configuration is the basis for the estimated weight given in Section 2.2.5. Some reduction from the weight quoted at this stage should be feasible with a more refined analysis to optimize the laminate along the length of the shell, and by the adoption of a less conservative approach to compliance with the specified EMP requirement.

2.2.1.4 Compliance with Design Requirements. During the feasibility phase of the study the requirements specified in the GE-RESD design requirements document have been satisfied except as noted below. The explanations use the paragraph numbers of the design requirements document for ready reference.

3.1 Item Definition

Further work is required with respect to the transmission of electrical signals to the AFS.

3.1.1.2 Electromechanical

Each of the electrical connectors at Sta. 32.18 for the RF cabling is installed at an angle of 99° - 5', that is, parallel to the shell skin instead of normal to the station plane as in the aluminum midbay. This is required to clear the forward flange of the nonintegral ring.

3.1.1.4 Mid-Section Structure and Thermal Shield

Per G.E. directive, a heat shield bond line thickness of 0.04 inches has been used in thermal calculations.

3.1.1.6 Mid-Section to Radar Antenna Assembly

Sufficient definition of the antenna housing for the purpose of a feasibility study has been included in this report.

3.2.1.1.5 Electrical

Further work is required in this area. The following outlines a possible approach.

This paragraph requires that the conducting parts of the structure be "electrically" bonded together. This particular structure, however, cannot use the methods illustrated in MIL-B-5087. It is proposed that the intent of MIL-B-5087 can be accomplished by the use of aluminum foil cemented with conductive cement to both the aluminum structure and the graphite composite material. For the three aluminum ring structures a single ribbon of foil about 2 cm wide cemented with conductive cement at one edge around the entire periphery would suffice. For the aluminum antenna supports, however, the foil ribbon should cover all edges due to possible RF fields. MIL-B-5087 requires a bonding demonstration test which could be made on the completed structure.

3.2.1.1.5.1 Impedance

This paragraph requires a DC impedance of less than 0.0025 ohms between parts and an AC impedance which can increase to 1 ohm at 50 MHz.

Due to the nonhomogenous nature of the electrical conductivity of the composite material, bonding into the surface normal to the graphite filaments requires a much larger contact area than would be required for bonding to metals. The foil ribbon technique extended around the periphery includes sufficient contact area to achieve a bonding resistance well below the 0.0025 ohm limit. Since the ribbon goes directly from the aluminum structure to the composite material there is essentially no series inductance to increase the impedance with frequency. In fact there is capacitive coupling spanning the nonconductive structural cement which would tend to decrease the impedance with frequency.

3.2.1.1.5.2 Perimeter Bonds

The technique described in the above paragraphs meets this requirement.

3.3.1 Shock

This requirement has not been addressed in the feasibility study.

3.3.2 Vibration

This requirement has not been addressed in the feasibility study.

3.3.5 Acceleration

Phase 7

(1) Limit

Phase 7 loads only have been used for the feasibility study.

(2) Ultimate

Phase 7 loads only have been used for the feasibility study.

Phase 7

(b1) Peak Longitudinal and Laterial

The limit load distributions of Figures 14 through 28 have been applied except that values from GE letter #3735-1169 have been used where these are more critical.

(b2) Spin

The effects of spin have not been addressed in the feasibility study.

3.3.7 Sand

This requirement has not been addressed in the feasibility study.

3.3.9 Acoustic Noise

This requirement has not been addressed in the feasibility study.

3.3.10 ERDA Radiation

Requirements not supplied.

3.3.13 Special Effects

This is primarily a GE responsibility. Convair does not have the data for the evaluation of these effects.

3.4 Transportability

This requirement has not been addressed in the feasibility study.

3.5.1 Materials, Processes, and Parts

Graphite/epoxy and Lexan material properties are not specified in MIL-HDBK-5B. Preliminary properties have been derived from available data.

2.2.2 FIBER/RESIN SYSTEM SELECTION AND ANALYSIS. The conceptual design study considered three graphite fiber reinforcements in conjunction with two classes of resins, i.e., epoxies and addition polyimides. The fibers selected for the study were the most prevalently used fiber in each of the three main categories of fibers, i.e., Thornel 300 (high strength), HM-S (high modulus), and GY-70 (ultra-high modulus). Thornel 300 is a product of Toray (distributed in the USA by Union Carbide Corp.) and has a modulus of 30 to 34 msi. HM-S is produced in the USA by Hercules, Inc., and has a modulus of 50 to 55 msi. GY-70 is produced in the USA by Celanese Corp. and has a modulus of 70 to 80 msi.

Epoxies considered in this study were selected based on usage in current production applications and availability of mechanical and physical property data. The fiber/resin systems were Narmco's T-300/5208, Fiberite's HM-S/934, and Fiberite's GY-70/934. Details of current usage of these systems are given in Reference 1. Testing of graphite/epoxy systems was not part of the conceptual design study, and therefore properties used in the study were based on a survey of large quantities of data available from previous programs.

Three addition polyimide resins were selected as candidates for the conceptual design study. The resins were Narmco's 5230, Hexcel's F-178, and Hercules 4397. Addition polyimides were included in this program for the following reasons: (1) the Mark 12A heat shield backside temperature was originally considered to be 600F, (2) future reentry vehicles including maneuverable reentry systems would require high-temperature resistant composites, and (3) addition polyimides process similarly to epoxies with only an added requirement of a simple postcure. Five systems were studied for their applicability to the Mark 12A and future reentry vehicles. These systems were T300/5230, T-300/F-178, HM-S/5230, HM-S/4397, and GY-70/5230. A survey (Reference 2) was made during the first week of the program of available composite data on graphite reinforced addition polyimides (F-178, 5230, and 4397). To supplement this data, a comprehensive screening program was initiated on the five graphite/polyimide systems. This included longitudinal tension, longitudinal compression, in-plane shear, and interlaminar tension testing at room temperature (RT), 350F, and 600F. Specimen configurations and test data generated by this program are summarized in Section 3.

At the end of the second week of the program, revised temperature plots were received from General Electric. These showed a maximum heat shield backface temperature of 400F. For the recommended midbay composite structure, the maximum composite front face and backface temperatures are 260F and 232F, respectively (see Section 2.2). These temperatures are well within the capability of current 350F curing epoxy systems, even after long term ambient aging. Therefore, graphite/epoxy rather than graphite/polyimide is recommended for the Mark 12A midbay structure. The advantages of graphite/epoxy are quite obvious, i.e., (1) greater data base and use history, (2) lower material costs, and (3) less likelihood for microcracking.

There are several factors which make graphite/polyimide an attractive alternate for the midbay structural material. A redesign eliminating the adhesive bond between the heat shield and the midbay structure or a reduction in heat shield thickness could result in significant weight savings. These potential design concepts would result in increased temperatures for the composite structure, and would drive the material selection toward addition polyimides. An unknown factor during the study was the relative resistance of the two classes of composites to potential nuclear threats. Should AGT/UGT show significant differences, then this too might warrant revision of the material selection.

An examination of the existing aluminum shell, carbon/phenolic (C/P) heat shield design led to the conclusion that the heat shield back face tension strain allowable at room temperature of 2300$\mu\epsilon$ was the governing failure mode. This divided the graphite fibers into two classes; those with strain allowables less than 2300$\mu\epsilon$, and those with strain allowables greater than 2300$\mu\epsilon$. For the graphites with less than 2300$\mu\epsilon$ allowables, enough material must be used to prevent failure in the graphite and a strength critical design results. For the graphites with greater than 2300$\mu\epsilon$ tension allowable, a stiffness critical design results.

In order to study the tradeoff between the different materials, the aft section with the most area was chosen. An ultimate load intensity of 2447 lbs./in. was selected since this load acting alone causes 2300$\mu\epsilon$ in the C/P in the existing design for the URNB condition. Layups were assumed to yield 45% of the unidirectional modulus. The study results are in Table 2.2.2-1.

Table 2.2.2-1. Results of Material Trade

Material	PSI X Ply Modulus	ϵ_{11} tu	ρ lbs/in^3	t_{req} in	W $\frac{\text{lbs}}{\text{in}^2 \times 10^{-3}}$	Δ %	Critical
GY-70	19 x 10^6	1400$\mu\epsilon$	.063	.0677	4.26	53	Strength
HM-S	13 x 10^6	3800$\mu\epsilon$	.060	.0463	2.78	0.0	Stiffness
T-300	9.5 x 10^6	8400$\mu\epsilon$	.058	.0634	3.68	32	Stiffness

The results clearly indicated that HM-s is the optimum fiber for the Mark 12A design.

In a parallel effort, Convair provided a series of panels for evaluation as part of a SAMSO/ABRES program. The panels were of a 0/±60 2_S configuration, and were bonded by Hitco to tape wrapped carbon phenolic (TWCP) heat shield material using Hysol's EA-934 epoxy adhesive and controlling the bondline thickness to 0.040 in. The materials evaluated as substructures were three graphite/epoxies (T-300/

5208, HM-S/934, and GY-70/934 and three graphite/polyimides (T-300/F-178, HM-S/4397, and GY-70/5230). An impact test program was conducted at the AFWL Material Response Impact Facility to assess the resistance of the six systems to impulsive loading damage. The flat composite samples represented a typical reentry vehicle cross section (heat shield/bond/substructure).

Reference 14 summarizes the data obtained from the impact tests. Impulsive loading conditions used in the screening program were designed to provide simulation of dynamic conditions experienced in UGT. Several different loading conditions were simulated. The repeatability of the mode and extent of damage on duplicate tests was excellent. The GY-70 and HM-S fiber reinforced panels with both epoxy and polyimide resins suffered extensive delamination under the worst test conditions, with the damage slightly greater with the GY-70 than with the HM-S and slightly greater with the polyimide than with the epoxy. The failure mode was complete delamination and interply separation. Under the worst case conditions, the T-300 reinforced polyimide (T-300/F-178) showed a midplane delamination and separation, while the T-300/5208 graphite/epoxy showed a partial midplane delamination. The T-300 panels were significantly more resistant to impulsive loading damage than the HM-S and GY-70 panels.

The data from the brief impulsive loading screening program were presented at the conceptual design review. The Mark 12A Midbay Substructure program was redirected at this point to evaluate a T-300/5208 midbay design rather than the more structurally efficient HM-S/934 design.

The above flat panel specimens, described in Section 3 as group "A" specimens, were layed up with a ply and orientation configuration as recommended in the conceptual study, reference paragraph 2.2.1.3. Section 3 also describes group "B" and "C" specimens, which by customer direction were configured with a ply and orientation as proposed for the Advanced Ballistic Reentry Vehicle (ABRV) - composite structure study - under a contract with AVCO. Results of impulsive loading screening tests on group "B" and "C" were unknown during preparation of this report. However, results will be available in a forthcoming report (Reference 16) by Ktech Corporation.

2.2.2.1 Fungus. A variety of cured epoxy-resin compounds exposed to standard fungus-resistance tests have all been shown to be non-nutrient to fungus. Cured epoxy-resin compounds were also not attacked by marine bacteria when incubated at either 5° or 20°C (Reference 4). Some amount of moisture must be present to support fungus growth. It is necessary, therefore, to determine the effect of moisture alone to establish the effect of fungus. It has been determined (see Reference 5) that moisture combined with fungus growth reduces mechanical properties of reinforced plastics but

that the combined effect is identical to the effect of moisture without fungus growth. The growth of fungus was more dependent on whether the reinforcement was organic such as cotton and paper or inorganic such as fiberglass. It was generally concluded that fungus growth has negligible effect on the mechanical properties of reinforced plastics. Graphite and boron reinforced epoxy composites (References 6 and 7) have shown little or no deterioration when exposed to standard fungus testing. Again whatever deterioration in properties has been encountered has been attributed to moisture rather than fungus effects. No fungus growth was encountered with graphite/epoxy laminates when tested per MIL-STD-810B, Method 508.

2.2.2.2 Permeability. The upper bound on the amount of water vapor which a midbay 0.050-inch T300/5208 system will diffuse is estimated to be 1.13×10^{-3} std cc/sec.: and is representative of the values to be expected in other graphite/epoxy systems considered in this study. The derivation of the 1.13×10^{-3} std cc/sec value is given as follows and is considered to be conservative.

$W = \frac{KC}{t}$ assumes one face wet, other face dry.

$W = \frac{\text{Weight of diffused water}}{\text{time x area}} = \frac{\text{lbs}}{\text{day x in}^2}$

$K = 7.5 \times 10^{-6}$ in^2/day at 80° F T300/5208

C = maximum weight of water per unit volume of composite. Max. weight percent for T300/5208 = 1.7%. T300/5208 density = 0.058 lbs/in^3
Note: usual values are 1.2% to 1.4%

t = thickness = 0.005 x 10 ply = 0.050 inches

$$W = \frac{7.5 \times 10^{-6} \times 9.86 \times 10^{-4}}{0.05} = 1.479 \times 10^{-7} \text{ lbs/day in}^2$$

$$\frac{1.479 \times 10^{-7} \text{lbs}}{\text{day x in}^2} \times \frac{\text{day}}{86400 \text{ sec}} \times \frac{453.6\text{g}}{\text{lb}} \times 1300 \text{ in}^2 = 1.0 \times 10^{-6} \text{g/sec}$$

$$\frac{22,400 \text{ cc}}{\text{g mole}} \quad \frac{\text{g mole}}{18\text{g}} \quad \frac{1.0 \times 10^{-6} \text{g}}{\text{sec}} \times \frac{273\text{K}}{300\text{K}} = 1.13 \times 10^{-3} \frac{\text{std cc}}{\text{sec}}$$

The addition of the 0.040 inch thick EA934 adhesive bond and the 0.415-inch TWCP heat shield will reduce this upper bound estimate. The use of aluminum foil on the outside of the substructure for electrical continuity would also result in an effective moisture barrier.

2.2.3 STRUCTURAL ANALYSIS. Several areas of the MK12A G/E midbody structural shell have been subjected to stress analysis in order to demonstrate the feasibility of application of graphite/epoxy to the design and in order to give some confidence to the weight estimate. The analyzed areas include the highly loaded load introduction rings at Station 25.55 and 32.18 as well as the basic shell wall. Prior to the first design review, almost all of the analysis was directed toward a HMS design. At the first design review, Convair was directed to work on a T300 design. The analysis presented here is of the T300 design.

The majority of the analysis was performed using finite element code GDSAP which is Convair's version of SAP which was developed by E. L. Wilson of the University of California at Berekley. The ring analyses using GDSAP were performed using the axisymmetric solid option with the loads being peak values from combined axial load and moment.

Section 3 describes tests performed to verify the following structural analysis/ adequacy of design in the areas of material properties, stress concentrations, bond capabilities and joints.

2.2.3.1 Material Properties. The G/E material properties used in the analysis of the MK12A are summarized in Table 2.2.3-1.

Table 2.2.3-1. G/E Material Properties

Property	Units	Material		
		T-300/5208	HM-S/934	GY-70/934
E_{11}	10^6 psi	20.8	28.0	42.0
E_{22}	10^6 psi	1.46	1.0	0.95
ν_{12}	-	0.30	0.30	0.30
G_{12}	10^6 psi	0.52	0.67	0.95
α_{11}	$\mu\epsilon/^\circ F$	-0.40	-0.45	-0.51
α_{22}	$\mu\epsilon/^\circ F$	16.2	16.2	16.0
$\epsilon_{11\ tu}$	-	8400	3800	1400
$\epsilon_{11\ cu}$	-	9200	3800	1400
ρ	lbs/in^3	0.058	0.060	0.063
t	in/ply	0.0055	0.0053	0.0050

The values listed are room temperature properties since all significant load conditions occur with the structure near room temperature. Only fiber direction strain allowableless are shown since for crossplied laminates subjected to single flight loads, first fiber failure criteria for laminate analysis is appropriate.

The data bases for GY-70 and T-300 are quite extensive. However, Convair does not have a large data base on HM-S and the values shown are judged to be reasonable based on literature searches.

The adhesive used for analysis was Hysol EA934. The room temperature properties used for analysis are shown in Table 2.2.3-2. This adhesive was used in this study since Convair has used it successfully on many programs. The test program showed that Hysol 9309 was generally stronger in lap shear when bonding G/E or G/PI to aluminum. EA9309 is called out on the drawings based on the test results. Figure 2.2.3-1 shows that EA9309 gives average shear strengths greater than 3500 psi for the range of bondline thicknesses of 0.005 to 0.025 inches which are the limits called out on the drawings.

Table 2.2.3-2. EA934 Properties

Property	Units	Value
E	10^6 psi	0.70
ν	-	0.30
G	10^6 psi	0.27
α	$\mu\epsilon/^\circ F$	28.8
ρ	lbs/in^3	0.049
$F_{su_{peak}}$	psi	3100

The shear allowable of 3100 psi peak for EA934 is based on a linear analysis of a standard half-inch overlap test specimen subjected to 1500 psi average stress. The analysis used 0.050 × 0.020 finite elements. A plot of the normal and shear stresses in a test specimen subjected to 1500 psi is shown in Figure 2.2.3-2. These stresses are based on a finite element analysis using 0.050 long by 0.020 thick finite elements just as the finite element models of the MK12A midbody use.

2.2.3.2 Applied Loads. The applied loads for use in this study are taken from:

"MK12A Graphite Composite Structure Design Requirements to Support Feasibility Studies," dated 7 July 1976 by GE-RESD.

EA9309 Adhesive T300/5208 to Aluminum

Δ - 0.50 Inch overlap double shear specimens

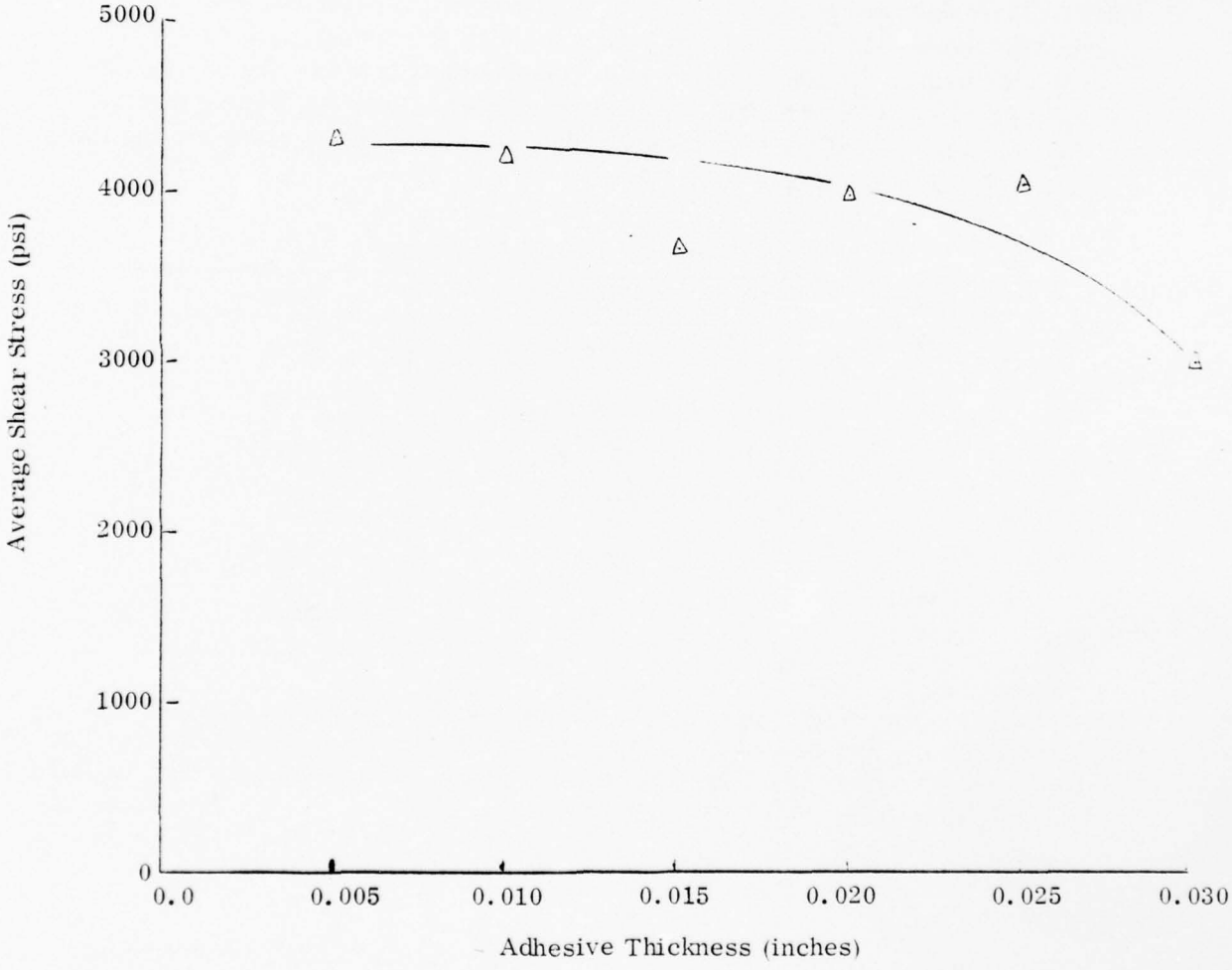

Figure 2.2.3-1. Shear Strength Vs. Bond Thickness

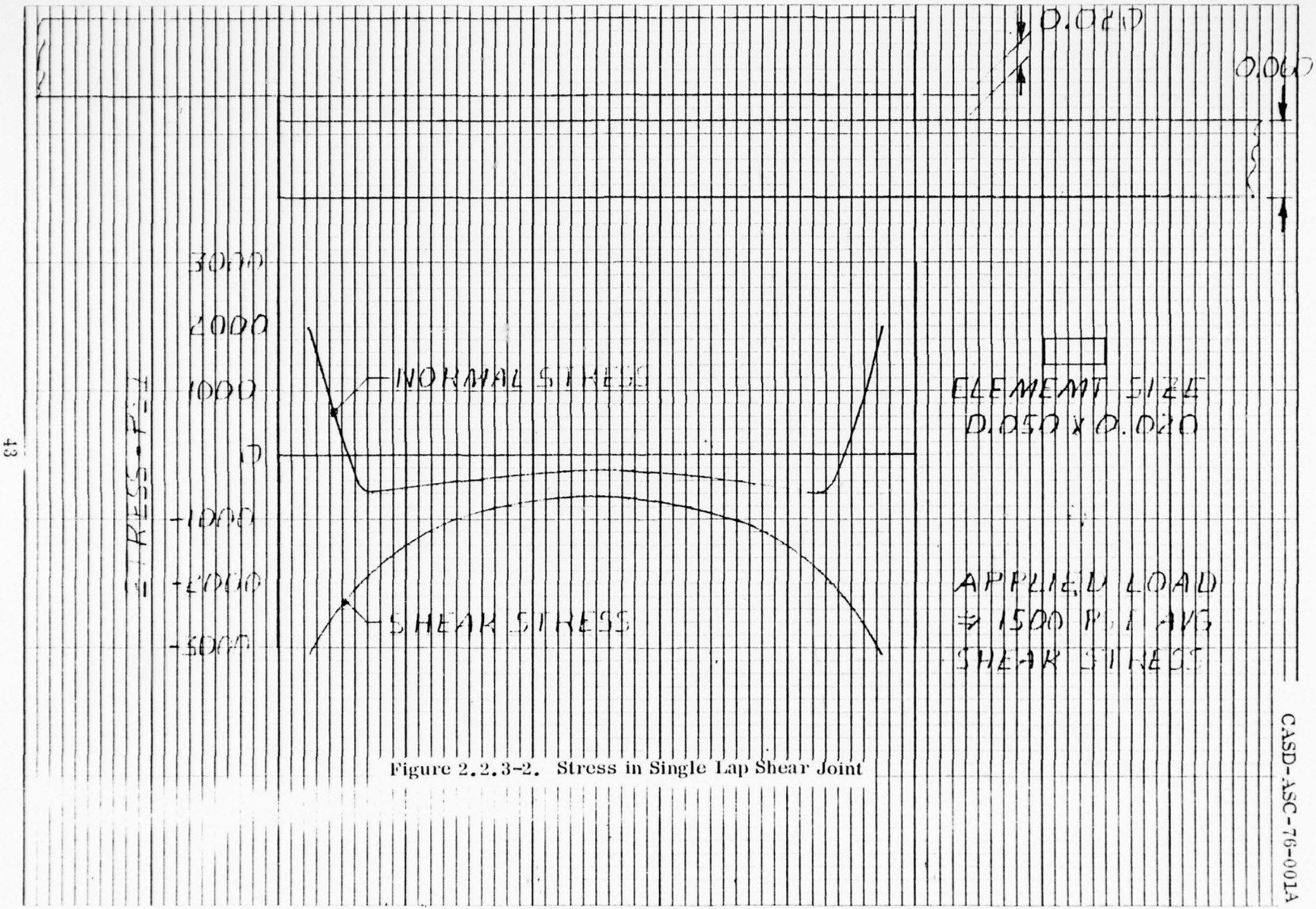

Figure 2.2.3-2. Stress in Single Lap Shear Joint

This document lists the overall dynamic requirements and gives two critical equivalent steady state load conditions for use in this study. These two conditions are designated URNB which is the maximum lateral acceleration case on ULRR which is the maximum temperature with the thinnest heat shield case.

The above document is assumed available and the numerous load charts are not reproduced here. For specific analyses, the applied external loads are stated with the analysis.

2.2.3.3 Mark 12A Laminate Definition. In order to evaluate various laminates that can adequately replace the present aluminum design the following approach was used.

1. Load intensities were evaluated at various stations.
2. The station with greatest load intensity (Sta. 32.18) was used as a baseline in comparing aluminum versus composite designs.
3. The two specified conditions (ULRR and URNB) were used to define the temperature state and thickness of the heat shield. Also defined were the axial loads, shears and bending moments that were used to compute the axial, and shear load intensities to be applied to the candidate composite designs (reference Table 2.2.3-3).

Table 2.2.3-3. Applied Loads on Laminate at Sta. 32.18 Aft (Ultimate)

Load	URNB @ Pad	URNB @ Groove
N_x (lb/in)	2577	1435
N_y (lb/in)	1813	1518
N_{xy} (lb/in)	0	0
M_x (in-lb/in)	-219	-70
M_y (in-lb/in)	-189	77.5
M_{xy} (in-lb/in)	0	0

4. The laminates studied considered the following components:

   a) The heat shield was divided into four equal thicknesses (.129/4 for ULRR and .202/4 for URNB) with each layer being assigned its particular stiffness and thermal expansion properties as a function of its particular temperature (reference Table 2.2.3-4).

   b) The adhesive between the heat shield and basic cone was considered to be the fifth layer (t = .040 in.) with its temperature dependent properties (reference Table 2.2.3-4).

c) The basic cone was modeled alternately as the original aluminum design and then various graphite composite systems with various orientations.

Table 2.2.3-4. Laminae Properties used in Laminate Analysis

No. Layer (Temp) (°F)	t (in)	E_1 (msi)	E_2 (msi)	ν_{12}	G (msi)	CTE_1 (in/in° F)	CTE_2 (in/in° F)
URNB STA 32.18 AFT							
1 (440)	.0505	1.1	1.6	.3	.42	177.	123.
2 (150)	.0505	2.25	2.25	.3	.87	50.	50.
3 (100)	.0505	2.45	2.45	.3	.94	13.6	13.6
4 (81)	.0505	2.55	2.55	.3	.98	4.5	4.5
5 (81)	.040	.58	.58	.62	.18	41.1	41.1
6 Al (81)	.100	10.0	10.0	.33	3.8	13.1	13.1
6 T300/5208 (81)	.005x20	20.8	1.42	.30	.54	-.45	16.2
ULRR STA 32.18 AFT							
1 (740)	.0322	.41	.41	.3	.16	3.89	3.89
2 (440)	.0322	1.00	1.00	.3	.38	4.29	6.18
3 (260)	.0322	1.97	1.97	.3	.76	5.02	6.02
4 (150)	.0322	2.30	2.30	.3	.88	4.78	4.78
5 (100)	.040	.62	.62	.30	.24	28.8	28.8
6 Al (91)	.100	10.0	10.0	.33	3.8	13.1	13.1
6 HMS (91)	.005x20	28.0	1.0	.30	.67	-.45	16.2

5. The analytical tool used was GDC's SQ5 laminate analysis program. This program computes laminate stiffness properties, distributes loads to each laminate to maintain the constitutive relationship of stresses and strain, computes strains resulting from specific applied loads and thermal conditions in the laminae's principal axis and compares these strains to input allowable values to obtain a margin of safety. Due to the curvature of the conical shell, no change in curvature was allowed due to body loads, air loads or thermal effects. Loads due to discontinuity were allowed to produce rotations.

Results

The analysis of the aluminum "control" configuration yields a margin of safety of

$$M.S._{A1} = -.047 \begin{pmatrix} \text{URNB Max } N_x \\ \text{Aft of Sta. } 32.18 \end{pmatrix}$$

in the heat shield layer.

Using T300/5208 fiber system in the orientation $(0,45,90,-45,0)_S$ $(0_2 90)_5 (0_2)$ yields a margin of safety of

$$M.S._{T300/5208} = +.048 \begin{pmatrix} \text{URNB Max } N_x \\ \text{Aft of Sta. } 32.18 \end{pmatrix}$$

in the same heat shield layer.

The margin of safety of T300/5208 laminate forward of Sta. 32.18 was also checked. With a 10-ply laminate of $(0,45,90,-45,0)_S$ resulting in a .050 thickness, a margin of

$$M.S._{T300/5208} = -.036 \begin{pmatrix} \text{ULRR Max } N_x \\ \text{Fwd. of Sta. } 32.18 \end{pmatrix}$$

was computed in the outer one-fourth of the heat shield. The allowable compressive strain of the heat shield was assumed to twice the allowable tensile strain which is believed to be conservative and therefore there is room for further optimization in this area.

2.2.3.4 Station 25.55 Ring. The Station 25.55 ring was modeled using axisymmetric solid finite elements and loaded axisymmetrically. This analysis contains no peaking factors to account for the discontinuous nature of the tension load being applied through the threads.

The loads applied to Station 25.55 are taken from Letter No. 3735-1169 (Reference 7) and are critical for URNB 15245 ft:

P = 7,000 lbs.
M = 68,000 in.-lbs.
θ = 9,900 degrees/sec. ult. (ref. paragraph 3.3.5)
p = 100 psi limit crush

Temperatures are taken from reference 7 revised at centers of elements. These applied loads were converted to running loads using thin shell equations.

N_{x_T} = 1496 lbs./in. limit

N_{x_c} = 2142 lbs./in. limit

The compression loads are assumed uniformly distributed along the contact plane at Station 25.55. The tension loads are assumed uniformly distributed at the mid-height of the threads.

The joint and about three inches of skin were modeled for analysis by GDSAP. A computer plot of the joint portion of the model is shown in Figure 2.2.3-3. The model was altered iteratively to minimize shear stresses in the bondline. The stresses are shown in Figure 2.2.3-4. The +0.25 margin of safety in the C/P was maintained to account for the unanalyzed peaking due to discontinuous threads.

2.2.3.5 Station 32.18 Ring. The station 32.18 ring and about six inches of adjacent shell were modeled using axisymmetric finite elements. All loads were applied axisymmetrically with values as follows:

		Fwd of 32.18	Aft of 32.18
P	=	-7000	-17,500 lbs. limit
M	=	72,000	115,000 in-lbs. limit
θ	=	9900	9900 degrees/sec ult
p_{max}	=	175	175 psi limit crush
p_{min}	=	35	35 psi limit crush
t	=	taken from Figure 7 revised at element centers	

The differential load was applied at a 4.22 inch radius where the payload support shell bears on the Station 32.18 ring.

The central portion of the finite element model of the Station 32.18 ring is shown in Figure 2.2.3-5. Four load conditions were run for the URNB condition which were the combinations of maximum and minimum shell load intensity and maximum and minimum crush pressure. The resulting bondline stresses are shown in Figure 2.2.3-6. The low margin of safety in the C/P is in a region where the G/E is stiffer than the existing aluminum design and is adequate by comparison.

Several iterations were required in order to achieve an acceptable shear and normal bondline stress distribution. Initial iterations were made with shorter and thinner legs on the ring. The shear peak stresses were on the order of 5000 psi and the normal tension stresses were approximately 3000 psi. Beryllium was tried in an attempt to reduce the normal stress peaks. However, this only increased the severity of the shear stress peaks as all the shell load tried to immediately transfer into the very stiff beryllium. Thickening and carefully tapering the aluminum ring yielded the current design.

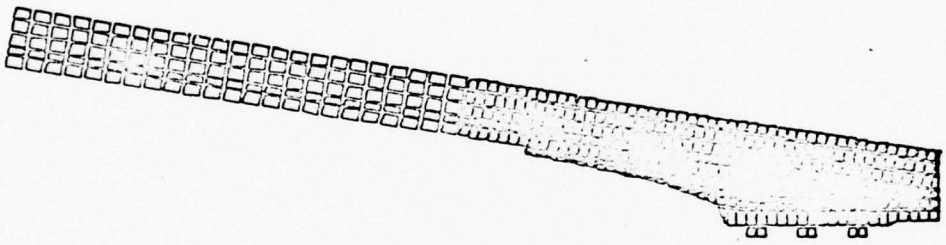

Figure 2.2.3-3. Finite Element Model of Station 25.55 Ring

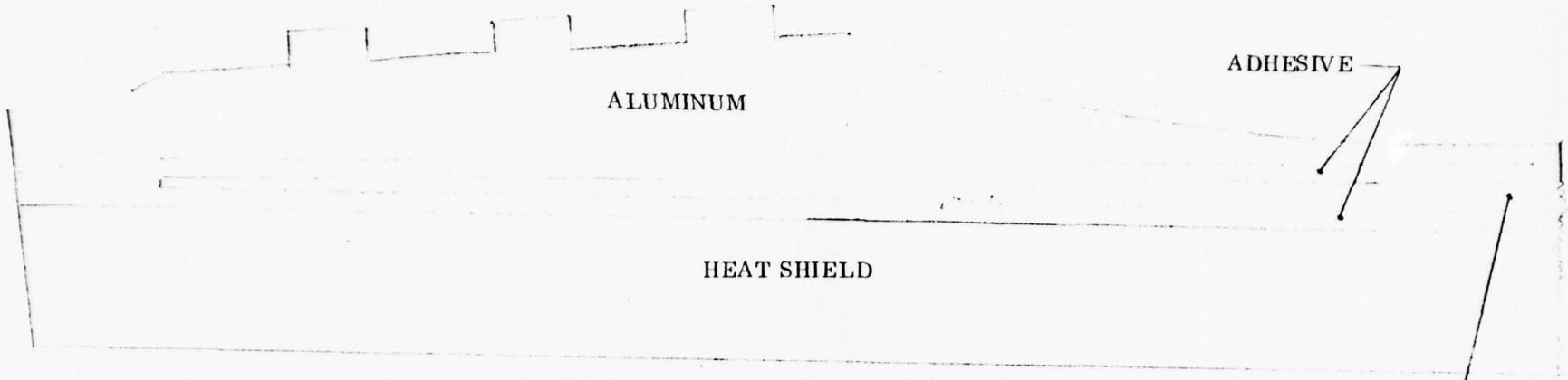

STRESSES IN STA 25.55 JOINT URNB 15K FT.

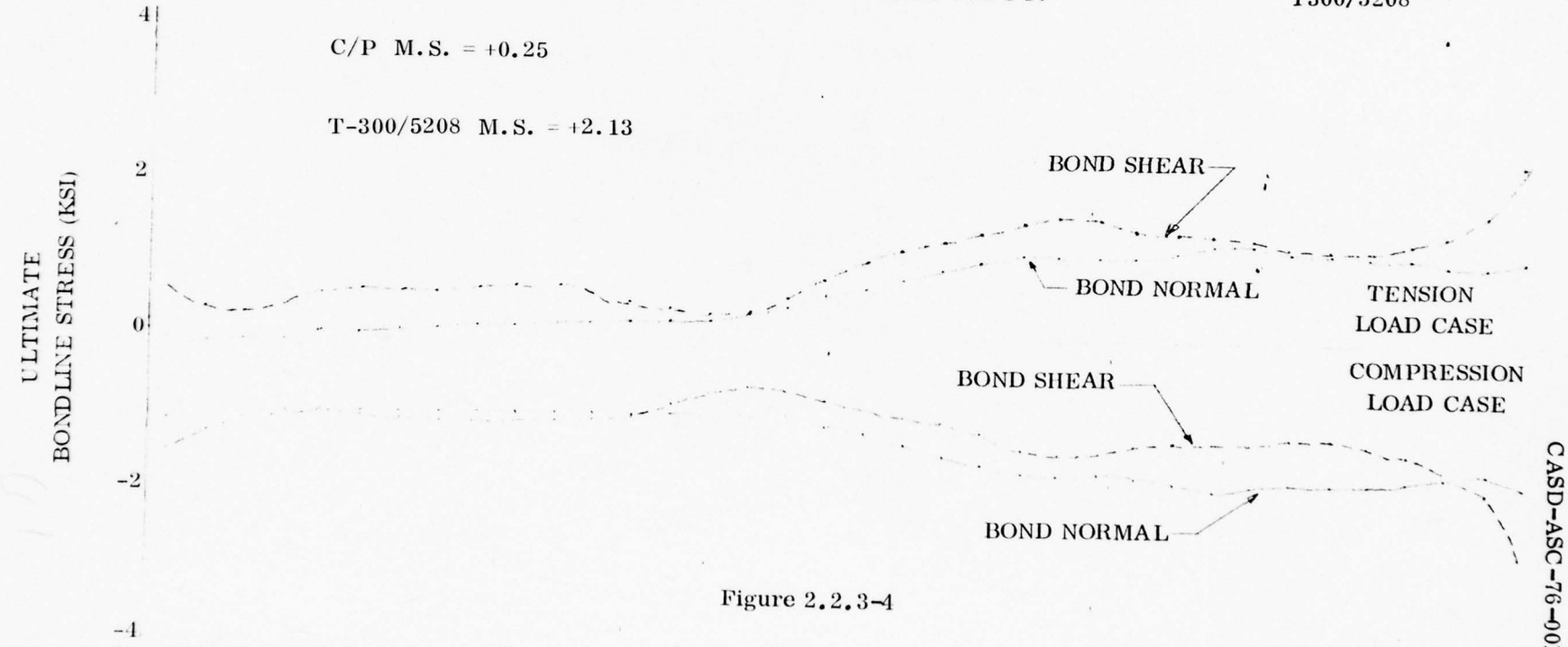

Figure 2.2.3-4

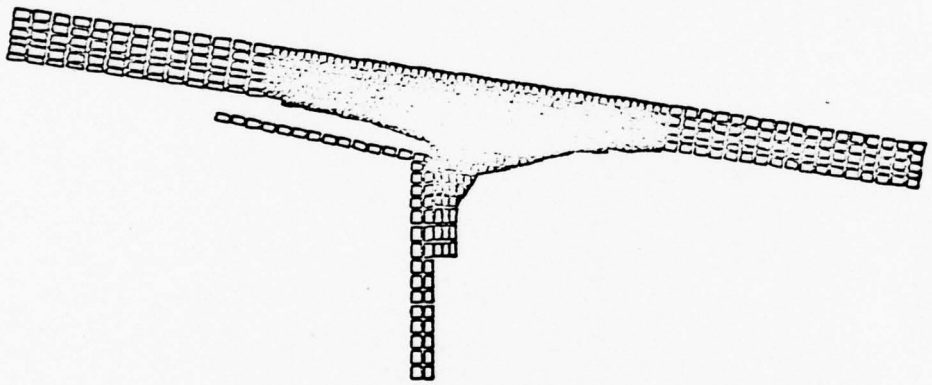

Figure 2.2.3-5. Finite Element Model of Station 32.18 Ring

Figure 2.2.3-6. Stresses in Station 32

2.2.3.6 Shell Stability Analysis. Shell stability analysis at Station 50 was done on the computer program SS8 which performs anisotropic curved panel stability analyses. SS8 was developed by D. J. Wilkins of General Dynamics Fort Worth Division under Contract F33615-69-C-1494. This program was selected due to the fact that it can perform the analysis of laminated-composite cylindrically curved shells. Unfortunately, it does not consider conical shells. This limitation was overcome in the following manner. A circular cylindrical analysis was performed on the aluminum configuration at Station 50. A cylinder of 15 inches of length was used. The analysis yielded an Eigenvalue = 1.35. It then was assumed that if a laminated cylindrical shell with the same geometry as the aluminum shell yielded an Eigenvalue ≥ 1.35, then that laminated section satisfied the stability criteria. The input for the baseline aluminum is as follows:

The cylinder length was derived as 15 inches unsupported shell between the pads and Station 50 ring. A slant radius of 7.64 inches was used. The laminates were chosen as 4 plies of heat shield with t = 0.0322 inch, 1 ply of bond with t = 0.04 inch, and 1 ply of aluminum with t = 0.06 inch. These dimensions yielded an Eigenvalue of 1.365110. The composite cylinder also had the same length and radius. Again the cylinder had the same 4 ply of heat shield and 1 ply of bond followed by an 0.005 inch ply of aluminum, 1 ply of glue with t = 0.003 inch, an 0.005 inch ply of glass, and 10 ply of G/E with $(0, +45, 90, -45, 0)_S$ layup with ply t = 0.0055 inch. These dimensions yielded an Eigenvalue of 1.341223.

The loads applied to each cylinder was derived by extracting P_{axial} and M_x at Station 50 from Figures 26 and 27 of MK12A Graphite Composite Structure Design Requirements to Support Feasibility Study. Loads were determined by the equations:

$$N_x = \sigma t$$

where

$$\sigma = \left(\frac{1}{.726}\right)\left(\frac{P}{A}\right) \pm \left(\frac{1}{.778}\right)\left(\frac{M_c}{I}\right) \quad \text{and}$$

$$N_o = \frac{P_r}{0.75}$$

The knockdown factors were obtained from report NASA SP-8007, Buckling of Thin-Walled Circular Cylinders, August 1968. The knockdown factor for axial load is

$$\gamma = 1 - .901(1-e^{-\varphi}) \qquad \text{(page 18)}$$

For bending,

$$\gamma = 1 - .731(1-e^{-\varphi}) \qquad \text{(page 19)}$$

and external pressure

$$\gamma = 0.75 \qquad \text{(page 20)}$$

where

$$\varphi = \frac{1}{29.8} \left[\frac{r}{\sqrt[4]{\frac{\bar{D}_x \bar{D}_y}{\bar{E}_x \bar{E}_y}}} \right]^{1/2}$$

The applied loads are as follows

N_x = 1517 lb/in

N_θ = 1015 lb/in

This stability analysis shows that the $[0, +45, 90, -45, 0]_s$ graphite/epoxy layup is equivalent to the aluminum shell at Station 50.

2.2.4 THERMAL ANALYSIS.

2.2.4.1 Analysis Objectives. There were two thermal analysis objectives:

1. To predict the maximum graphite/epoxy composite structure and Epon 934 adhesive temperatures during the reentry time period.

2. To predict the temperature gradients at the Station 32 thrust ring area.

2.2.4.2 Thermal Models. Two analysis locations were selected. The minimum structural thickness area at Station 42 was selected because the local predicted composite and adhesive temperatures would be a maximum. The Station 32 thrust ring area was analyzed to demonstrate that thermal expansion of an aluminum ring would not induce unacceptable strain in the graphite/epoxy shell.

The Station 42 thermal model employed nominal material thicknesses of 0.050 inches for the Epon 934 adhesive. Station 42 thermal model nodes are illustrated in Figure 2.2.4-1, which shows the adhesive to be divided into five nodes (2 through 6) and the

NODALIZED THERMAL MODEL
STATION 42, GRAPHITE/EPOXY

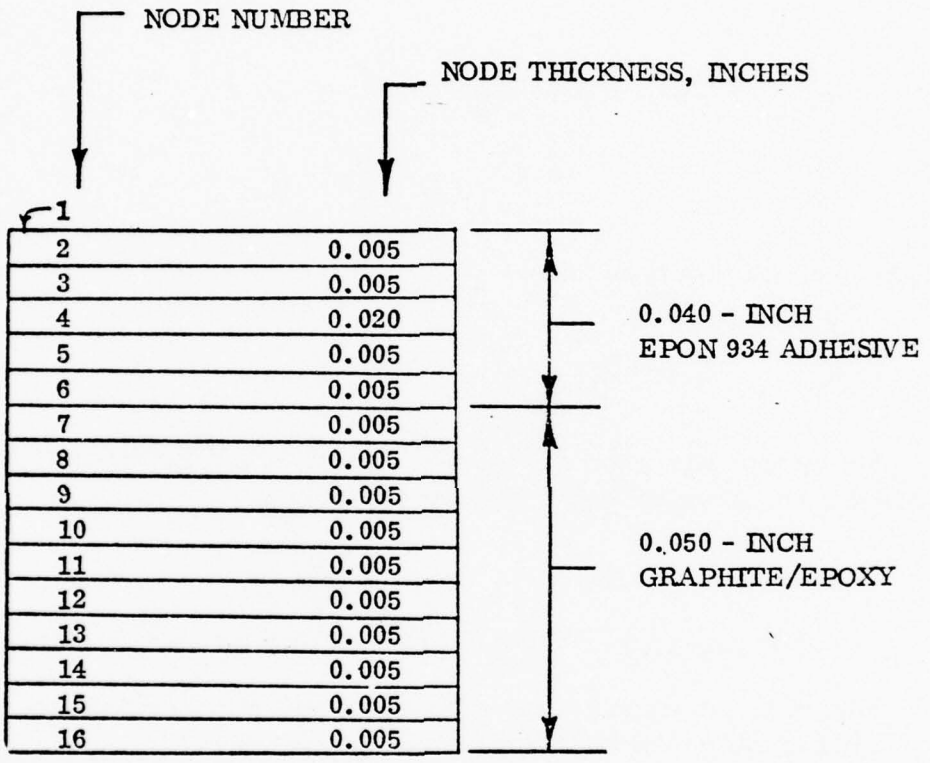

Note: Node 1 is a surface node that has its temperature driven versus time corresponding to the heat shield inner surface temperature for the ULRR conditions.

Figure 2.2.4-1. Mark12A Midbay Graphite/Epoxy Structure — Concept #1, Baseline

graphite/epoxy divided into ten nodes (7 through 16). A surface node (Node 1) represents the inner surface of the heat shield, for which the temperature history was provided by General Electric (Reference 8) and is shown as the upper temperature history in Figures 2.2.4-3 through 2.2.4-6. These temperatures, which were considered to be two-sigma hot values, were based upon an analysis of flight data for an aluminum midbay structure. These data were used in this analysis because heat shield inner surface temperatures were available for an aluminum midbay structure only. It should be noted that the heat shield inner surface temperature would have been somewhat higher for a composite material midbay structure because the composite material thermal mass and conductivity are lower than that of aluminum.

The Station 32 ring area thermal model is shown in Figure 2.2.4-2. A large thermal model was employed in order to account for the axial heat conduction from the high temperature thin skin to the lower structural temperature adjacent to the ring where the material mass is large. The heat shield inner surface is represented by nodes 1, 10, 23, 43, 56, 65 and 74. A nominal adhesive thickness of 0.040 inches was employed for the graphite/epoxy-to-heat shield bond, and 0.015 inches for the ring-to-graphite/epoxy bond. The graphite/epoxy thickness was assumed to be 0.100 inches thick in the ring area and 0.050 inches thick in the basic skin area. The dimensions of the aluminum ring are based upon the Reference 9 sketch, and have been reduced in size to account for the holes and spotfaced surfaces on the ring upstanding leg.

The Reference 10 computer program input listings for the Station 32 and 42 thermal models, are provided in Appendix A.

2.2.4.3 Analysis Assumptions. It was assumed that the heat shield inner surface temperature (Reference 8) would be unaffected by axial variations in the midbay structural thickness. It was further assumed that radiation and conduction energy exchange between the midbay internal surface and the payload would be negligible.

The problem starting time (flight time equals zero seconds) corresponds to a reentry altitude of 40,000 feet (Reference 8).

The ULC trajectory was employed to relate the heat shield temperature versus altitude (Reference 8) to heat shield temperature versus flight time.

The heat shield temperatures correspond to the upper left, roll resonance condition.

2.2.4.4 Material Properties.

Graphite/Epoxy

Density, 97 lb/ft^3 (Reference 11)

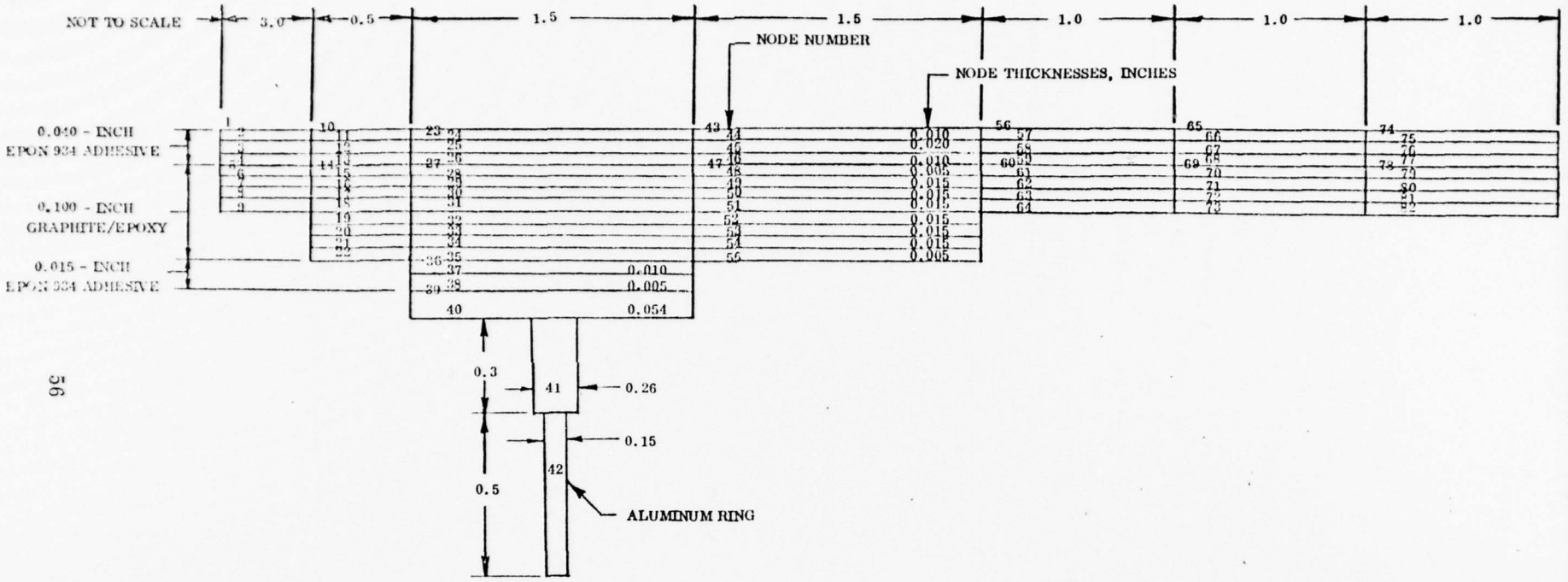

Note: Nodes 1, 10, 23, 43, 56, 65, and 74 are surface nodes having thier temperatures driven versus time corresponding to the heat shield inner surface temperature for the ULRR condition.

Figure 2.2.4-2. Nodalized Thermal Model, Station 32
Ring Area — Concept #1, Baseline

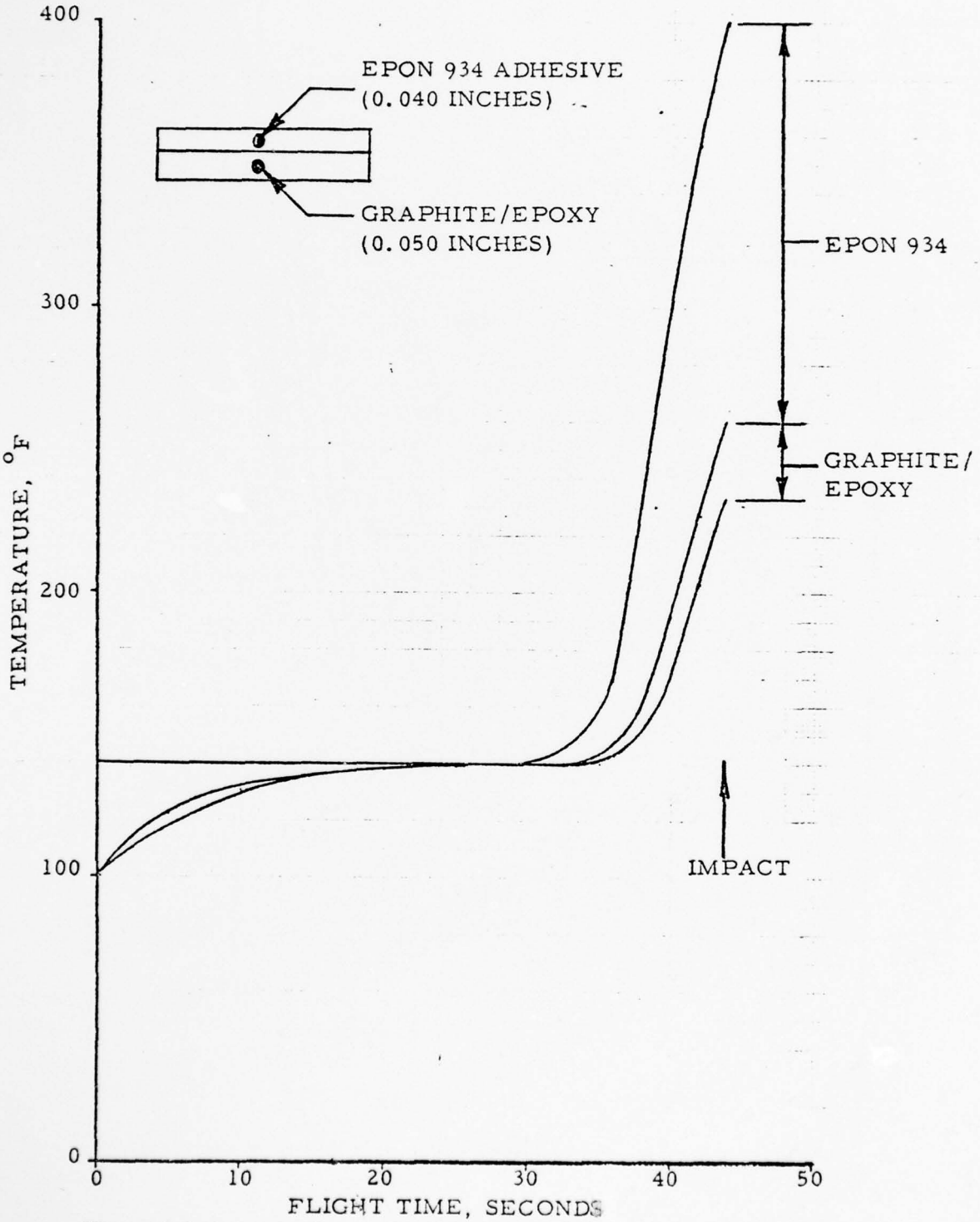

Figure 2.2.4-3. Station 42 Predicted Temperatures (0.040 adhesive) Concept #1, Baseline

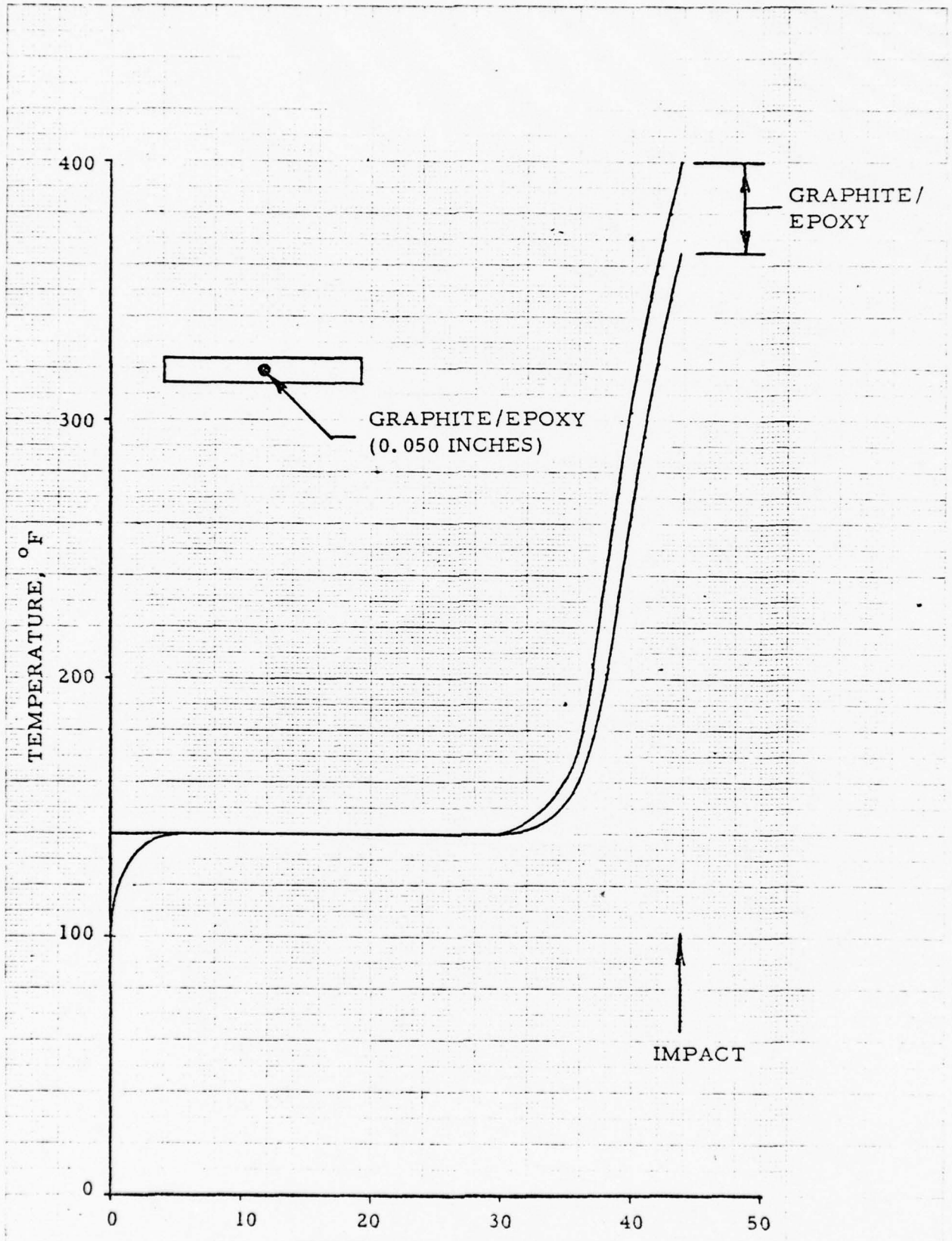

Figure 2.2.4-4. Station 42 Predicted Temperatures (No Adhesive) Concept #1, Baseline

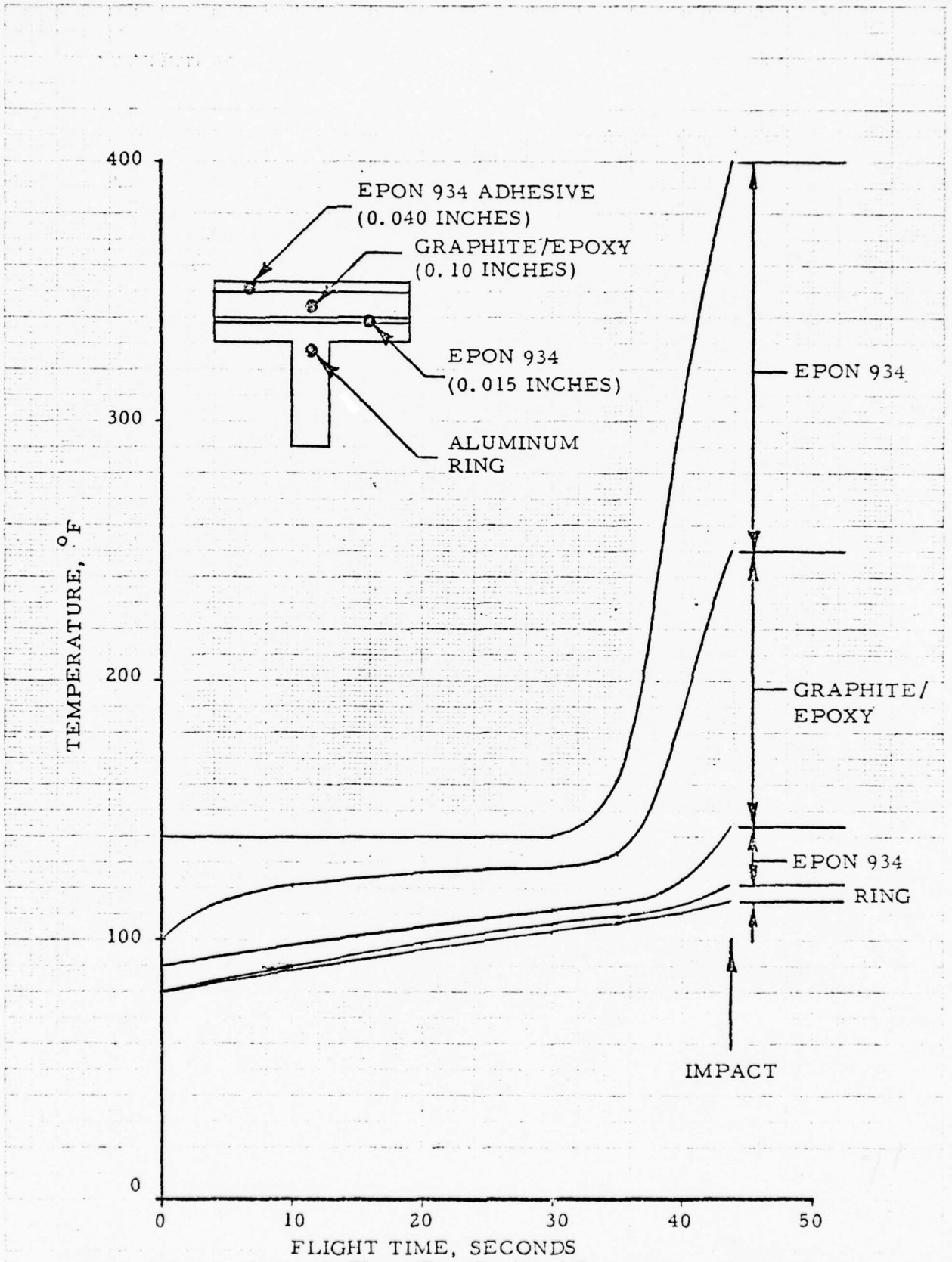

Figure 2.2.4-5. Station 32 Thrust Ring Predicted Temperatures (0.040 adhesive) Concept #1, Baseline

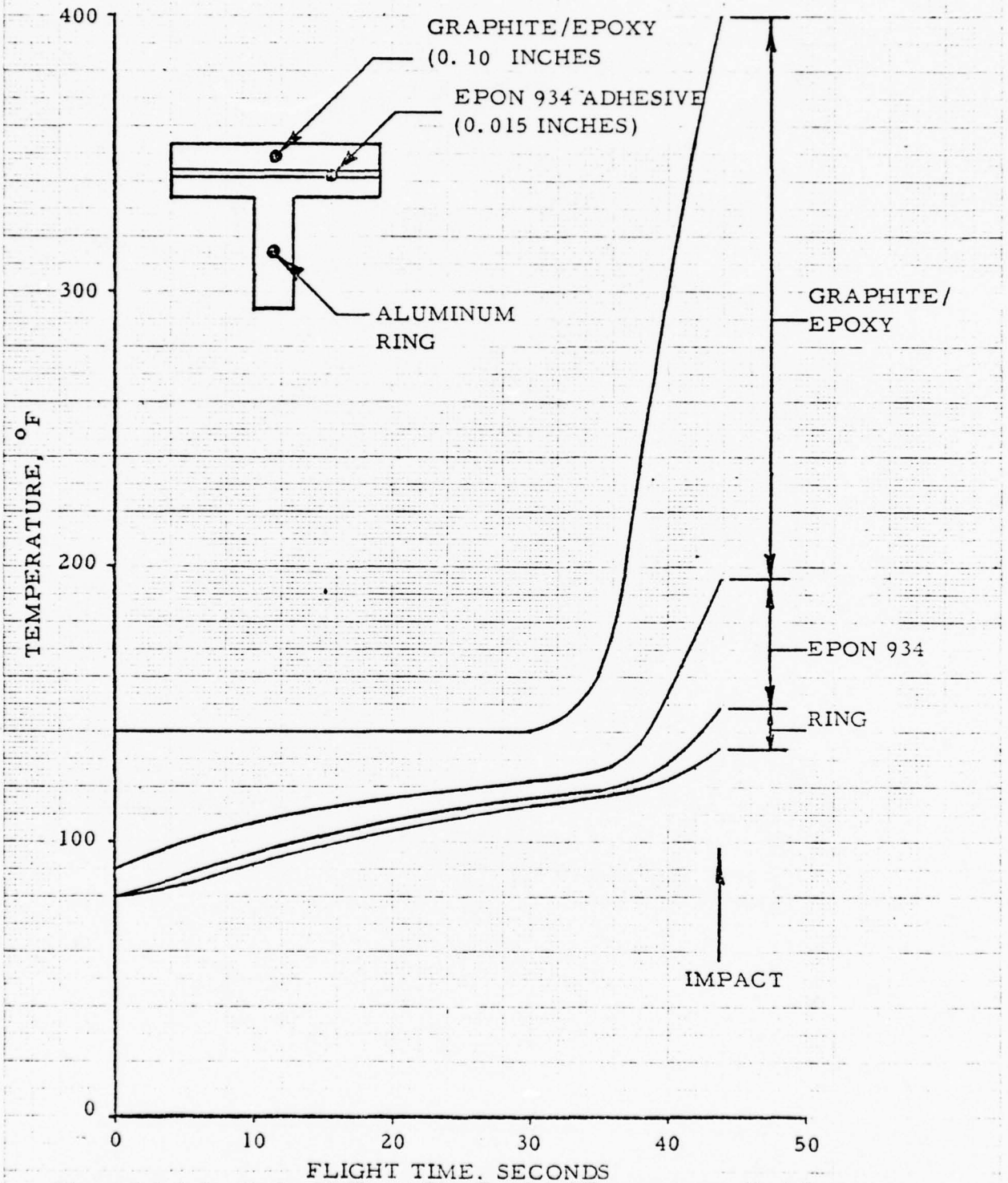

Figure 2.2.4-6. Station 32 Thrust Ring Predicted Temperatures (No Adhesive) Concept #1, Baseline

°R	Specific Heat, Btu/lb-°R (Reference 11)
160	0.075
810	0.330

°R	Conductivity (thickness direction), Btu/hr-ft-°R (estimated)
160	0.13
540	0.59
810	0.70

°R	Conductivity (in the plane of layup), Btu/hr-ft-°R (Reference 11)
160	6.5
760	29.0

Epon 934 Adhesive (Reference 12)

Density, 91.7 lb/ft^3

Specific Heat, 0.315 Btu/lb-°R

Thermal Conductivity, 0.266 Btu/hr-ft-°R

Aluminum (Reference 13)

Density, 173 lb/ft^3

°R	Specific Heat - Btu/lb-°R
500	0.20
1000	0.24

°R	Thermal Conductivity - Btu/hr-ft-°R
500	67
1000	106

2.2.4.5 Analysis Results.

Station 42

Predicted temperatures are plotted versus flight time in Figure 2.2.4-3. The maximum predicted temperature of the graphite/epoxy is 260° F, and the maximum Epon 934

predicted temperature is 400° F. The plot of the maximum Epon 934 temperature corresponds to the heat shield inner surface temperature. The graphite/epoxy starting temperature of 100° F corresponds to the Reference 8 data.

Graphite/epoxy temperatures predicted for a condition having no adhesive are shown in Figure 2.2.4-4. It can be seen that the maximum predicted graphite/epoxy temperature would increase to 400° F.

Station 32 Ring Area

Predicted temperatures are plotted versus flight time in Figure 2.2.4-5. The maximum predicted temperatures are 400° F on the 0.040-inch thick adhesive, 250° F on the graphite/epoxy, 144° F on the 0.015-inch adhesive, and 122° F on the aluminum ring. The graphite/epoxy starting temperature of 100° F corresponds to the Reference 8 data. The ring starting temperature was assumed to be 80° F.

Without the 0.040-inch layer of adhesive, the maximum predicted graphite/epoxy temperature would increase to 400° F (Figure 2.2.4-6), and the maximum ring temperature would increase to 149° F.

Substituting beryllium in place of the aluminum ring would reduce the maximum ring temperature by 10° F for the two cases considered in this analysis with and without adhesive.

It should be noted again that substituting graphite/epoxy for an aluminum midbay structure would cause somewhat higher temperatures to exist on the heat shield inner surface as well as on the graphite/epoxy structure.

2.2.5 MASS PROPERTIES. Table 2.2.5-1 compares the weight and balance of the conceptual design(s) of the midbay substructure with the reference all-aluminum design. The preliminary design utilizing T300/5208 weighs 14.54 pounds, a 3.47 pound reduction from the reference design. The longitudinal center of gravity is at Station 45.50.

Table 2.2.5-2 is a material matrix, showing the type and weight distribution of the various materials used in the preliminary design of the composite midbay substructure.

Table 2.2.5-1. Weight and Balance Comparison - Conceptual/Preliminary Design

	Aluminum Design		Composite HMS/934 Conceptual Design			Composite T-300/5208 Composite Preliminary Design		
	Weight(lb)	C. G.	Weight(lb)	C. G.	Δ vs(1)	Weight(lb)	C. G.	Δ vs(1)
Ring, Forward Threaded	.57	26.29	.64	26.32	+ .07	.73	26.35	+.16
Shell, Sta. 25.55 - 57.525	7.33	43.63	3.95	43.83	-3.38	4.46*	43.81	-2.87
Thrust Ring, Sta. 32.18	.72	32.10	.87	32.08	+ .15	.77	32.08	+.05
Payload Support Pads	1.64	37.55	1.19	36.80	- .45	1.43	36.23	-.21
Ring at Sta. 50.705	.43	50.71	.29	50.71	- .14	.31	50.82	-.12
Antenna Housing (2)	1.12	53.20	.49	52.31	- .63	.49	52.31	-.63
Ring at Sta. 55.932	1.70	56.10	1.87	56.05	+ .17	1.85	56.05	+.15
Ring, Aft, Threaded	2.05	57.98	2.05	57.98	0	2.05	57.98	0
Subtotal	15.56	45.96	11.35	46.32	-4.21	12.09	45.83	-3.00
Heat Shield Bond	2.45	43.80	2.45	43.80	0	2.45	43.80	0
Total Midbay	18.01	45.66	13.80	45.87	-4.21	14.54	45.50	-3.47

*Includes 1.16 lb. Foil Penalty

Table 2.2.5-2. Material Matrix, Composite Midbay Substructure - Preliminary Design

	G/E T-300/5208	Bond Material	Lexan	Aluminum	Total (lb)
Ring, Forward Threaded		.03		.70	.73
Shell, Sta. 25.55 - 57.525	4.33			.13	4.46
Thrust Ring, Sta. 32.18		.05		.72	.77
Payload Support Pads	1.08	.06	.29		1.43
Ring at Sta. 50.705	.28	.03			.31
Antenna Housings (2)		.03	.46		.49
Ring at Sta. 55.932		.07		1.78	1.85
Ring, Aft, Threaded				2.05	2.05
Subtotal	5.69	.27	.75	5.38	12.09
Heat Shield Bond		2.45			2.45
Total Midbay	5.69	2.72	.75	5.38	14.54

SECTION 3

SPECIMEN AND SUBCOMPONENT TESTING

3.1 INTRODUCTION

Section 3 describes test panel/subcomponent configurations and test methods used to acquire data in support of the conceptual design phase. The fiber/resin systems studied are identified and test results are tabulated.

3.2 SPECIMEN CONFIGURATIONS

A groundrule of the conceptual design study was that no testing would be performed on graphite/epoxy systems because of the extensive data already available. In the case of graphite/polyimide systems, Convair selected four tests to screen the candidate composite systems and obtain preliminary design data. These tests were longitudinal tension, longitudinal compression, in-plane shear, and interlaminar tension. Panel cure and post cure cycles were generally those recommended by the material suppliers, and a summary of those cycles are given in Appendix D.

Longitudinal tension tests were run on $[0]_8$ laminates. The specimens were straight-sided, 8.0 to 9.0 inches long, 0.5 inch wide, and had bonded doublers. Doublers were 2.5 inches long with 0.5-inch tapered section. Doubler material was fiberglass/epoxy for the RT and 350F specimens and perforated, annealed 6Al-4V titanium alloy for the 600F specimens. The RT test specimens were made using Hysol's EA9309 or EA934 adhesives for doubler bonding. American Cyanamid's HT-424 adhesive was used for doubler bonding on the 350F and 600F test specimens. The EA9309 and EA934 were cured for approximately 24 hours at RT followed by a one hour cure at 150F. The HT-424 was cured for one hour at 350F. The RT curing adhesives were bonded using contact pressure, and the HT-424 was cured using either vacuum bag pressure or vacuum bag plus 50 psig pressure. Strain gages were used to obtain load versus strain data, which in turn was used for modulus and Poisson's ratio calculations.

Longitudinal compression tests were run on $[0]_{24}$ laminates. The specimens were straight-sided, 5.5 inches long, 0.25 inch wide, and had bonded doublers. The total allowable thickness in the doubler area to allow conformance to the Celanese test fixture is 0.160 to 0.175 inches. The doublers were 2.5 inches long, leaving a 0.5 inch test section. Doublers for the RT and 350F specimens were made of quartz/polyimide, while these for the 600F specimens were made of perforated, annealed 6Al-4V titanium alloy. Adhesives and adhesive bonding cycles were

identical to those used in preparation of the tensile specimens. Strain gages were used to obtain load versus strain data, which in turn was used for modulus and Poisson's ratio calculations.

In-plane shear was determined by the testing of $[\pm 45]_{2S}$ laminates in tension. The specimens were 8.0 inches long by 1.0 inch wide, and had bonded doublers which were 2.5 inches long with a 0.5 inch tapered section. Doubler material and adhesives for doubler bonding were identical to that used for the longitudinal tension specimens. Strain gages were used to obtain load versus strain data. Shear strength and modulus values were calculated from the tension data.

Interlaminar tension specimens were prepared by machining 0.75 inch discs from $[\pm 45]_{2S}$ laminates. The discs were bonded between 0.75 inch threaded steel rods. Hysol's EA9309 was used for bonding the RT specimens, and HT-424 was used for the 350F and 650F specimens. Adhesive cure cycles were identical to those previously described for the longitudinal tension specimens. The pressure for the HT-424 bonds was 25 psig.

Resin contents and specific gravity measurements were made on each test panel. Fiber volume was calculated for each panel using the resin content and specific gravity measurements as well as theoretical or reported specific gravities for basic resins and fibers. Resin contents were obtained by the standard acid digestion method using a combination of sulfuric acid and hydrogen peroxide. Specific gravity was measured per ASTM D 792. Pieces of the crossplied panels were mounted, polished, and photographed to document microstructure.

3.3 SPECIMEN TESTING

All testing was conducted at a head travel rate of 0.05 in./min. The 350F and 600F specimens were heated as rapidly as possible and held for one minute at temperature prior to testing. An Instron test machine or equivalent was used for all testing. A Missimer's high temperature chamber was used for the heating of the specimens. The chamber was stabilized at the test temperature prior to the rapid insertion of the specimen into the test grips. It took about 3 to 4 minutes for the longitudinal tension, interlaminar tension, and in-plane shear specimens to get to 350F and about 5 to 6 minutes to get to 600F. Compression specimens use the very massive Celanese fixture, and these took about one minute longer to get to the respective temperatures. An automatic strain recording system, B&F Instruments Model 161 Minisystem, was used to measure and record the output from strain gages.

Table 3.3-1 summarizes the test program for the five graphite reinforced addition polyimides. The program was designed to measure panel-to-panel variation, and

Table 3.3-1. Test Program

Material / Properties	T-300/F-178	T-300/5230	HM-S/4397	HM-S/5230	GY-70/5230
Tension, σ, E, ν					
RT	6	6	3	6	6
350F	6	6	3	6	6
600F	6	6	3	6	6
Compression: σ, E, ν					
RT	6	6	3	6	6
350F	6	6	3	6	6
600F	6	6	3	6	6
In-Plane Shear: G, ν					
RT	6	6	3	6	6
350F	6	6	3	6	6
600F	6	6	3	6	6
Interlaminar Tens. Str.					
RT	6	6	3	6	6
350F	6	6	3	6	6
600F	6	6	3	6	6
Resin Content					
$[0]_8$	4	4	2	4	4
$[0]_{24}$	4	4	2	4	4
$[\pm 45]_{2s}$	4	4	2	4	4
Fiber Volume					
$[0]_8$	4	4	2	4	4
$[0]_{24}$	4	4	2	4	4
$[\pm 45]_{2s}$	4	4	2	4	4
Specific Gravity					
$[0]_8$	4	4	2	4	4
$[0]_{24}$	4	4	2	4	4
$[\pm 45]_{2s}$	4	4	2	4	4
Microsection	1	1	1	1	1

therefore, two separate laminates prepared and cured at different times were used for machining the mechanical property test specimens. Only one panel of HM-S/4397 was evaluated because of repeated problems with the cure and postcure of this system and because of the poor high temperature test results obtained with the material. Three specimens were machined from each panel for each test temperature. Results are summarized in Tables 3.3-2 to 3.3-4. Individual test results are given in Appendix E.

In general, the tensile test data reflects what might be expected out of current graphite reinforced epoxies, and the fact that the data was obtained on graphite reinforced polyimides is very encouraging. There was good translation of fiber modulus properties into composite modulus values for all the systems. The tensile strength data for T-300/F-178 is not as high as one would expect, and this could be a result of residual stresses resulting from the high temperature cure and postcure coupled with shrinkage stresses. The loss of strength for HM-S/4397 at 600F was expected, since the 4397 is an epoxy modified polyimide. The other systems performed well for the short duration 600F exposure. In compression, the poor high-temperature resistance of the 4397 was even more evident. In fact, at 600F the HM-S/4397 could not support any load. The compression and shear properties are typical of graphite/epoxy systems. Interlaminar tension strength of the T-300 systems was better than that obtained with the HM-S and GY-70 systems. This is true also with graphite/epoxy composites.

3.4 INTERLAMINAR TENSION AND SHORT BEAM SHEAR SCREENING TESTS

It was determined that interlaminar tension and short beam shear testing correlated well with the data obtained from the impulsive loading screening program (reference Sect. 2.2.2). A brief screening program was therefore conducted on high strength graphite reinforced resin matrix systems to determine parameters which influence interlaminar tension and short beam shear strengths. The parameters evaluated were fiber volume, cure temperature, fiber modulus, and form of reinforcement.

Crossplied laminates, $[0/\pm60]_{2s}$, were used for all testing. The cure cycles are included in those detailed in Appendix D. The short beam shear testing utilized standard 0.6 by 0.25-inch specimens. The span-to-depth ratio was kept constant at 4 to 1. Loading head and supports were 1/16-inch radius rods. A head travel rate of 0.05 in./min. was used. Three specimens from each laminate were tested. Interlaminar tension specimens were prepared by bonding 0.75-inch diameter discs of composite between two 0.75-inch diameter threaded steel rods. The adhesive used was Hysol's EA9309, and all bonding utilized a RT cure. The specimens were loaded in tension at a head travel rate of 0.05 in./min., and three specimens were tested from each laminate.

Table 3.3-2. Average Tension Properties of $[0]_8$ Graphite/Polyimide Composites

		T-300/F-178	T-300/5230	HM-S/4397	HM-S/5230	GY-70/5230
0° Tensile Strength, ksi						
	RT	172	214	175	141	114
	350F	178	207	201	169	116
	600F	159	181	131	170	126
0° Tensile Modulus, msi						
	RT	21.1	23.1	29.5	31.6	45.6
	350F	22.1	24.1	-	32.8	41.0
	600F	21.2	22.9	29.9	29.8	48.9
0° Tensile Strain, μ-in						
	RT		9,250	5,970	4,470	2,510
	350F	8,030	8,610	-	5,130	3,010
	600F	7,260	7,770	4,390	6,100	2,400
Poisson's Ratio						
	RT	0.32	0.30	0.27	0.26	0.36
Resin Content, %		29.32	26.44	27.56	32.33	25.69
Fiber Volume, %		64.10	67.72	64.83	60.10	65.85
Specific Gravity		1.597	1.608	1.605	1.593	1.703

Table 3.3-3. Average Compression Properties of $[0]_{24}$ Graphite/Polyimide Composites

		T-300/F-178	T-300/5230	HM-S/4397	HM-S/5230	GY-70/5230
0° Compression Strength, ksi						
	RT	142	163	106	88.6	75.5
	350F	151	155	96.0	93.1	73.2
	600F	74.7	90.9	-	57.1	65.8
0° Compression Modulus, msi						
	RT	19.0	21.1	28.0	25.7	46.6
	350F	20.3	24.3	31.9	26.6	45.2
	600F	18.4	22.9	-	22.3	41.3
0° Compression Strain, μ-in						
	RT	8,060	7,180	4,290	3,680	1,540
	350F	7,910	5,360	2,740	4,080	1,720
	600F	4,000	3,970	-	2,270	1,600
Poisson's Ratio						
	RT	0.38	0.29	0.42	0.44	0.46
Resin Content, %		29.80	25.05	30.44	30.59	22.91
Fiber Volume, %		63.58	69.26	61.60	62.02	69.17
Specific Gravity		1.595	1.609	1.587	1.618	1.709

Table 3.3-4. Average Properties of $[\pm 45]_{2S}$ Graphite/Polyimide Composites

	T-300/F-178	T-300/5230	HM-S/4397	HM-S/5230	GY-70/5230
0° Tensile Strength, ksi					
RT	19.8	18.6	11.9	11.8	11.0
350F	16.1	13.9	12.8	11.3	9.7
600F	7.9	6.7	3.8	10.4	8.6
0° Tensile Modulus, msi					
RT	2.8	2.8	2.4	2.3	2.9
350F	3.0	3.1	1.8	2.0	2.3
600F	1.4	1.3	0.6	1.3	1.5
Calculated Shear Strength, ksi					
RT	9.8	9.3	5.9	5.9	5.5
350F	8.1	6.9	3.4	5.7	4.9
600F	4.0	3.4	1.9	5.2	4.3
Calculated Shear Modulus, msi					
RT	0.81	0.78	0.66	0.63	0.76
350F	0.86	0.87	0.49	0.54	0.62
600F	0.39	0.34	0.15	0.33	0.38
Interlaminar Tension Strength, psi					
RT	2,544	2,015	1,371	1,196	1,302
350F	1,491	1,092	995	715	405
600F	689	498	403	539	396
Resin Content, %	32.41	27.18	31.62	37.10	27.69
Fiber Volume, %	60.78	66.82	60.28	54.98	63.47
Specific Gravity	1.575	1.593	1.581	1.583	1.721

The test results are summarized in Table 3.4-1. Included also are specific gravity, resin content and fiber volume determinations for each material. Reviewing the data on the T-300/5208, HM-S/934, GY-70/934, and T-300/F-178, it is readily apparent that the epoxy matrix is preferable to the polyimide and the T-300 performs better than the HM-S which in turn is better than the GY-70. The fiber modulus appears to be more important than the resin matrix. An attempt was made to lower the fiber volume in a second T-300/5208 panel, but there was no significant effect from the rather small change in fiber volume. Another 350F curing epoxy resin, Fiberite 934, was evaluated in conjunction with the T-300 since it is not considered quite as rigid a matrix. The T-300/934 showed some improvement over the T-300/5208. A lower modulus fiber, Type AS, was evaluated by preparing the testing specimens of A-S/3501-5 (a 350F system obtained as a prepreg from Hercules, Inc.) Extensive work on cure cycle optimization has been conducted at Convair for several years with this latter system. The interlaminar tension and short beam shear strengths were markedly better with the A-S/3501-5 than with any of the other systems previously evaluated.

A 250F curing epoxy resin, Fiberite 948A, was evaluated in conjunction with two graphite fibers, T-300 and HM-S. It had been theorized that lower curing temperature would result in lower residual stresses, and this in turn might lead to higher interlaminar tension and short beam shear strengths. The results, however, showed poorer short beam shear strength but higher interlaminar tension strength than that obtained with the T-300/5208.

Laminates were prepared with both 948A and 5208 matrices using woven T-300 fabric. Specimens tested from these laminates showed improvements in tension and shear strengths over the same system made from unidirectional T-300 tape.

It is recommended that future impulsive loading evaluations concentrate on lower modulus fibers (A-S and T-300), more ductile resins (934, etc.), and woven fabric reinforcements. Woven fabrics of hybrid fibers may also be beneficial for some programs, particularly if the warp fibers can be high modulus and the fill fibers low modulus.

3.5 SUBCOMPONENT TESTING

The following paragraphs document the results of the test plan described in Report 646-0-76TD-009 under Contract DAAG-46-76-C-0073. A copy of this test plan is provided in Appendix F. Unless otherwise specified, all testing was done at room temperature. The failures recorded include ultimate load, ultimate stress, and the failure mode. All dimensions are in inches. All bonding was done at room temperature.

Table 3.4-1. Screening Tests on Candidate Mark 12A Graphite/Resin Composites

	$[0/\pm60]_{2S}$ T-300/5208	$[0/\pm60]_{2S}$ T-300/5208	$[0/\pm60]_{2S}$ HM-S/934	$[0/\pm60]_{2S}$ GY-70/934	$[0/\pm60]_{2S}$ T-300/934	$[0/\pm60]_{2S}$ A-S/3501
Resin Content, % by Wt.	25.50	27.16	34.33	26.98	28.59	28.31
Fiber Volume, %	68.16	66.23	57.92	64.35	65.26	64.48
Short Beam Shear Strength, ksi	6.73	6.22	6.30	4.63	7.70	11.1
Interlaminar Tension Strength, ksi	2.23	2.01	1.95	1.79	2.81	3.21
Specific Gravity	1.581	1.601	1.604	1.717	1.606	1.611

	$[0/\pm60]_{2S}$ HM-S/948A	$[0/\pm60]_{2S}$ T-300 Fabric/948A	$[0/\pm60]_{2S}$ T-300/948A	$[0/\pm60]_{2S}$ T-300 Fabric/5208	$[0/\pm60]_{2S}$ T-300/F-178
Specific Gravity	1.545	1.518	1.554	1.563	1.576
Resin Content, Wt. %	34.81	34.04	30.32	32.81	37.56
Fiber Volume, %	55.53	57.07	61.18	59.96	55.19
Short Beam Shear Strength, ksi	5.31	7.46	5.73	8.07	3.79
Interlaminar Tension Strength, ksi	2.91	3.02	2.84	2.08	1.43

3.5.1 LAP SHEAR TEST RESULTS. The lap shear tests were run as specified in paragraph 4 of MK12A test plan (Appendix F). The results of this test are shown in Table 3.5-1. In all cases the bond was composite to aluminum. Figure 3.5-1 and 3.5-2 illustrate the interaction between shear stress and bondline thickness. It should be noted that some of the specimens using EA934 adhesive used a glass scrim. On these specimens the failure occurred at the scrim rather than at the bond. Single lap tests without scrim were tested in order to obtain an appropriate knockdown factor. This data is also presented on Figure 3.5-2.

3.5.2 SIMULATED RING TEST. The simulated ring tests were run as specified in paragraph 5 of the test plan (Appendix F). The results of this test were to be used to determine the strength of the Station 32.18 ring. An ultimate applied load of 2116 lbs/in associated with a lateral acceleration of 190 G's was determined for URNB threat at 18,000 ft. A radius of 4.22 inches was used. The simulated ring ultimate load was tested at 3,130 lb/in or a M.S. = +0.48. The results are tabulated in Figure 3.5-3. It should be noted that all of the room temperature tests produced failures in the honeycomb elastic foundation. The elevated temperature conditions produce much lower loads as seen in Figure 3.5-3.

3.5.3 GORE CONCENTRATION TEST RESULTS. The gore concentration test was run as specified in the test plan (Ref. Appendix F). Due to length and width of the material supplied, it is often necessary to splice the layers in the composite section. The gore concentration tests were used to determine if an 0.08 gap in discontinuity or an 0.20 overlap of the plies would be more beneficial. Figure 3.5-4 shows the results of this test. The analysis used the 1.71 stress concentration factor.

3.5.4 LONGITUDINAL PLY TERMINATION STRESS CONCENTRATION. It may be necessary, due to load variance, to alter the layup within the shell. The purpose of the longitudinal ply termination stress concentration test is to reveal the impact of discontinuous layup in the shell. The longitudinal ply termination stress concentration test was run as specified in the test plan (Appendix F). The results of this test are displayed in Figure 3.5-5. The current configuration does not have this design feature; however, the effect is seen to be small.

3.5.5 FLEXURE AT DOUBLER TESTS. The midbody has discontinuous, cocured doublers in the vicinity of Station 40. There are significant flexure movements which are transmitted across these doublers. A series of flexure tests have been run to evaluate stress concentration and peel effects at doubler termination. The results are documented in Figure 3.5-6. The strength reduction is seen to be less than that due to gores. Since this concentration was judged to be independent of the gore concentration factor, it was not used.

Table 3.5-1. Lap Shear Test Results
Composite to Aluminum

TEST	OVERLAP	BOND	T300/5208 ULT LOAD LBS	T300/5208 ULT STRESS KSI	T300/5208 FAILURE MODE	T300/5230 ULT LOAD LBS	T300/5230 ULT STRESS KSI	T300/5230 FAILURE MODE
SINGLE LAP SHEAR	0.5	0.005						
		934	1787.	3.6	INTERFACE	1475	3.0	GLASS DELAM.
		9309	2519.	5.0		2017	4.0	
SINGLE LAP SHEAR	1.0	.005						
		934	2063.	2.1	INTERFACE	1775	1.8	GLASS DELAM.
		9309	4315	4.3		2557	2.6	
DOUBLE LAP SHEAR	0.5	.005						
		934	3532	3.5	INTERFACE	4300	4.3	INTERFACE
		9309	-	-	-	4317	4.3	INTERFACE
DOUBLE LAP SHEAR	0.5	.010						
		934	-	-	-	3420	3.4	INTERFACE
		9309	-	-	-	4210	4.2	INTERFACE
DOUBLE LAP SHEAR	0.5	.015						
		934	-	-	-	2413	2.4	INTERFACE
		9309	-	-	-	3658	3.7	INTERFACE
DOUBLE LAP SHEAR	0.5	.020						
		934	-	-	-	2050.	2.1	INTERFACE
		9309	-	-	-	3982	4.0	INTERFACE
DOUBLE LAP SHEAR	0.5	.025						
		934	-	-	-	1652	1.7	
		9309	-	-	-	4075	4.1	
DOUBLE LAP SHEAR	0.5	.030						
		934	2302	2.3	INTERFACE	2111	2.1	INTERFACE
		9309	-	-	-	2998	3.0	INTERFACE

Table 3.5-1. Lap Shear Test Results
Composite to Aluminum (Contd)

TEST	OVERLAP	BOND	T300/5208 ULT LOAD LBS	T300/5208 ULT STRESS KSI	T300/5208 FAILURE MODE	T300/5230 ULT LOAD LBS	T300/5230 ULT STRESS KSI	T300/5230 FAILURE MODE
DOUBLE LAP SHEAR	1.0	0.005	-	-	-	4366	2.2	
SINGLE SCARF	2.8	0.005						
		934	7143	2.6	DELAM.	6118	2.2	DELAM.
		9309	8502	3.1	DELAM.	7470	2.7	DELAM.

EA9309 Adhesive T300/5208 to Aluminum

Δ-0.50 Inch overlap double shear specimens

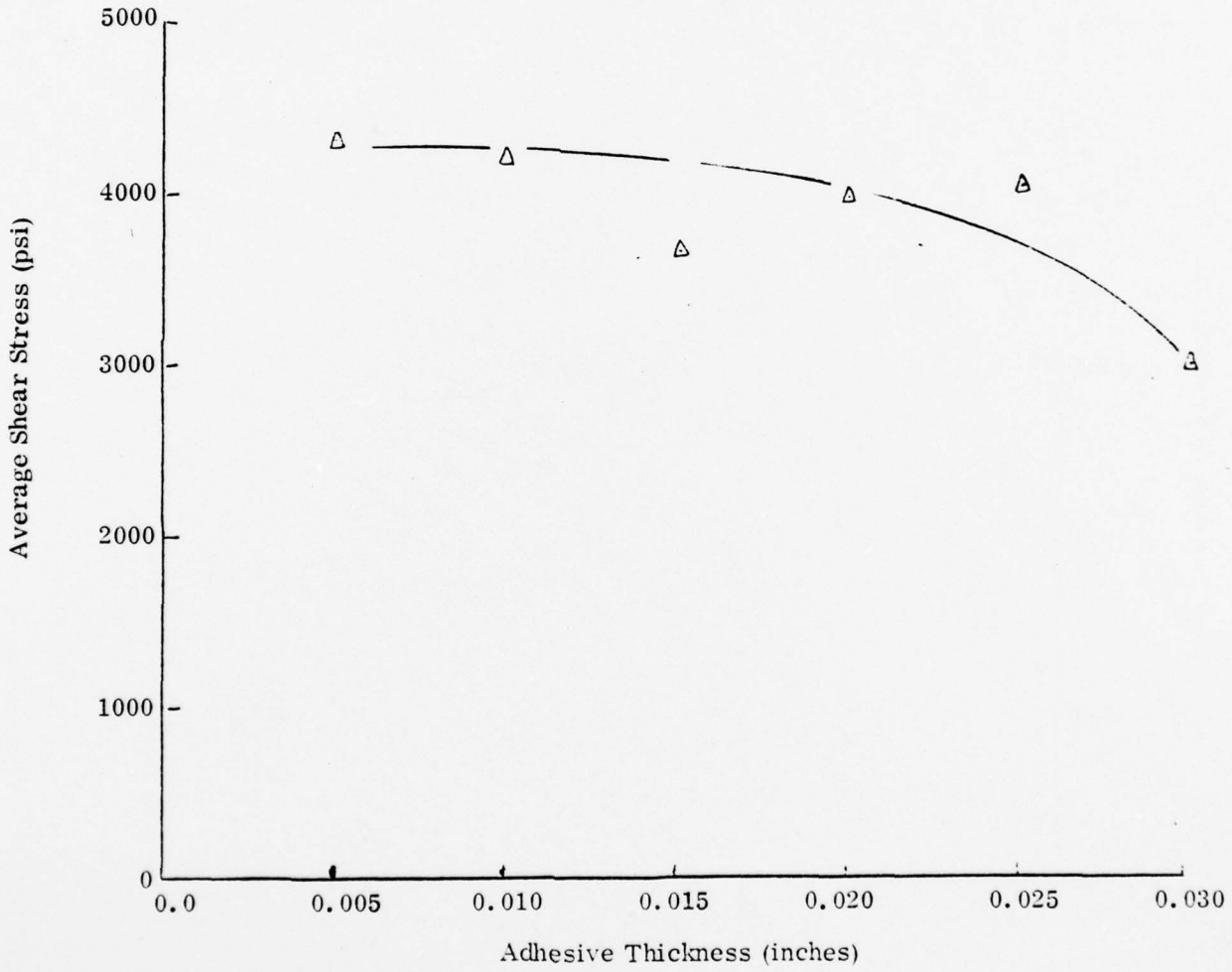

Figure 3.5-1. Shear Strength Vs. Bond Thickness

SHEAR STRENGTH VS. BOND THICKNESS

EA-934 Adhesive T300/5230 to Aluminum

——— △ — 0.50 inch overlap double shear specimens with glass scrim cocured with G/PI

– – – – * – 0.50 inch overlap single shear specimens without scrim

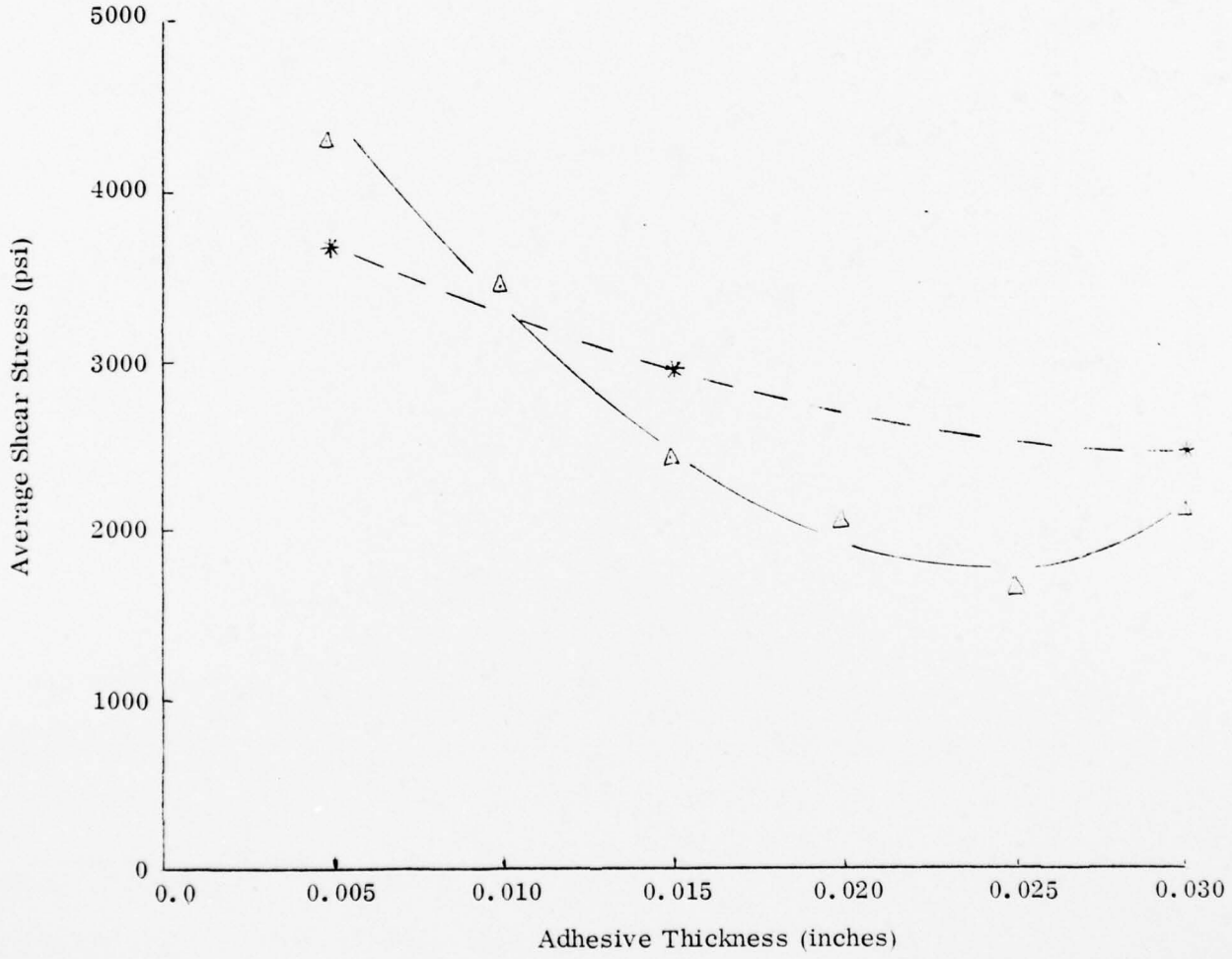

Figure 3.5-2. Shear Strength Vs. Bond Thickness

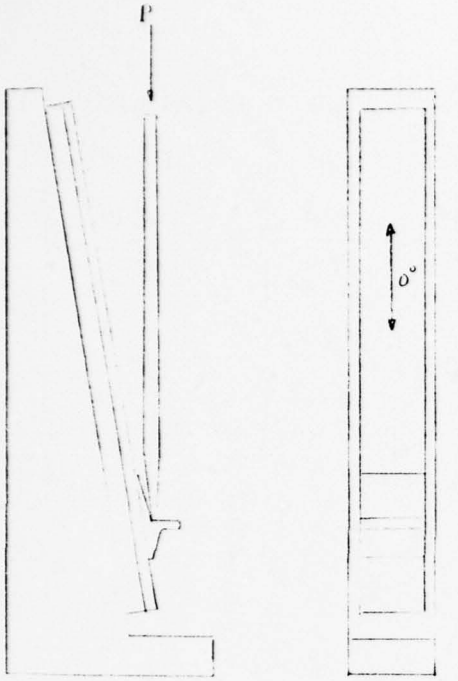

TEST	T300/5208		T300/5230		ULT APPLIED LOAD (LB/IN)
	ULT LOAD (LBS)	N_x (ULT) (LB/IN)	ULT LOAD (LBS)	N_x (ULT) (LB/IN)	
RT	6250	3130	6570	3290	2116
130° F	2940	1470	-	-	-
195° F	-	-	3357*	1680	-

MOST FAILURES AT HONEYCOMB
*FAILED AT BOND

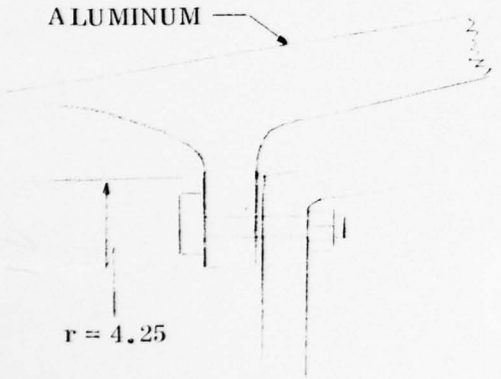

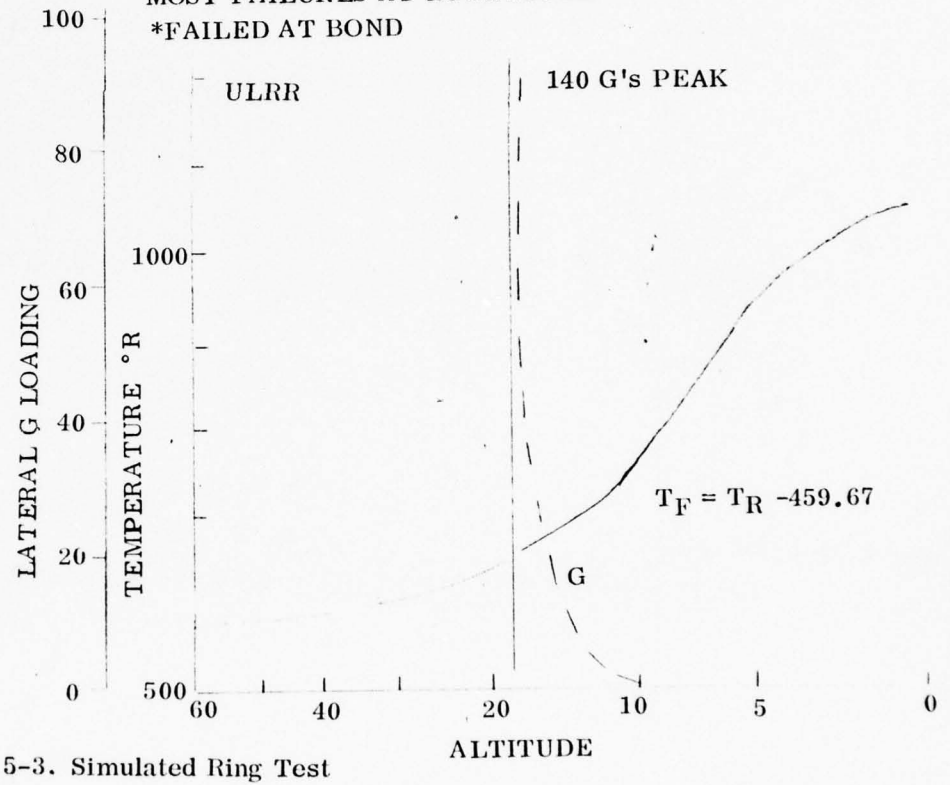

Figure 3.5-3. Simulated Ring Test

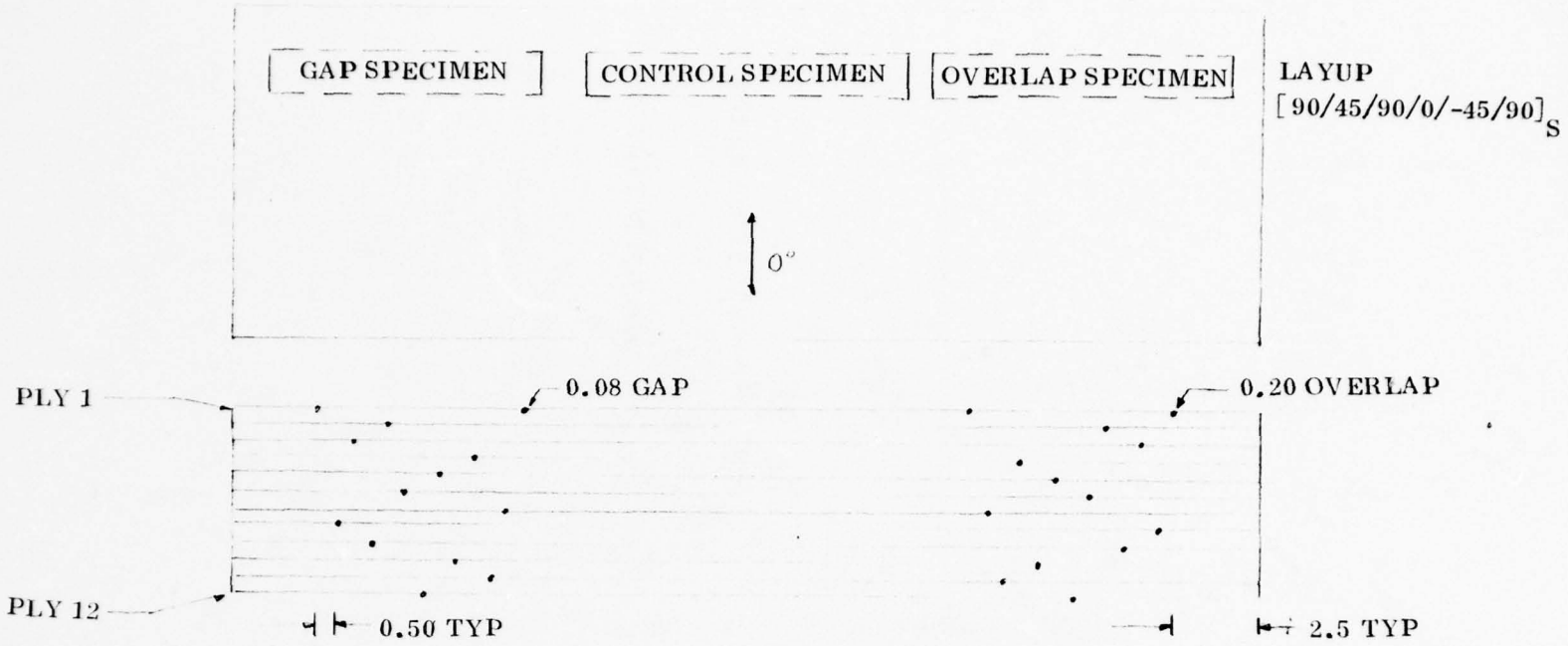

TEST	T300/5208						T300/5230					
	TENSION			COMPRESSION			TENSION			COMPRESSION		
	ULT LOAD (LBS)	ULT STRESS (KSI)	K_T	ULT LOAD (LBS)	ULT STRESS (KSI)	K_T	ULT LOAD (LBS)	ULT STRESS (KSI)	K_T	ULT LOAD (LBS)	ULT STRESS (KSI)	K_T
CONTROL	7584	124.5	-	4373	129.7	-	6889	102.1	-	4050	109.2	-
0.08 GAP	3939	53.4	1.96	3854	114.3	1.13	3515	53.1	1.92	3490	94.1	1.16
0.20OVERLAP	4575	73.0	1.71	3577	106.1	1.22	3556	52.0	1.96	3141	84.7	1.29

Figure 3.5-4. Gore Concentration Test Results

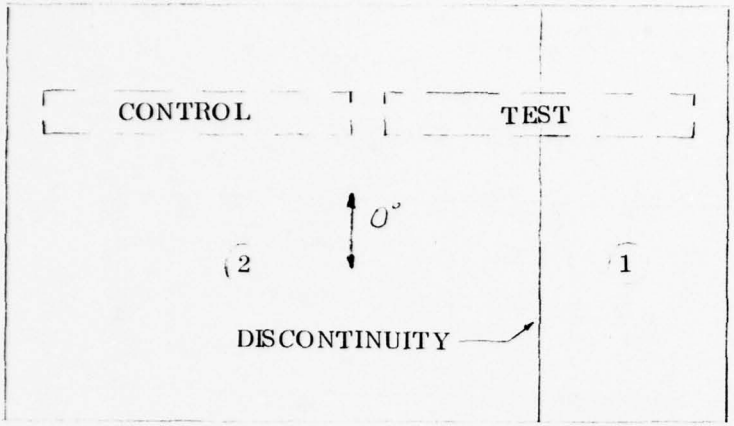

① $[0/45/0/-45/90/0/45/0/-45/90]_S$

② $[0/45/-45/90/0/45/90/-45/90]_S$

TEST	T300/5208				T300/5230			
	TENSION		COMPRESSION		TENSION		COMPRESSION	
	ULT LOAD (LBS)	ULT STRESS (KSI)	ULT LOAD (LBS)	ULT STRESS (KSI)	ULT LOAD (LBS)	ULT STRESS (KSI)	ULT LOAD (LBS)	ULT STRESS (KSI)
CONTROL	6060	63.5	2090	90.0	5491	53.3	1748	64.5
DISCONTINUITY	6116	62.6	1611	65.6	5700	52.1	1308	47.0

Figure 3.5-5. Longitudinal Ply Termination Stress Concentration Test

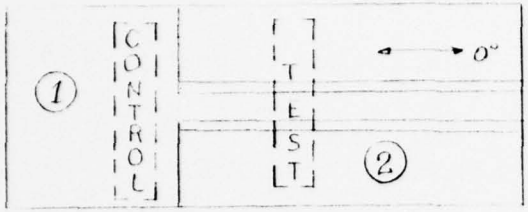

1 $[0/90/45/90/-45/0]_S$

2 $[0/90/45/90/-45/0]_{S2}$

TEST	T300/5208		T300/F-178*	
	ULT LOAD (LBS)	ULT STRESS (KSI)	ULT LOAD (LBS)	ULT STRESS (KSI)
Control	360	142	224	85
Step in Tension	328	129	187	72
Step in Compression	344	135	162	63

* ALL SPECIMENS DELAMINATED

Figure 3.5-6. Flexure at Doubler Termination Test

3.6 NUCLEAR VULNERABILITY AND HARDNESS TEST SPECIMENS

At completion of the MK12A composite midbay conceptual design study, the program effort was expanded and directed towards the design and fabrication of flat specimens and subcomponent elements, listed in Table 3.6-1 as as groups A, B, and C, for nuclear vulnerability and hardness (NV&H) screening tests by the Air Force Weapons Laboratory (AFWL). Results of the impulsive loading tests on group A laminates are described in reference 15. Results of tests on group B and C specimens were unknown during preparation of this report, but will be available in a forthcoming report from Ktech Corporation (Reference 16).

3.6.1 MATERIAL SYSTEMS. The group A material systems listed in Table 3.6-1 were selected by General Dynamics Convair (GD/C) in conjunction with AMMRC/AFML based on fiber/resin system analysis described in paragraph 2.2.2 and NV and H design considerations provided by Effects Technology, Inc. Laminates from material system AS/3501 were included, though not identified in the group A listing. The AS/3501 specimens were provided from a GD/C IRAD program.

The material systems selected for group B and C specimens were T-300/5208 and AS/3501 as a result of the screening tests (Reference 15) performed by the AFWL. Table 3.6-1 identifies each specimen in group A, B and C by part number (Reference Figure 3.6-1).

3.6.2 SPECIMEN AND SUBCOMPONENT DESIGN. Initially all specimens/subcomponent elements were to be layed up with plies and orientations under consideration in the MK12A composite substructure study. However, only the initial set of test specimens (group A) were fabricated to a ply and orientation representative of the proposed MK12A composite substructure configuration. By program redirection the remainder of the specimens, group B and C, were fabricated with ply(s) and orientation(s) as proposed in the Advanced Ballistic Reentry Vehicle (ABRV) composite structure study under contract with AVCO Systems Division. Plies and orientations are identified in Table 3.6-1.

The six 9" diameter × 9" long cylinder assembly configurations in group B represent a matrix of configurations for subcomponent element(s) of the ABRV substructure, with differences in material systems (i.e., T-300/5208 and AS/3501) and ply/orientation layup for the cylinder shell. From the standpoint of NV and H, the potentially critical bonded areas of the ABRV composite shell substructure/joints were identified as payload ring, equipment support ring, kick ring, breech lock ring(s) and antenna mounting pad. The design of the cylinder assemblies incorporates each of the areas identified above. Actual details of the subcomponent elements are shown in Figure 3.6-2 (Breach lock ring(s), part numbers 72C0772-113 and -115 are not shown).

Table 3.6-1. Summary of Test Specimens

TABLE A

	MATERIAL	COMPOSITE MATERIAL PLY AND ORIENTATION
72C0772-1 PANEL	T300/5208	
72C0772-3	T300/934	
72C0772-5	HMS/934	
72C0772-7	T300/F178	
72C0772-9	T300/5230	
72C0772-11 PANEL	HMS/5230	
72C0772-13 PANEL ASSY	T300/5208	.060 THICK $(0^\circ \pm 60^\circ)_{2S}$
72C0772-15	T300/934	
72C0772-17	HMS/934	
72C0772-19	T300/F178	
72C0772-21	T300/5230	
72C0772-23 PANEL ASSY	HMS/5230	
72C0772-25 PANEL	T300/5208	
72C0772-27	T300/934	
72C0772-29	HMS/934	
72C0772-31	T300/F178	.120 THICK $(0^\circ \pm 60^\circ)_{4S}$
72C0772-33	T300/5230	
72C0772-35 PANEL	HMS/5230	

TABLE B	AL ALY	LEXAN 40% GLASS	T300/ 5208 G/E	AS/3501 G/E	
72C0772-37 RING			X		$[0/45/90/135/0/90/\bar{0}]_S$
72C0772-39 RING				X	"
72C0772-101 CYLINDER ASSY	X		X		$[0/45/90/135/0/90/0_2/45/135/0_2/90/0/135/90/45/0]_T$
72C0772-103	X			X	"
72C0772-105	X		X		
72C0772-107	X	X		X	$[0/45/90/135/0/90/\bar{0}]_S$
72C0772-109		X	X		
72C0772-111 CYLINDER ASSY		X		X	

TABLE C	AL ALY	LEXAN 40% GLASS	T300/ 5208 G/E	AS/3501 G/E	
72C0772-127 PANEL			X		
72C0772-129 PANEL				X	
72C0772-141 TEST ASSY	X		X		
72C0772-143	X			X	
72C0772-145		X	X		
72C0772-147		X		X	
72C0772-149		X	X		$[0/45/90/135/0/90/\bar{0}]_S$
72C0772-151 TEST ASSY		X		X	
72C0772-153 DISC			X		
72C0772-155 DISC				X	
72C0772-37 RING			X		
72C0772-39 RING				X	

AD-A076 485 GENERAL DYNAMICS SAN DIEGO CA CONVAIR DIV F/G 22/2
COMPOSITE MATERIAL APPLICATION TO THE MK12A RV MIDBAY SUBSTRUCT--ETC(U)
SEP 79 W GARCIA , J HERTZ , J PRUNTY DAAG46-76-C-0073
UNCLASSIFIED CASD/ASC-76-001A AMMRC-TR-79-51 NL

2 OF 2
AD
A076485

END
DATE
FILMED
12-79
DDC

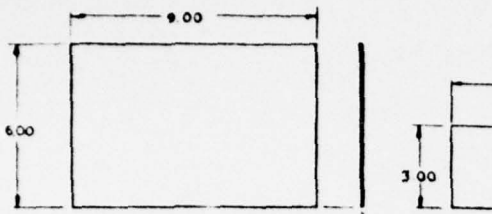

-1, -5 THRU -11 PANEL
FIG 1 ⚠4

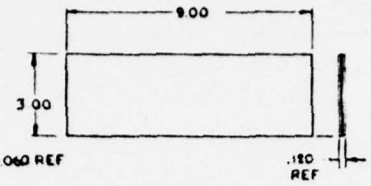

-13 THRU -23 BONDED ASSY ⚠1 ⚠4
FIG 2 ⚠4

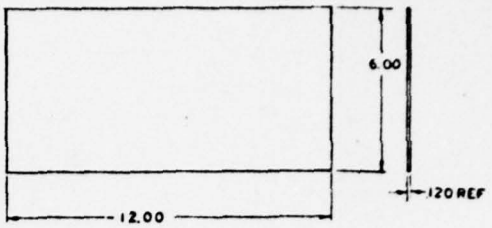

-25 THRU -35 ⚠4
FIG 3

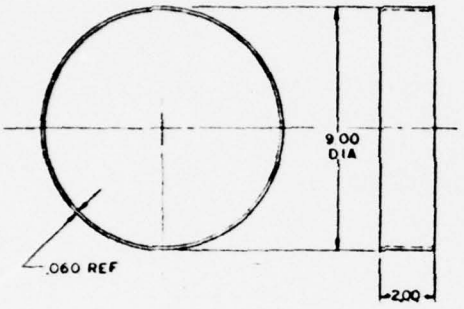

-37, -39
FIG 4

-153 DISC
-155
SCALE 1/1

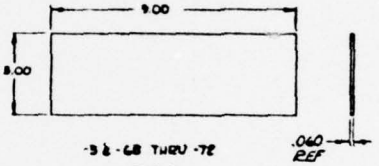

-3 & -68 THRU -72
FIG 9

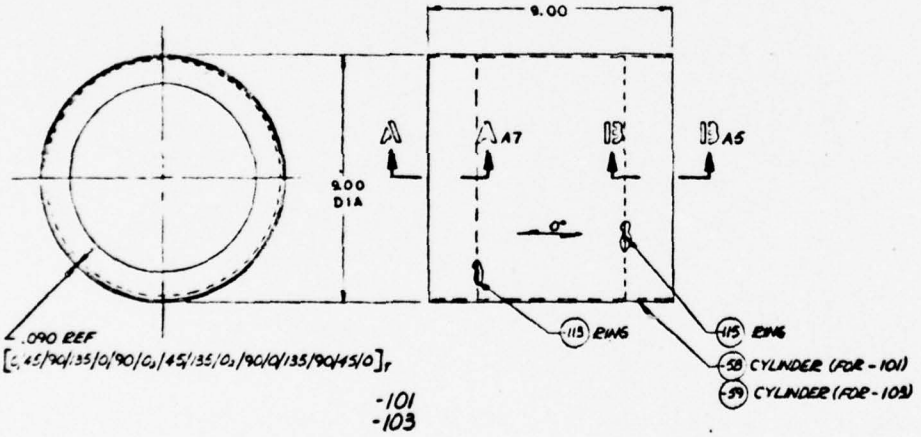

-101
-103

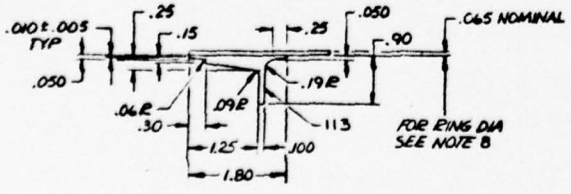

SECT A-A C17

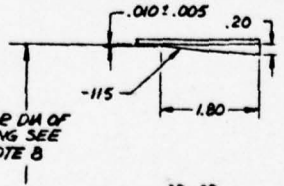

SECT B-B C6
SCALE 1/1

FOR NOTES SEE SH 3 NB

THIS PAGE IS BEST QUALITY PRACTICABLE FROM COPY FURNISHED TO DDC

QTY	ITEM OR FIND NO	CODE IDENT NO	PART OR IDENTIFYING NUMBER	NOMENCLATURE OR DESCRIPTION	ZONE	NO.		NOTE TEXT (STOCK SIZE, MATERIAL, SPECIFICATION, TYPE, HEAT TREAT, ETC.)	
18			-155	DISC	E	6	M	AS/3501 G/E	
18			-153	DISC	E	6	M	T300/5208 G/E	
3			-151	TEST ASSY	B	37			
3			-149	TEST ASSY	B	37			
3			-147	TEST ASSY	B	35			
3			-145	TEST ASSY	B	35			
3			-143	TEST ASSY	B	32			
3			-141	TEST ASSY	B	32			
			-139	PAD	E	38	M	.70x4.0x4.0, POLYCARBONATE (LEXAN) WITH 40% GLASS	
			-137	SEGMENT	C	3	M	.50x8.9x8.9, POLYCARBONATE (LEXAN) WITH 40% GLASS	
			-135	SEGMENT	C	32	M	.50x8.9x8.9, AL ALY, OPTIONAL	
			-133	PANEL	C	36	M	AS/3501 G/E	
			-131	PANEL	C	36	M	T300/5208 G/E	
3			-129	PANEL	F	32	M	AS/3501 G/E	
3			-127	PANEL	F	32	M	T300/5208 G/E	
9			-125	PANEL	S	3	M	AS/3501 G/E	
9			-123	PANEL	S	3	M	T300/5208 G/E	
			-64	RING			M	AS/3501 G/E	
AR			EA934	ADHESIVE					
			-72	PANEL				M/F -11	FIG 9
			-71					M/F -9	
			-70					M/F -7	
			-69					M/F -5	
2			-68	PANEL				M/F -1	FIG 9
			-61	CYLINDER			M	AS/3501 G/E	
			-60	CYLINDER			M	T300/5208 G/E	
			-59	CYLINDER	E	6	M	AS/3501 G/E	
			-58	CYLINDER	E	6	M	T300/5208 G/E	
			-57	RING			M	T300/5208 G/E	
			-121	MOUNT			M	[illegible] POLYCARBONATE (LEXAN) WITH 40% GLASS	
			-119	RING			M	[illegible] POLYCARBONATE (LEXAN) WITH 40% GLASS	
			-117	RING			M	.50x8.9x8.9, AL ALY OPTIONAL	
			-115	RING	E	6	M	.50x8.9x8.9, AL ALY OPTIONAL	
			-113	RING	E	6	M	.50x8.9x8.9, AL ALY OPTIONAL	
1			-111	CYLINDER ASSY	F	27			
1			-109	CYLINDER ASSY	A	27			
1			-107	CYLINDER ASSY	F	27			
1			-105	CYLINDER ASSY	F	27			
1			-103	CYLINDER ASSY	E	7			
1			-101	CYLINDER ASSY	E	7			
6			-39	RING				AS/3501 GR/E	FIG 4
6			-37	RING				T300/5208 GR/E	FIG 4
1			-35	PANEL				.75x6.0x12.0 HMS/5230	FIG 3
1			-33					T300/5230	
1			-31					T300/F178	
1			-29					HMS/934	
1			-27					T300/934	
1			-25	PANEL				1.20x6.0x12.0 T300/5208	FIG 3
1			-23	PANEL ASSY				(HMS/5230)	FIG 2
1			-21					T300/5230	
1			-19					T300/F178	
1			-17					HMS/934	
1			-15					T300/934	
1			-13	PANEL ASSY				(T300/5208)	FIG 2
1			-11	PANEL				.060x6.0x9.0 HMS/5230	FIG 1
1			-9	PANEL				.060x6.0x9.0 T300/5230	FIG 1
1			-7	PANEL				.060x6.0x9.0 T300/F178	FIG 1
1			-5	PANEL				.060x6.0x9.0 HMS/934	FIG 1
2			-3	PANEL				.060x3.0x9.0 GR T300/934	FIG 2
1			-1	PANEL				.060x6.0x9.0 GR T300/5208	FIG 1

NOTE SYMBOL: D - DOC NO; E - END ITEM; G - GENL NOTE; L - LIMIT; M - MATERIAL; N - NOMEN; R - REF DES; T - TYPE DES; U - USAGE DATA; V - VENDOR ITEM

PARTS LIST

UNLESS OTHERWISE SPECIFIED

SEE 0-70914 FOR ABBREVIATION CODE AND SYMBOL REQUIREMENTS

SEE 0-70902 FOR STANDARD MANUFACTURING AND INSTALLATION REQUIREMENTS

ASSOCIATED LIST REQUIRED SEE DOCUMENT SAME NUMBER PREFIXED

UNLESS OTHERWISE SPECIFIED DIMENSIONS ARE IN INCHES

TOLERANCES .X ±.1 .XX ±.03 .XXX ±.010 ANGULAR PER 0-70902

CONVAIR DIVISION OF GENERAL DYNAMICS SAN DIEGO CALIFORNIA

TEST SPECIMENS, MK12A MIDBAY ADVANCE COMPOSITE STRUCTURES (

E 14170 72C0772

FIG 3.6-1 A

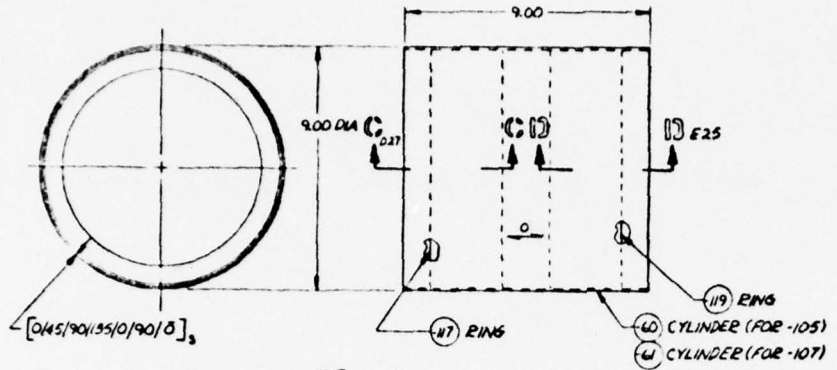

-105
-107

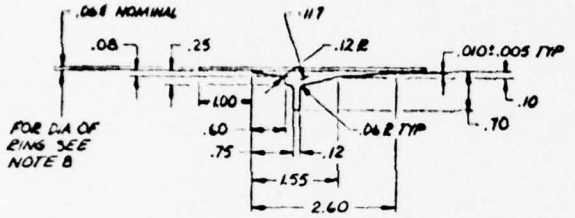

SECT C-C G26
SCALE 1/1

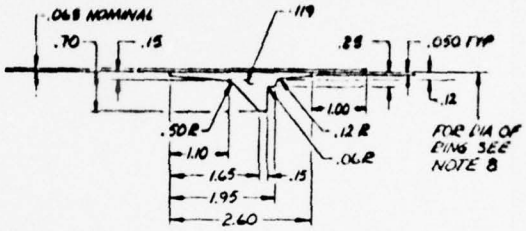

SECT D-D G26
SCALE 1/1

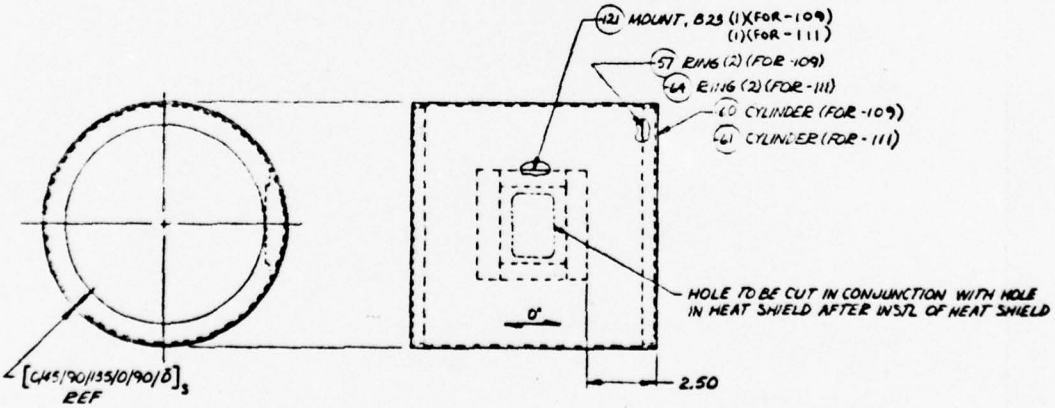

-109
-111

REVISIONS

ZONE	REV	DESCRIPTION	DATE	APPROVED

MODULE	PLY	ORIENTATION
1	1	0°
	2	45°
2	3	90°
	4	135°
3	5	135°
	6	90°
4	7	45°
	8	0°

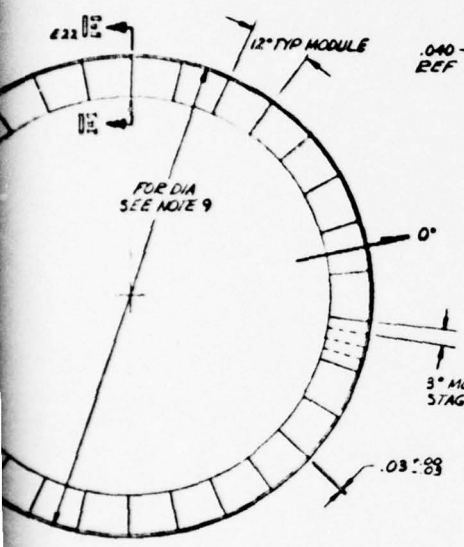

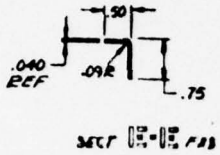

SECT E-E B23

-57 1-64 C126
SCALE 1/1

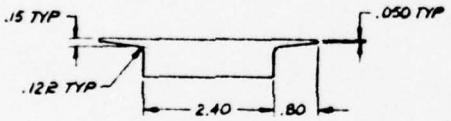

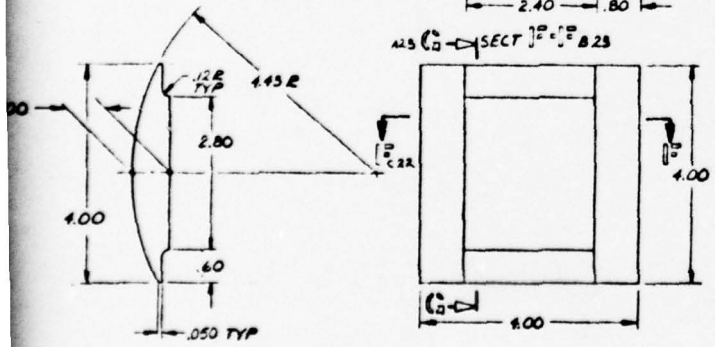

SECT C-C B22

-121
SCALE 1/1

UNLESS OTHERWISE SPECIFIED			
ALL UNMARKED SURFACES	√		
SHEET BASIC CODE ASSIGN			

SEE D- 70010 FOR ABBREVIATION CODE AND SYMBOL REQUIREMENTS

SEE D- 70003 FOR STANDARD MANUFACTURING AND INSTALLATION REQUIREMENTS

ASSOCIATED LIST REQUIRED SEE DOCUMENT SAME NUMBER PREFIXED
PL ☐ FOR PARTS LIST
UA ☐ FOR USAGE LIST

UNLESS OTHERWISE SPECIFIED DIMENSIONS ARE IN INCHES
TOLERANCES
X ± .1 XX ± .03 XXX ± .010
ANGULAR PER D- 70002

ENGR	
STRESS	
QE (QAE)	
DESIGN	
DRAWN	C. KAISER
CONTRACT NO.	

CONVAIR DIVISION OF GENERAL DYNAMICS
SAN DIEGO, CALIFORNIA

TEST SPECIMENS, MK12A
MIDBAY, ADVANCE COMPOSITE
STRUCTURES

SIZE	CODE IDENT	DRAWING NO.
E	14170	72C0772

SCALE — WEIGHT

23 | SEC CLASS | DOC | SEC CONT | GROUP | SUB GROUP

FIG 3.5-1 B

NOTES:

1. IDENTIFY SPECIMENS BY BAG & TAG PER MIL-STD-130. SPECIMENS TO BE SERIES IDENTIFIED (-X,-001 THRU -006). TRACEABILITY REQUIRED TO MATERIAL BATCH AND ROLL NUMBER WITHIN THE BATCH.
2. PERFORM ULTRASONIC INSPECTION PER THE APPLICABLE REQUIREMENTS OF MIL-I-8950 USING THROUGH TRANSMISSION. RECORD TEST RESULTS. CALIBRATE USING TEST STANDARD A NDT-5 AS/3501 OR EQUIVALENT.
3. BOND WITH EA 934.
4. PLY ORIENTATION .060 THK (0°±60°)23, 120 THK (0°±60°)43
5. ITEMS 1 THRU 35 TO BE GOVERNMENT TESTED PRIOR TO MFG OF OTHER ITEMS. MATERIAL WILL BE SELECTED AFTER TEST.
6. GD/CONVAIR TO RETAIN TEST SAMPLES OF EACH SPECIMEN DELIVERED PER CONTRACT.
7. ITEMS -13 THRU -23 ASSYS ARE MADE BY UTILIZING TWO, 3 BY 9 INCH SIZE PANELS OF THE SPECIFIED MATERIAL SYS & BONDING TOGETHER INTO A SANDWICH WITH EA 934 ADHESIVE.
8. DIA OF -57, -64, -113, -115, -117 & -119 RINGS TO BE DETERMINED AFTER FINAL DIM. CHECK OF CYL ID. OD OF RINGS TO BE .040 IN DIA SMALLER THAN ID OF CYL.

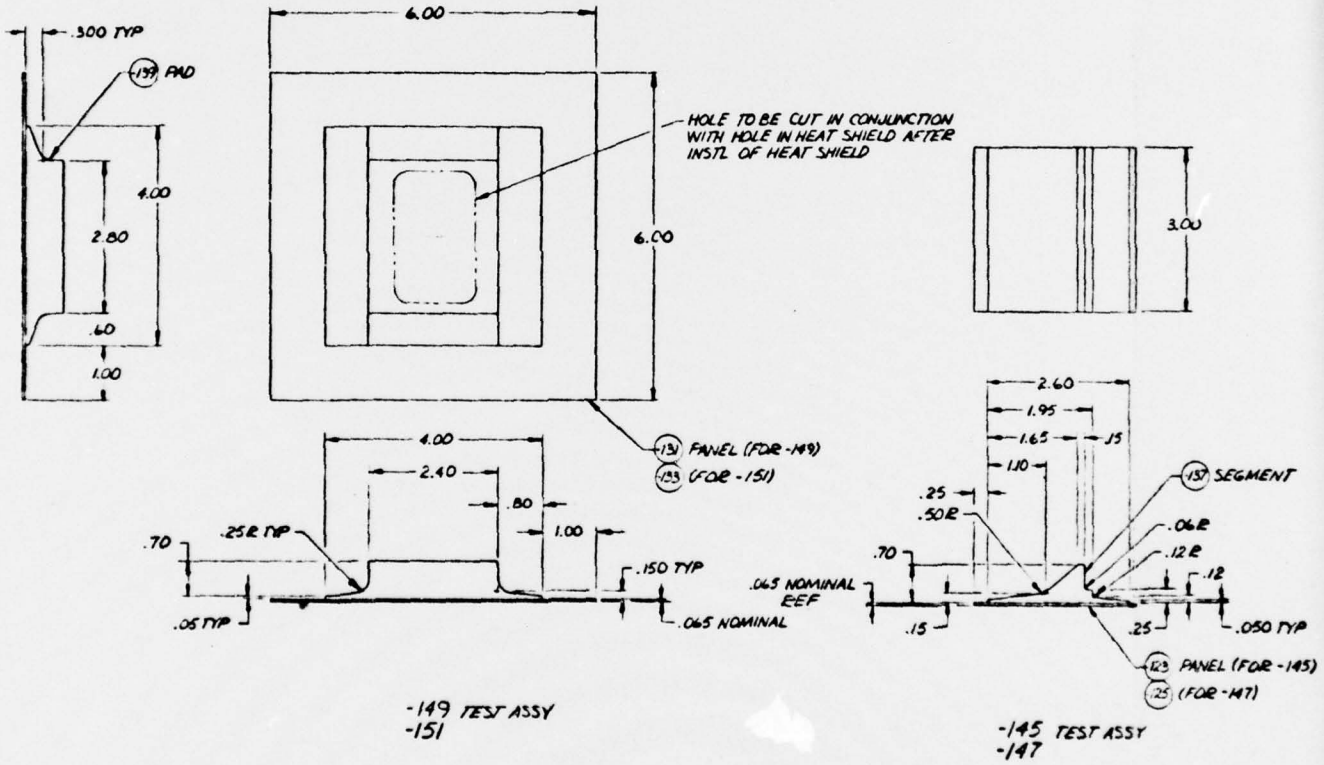

-149 TEST ASSY
-151

-145 TEST ASSY
-147

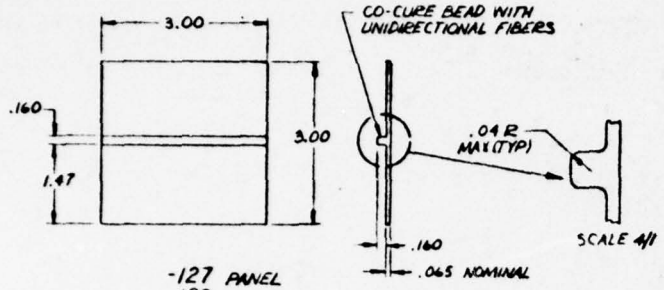

-127 PANEL
-129

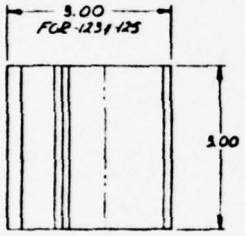

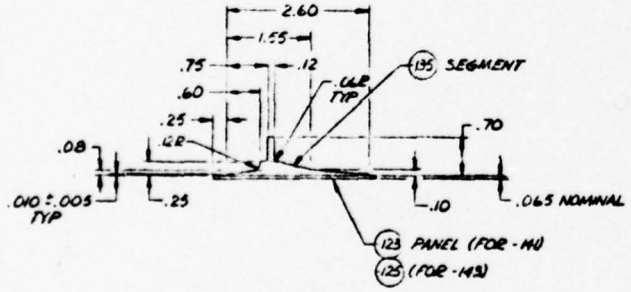

-141 TEST ASSY
-143

CONVAIR DIVISION OF GENERAL DYNAMICS SAN DIEGO, CALIFORNIA	
TEST SPECIMENS, MK 12A M.DBAY, ADVANCE COMPOSITE STRUCTURES	
SIZE E	CODE IDENT 14170
DRAWING NO 72C0772	

FIG 3.6-1 C

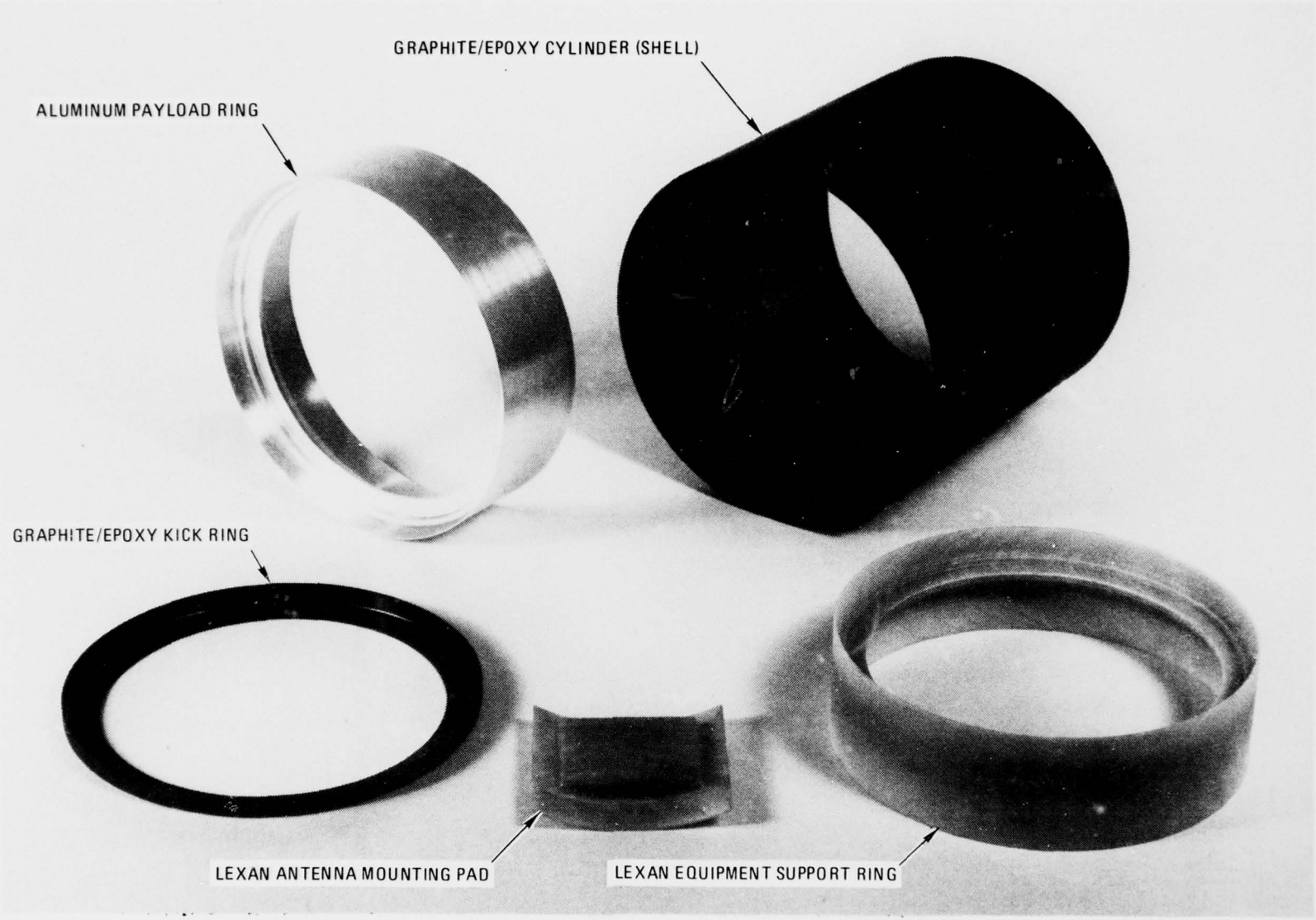

Figure 3.6-2. Typical Cylinder Assembly Details

Figure 3.6-3. Typical Cylinder Assembly with Heat Shield Applied

Bonding of the rings to the cylinders with EA934 adhesive was successfully accomplished by using the female mold in which the cylinder was cured and a holding fixture designed to position the ring in the mold. Before placing the holding fixture with ring into the mold, excessive adhesive was applied to the ring bond line surface. In placing the cylinder into the mold, to the required position relative to the ring, the excessive adhesive flows out of the bond line area through a .020" annular gap (bond line thickness), leaving essentially a void free bond.

Heatshield material was applied by AVCO Systems Division to all test specimens in group B and C. Figure 3.6-3 shows a typical cylinder with heatshield material applied.

3.6.3 ULTRASONIC TESTS. Each of the test specimens in group A, B, and C were ultrasonic tested. All specimens indicated a relative low number of voids. In particular, the cylinder/bond line, as indicated in Figure 3.6-4, showed excellent bonding. The illustrated photograph of a "C" scan chart for cylinder assembly 72C0772-105 is the worst case of the six cylinders.

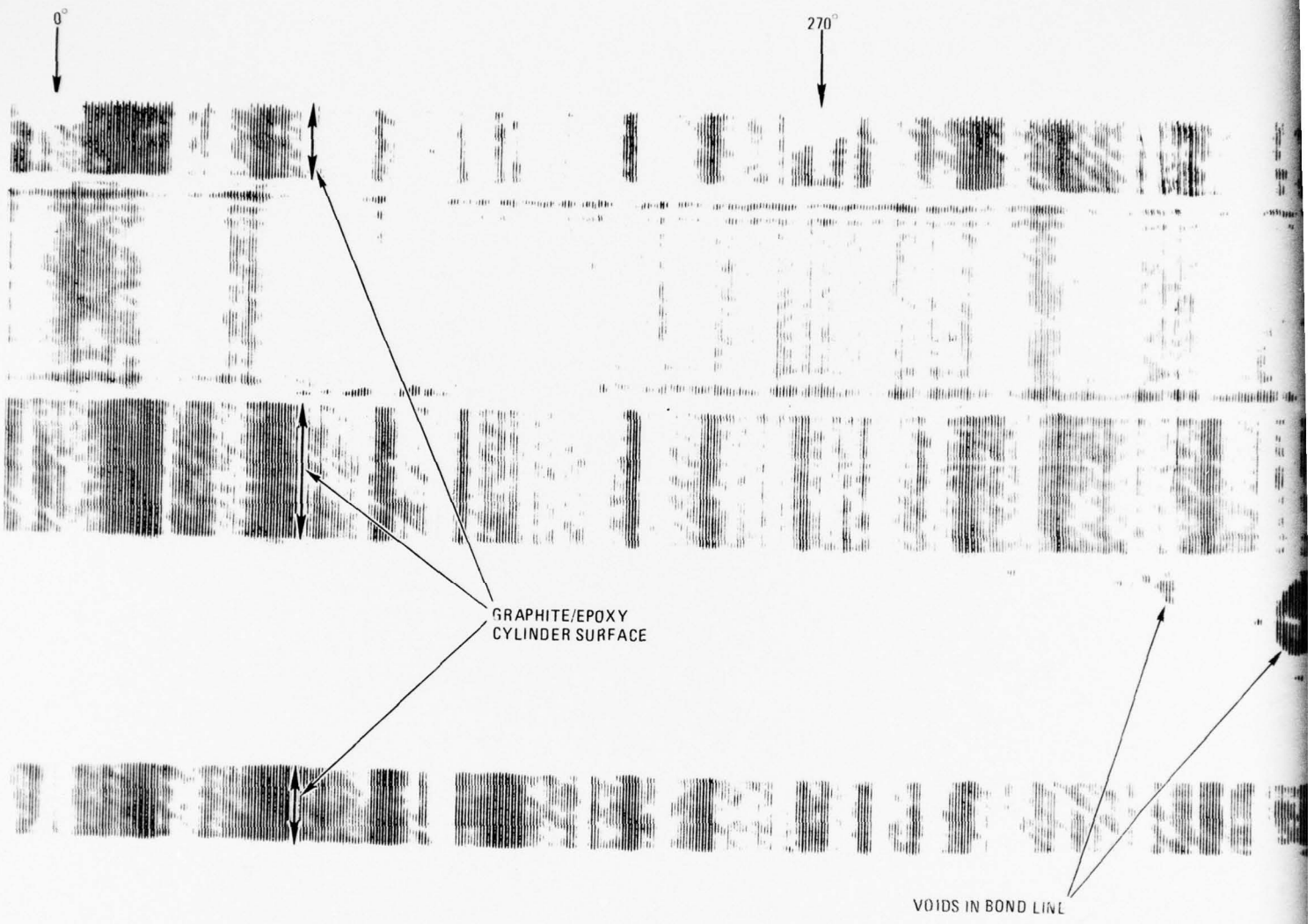
0°
270°
GRAPHITE/EPOXY
CYLINDER SURFACE
VOIDS IN BOND LINE

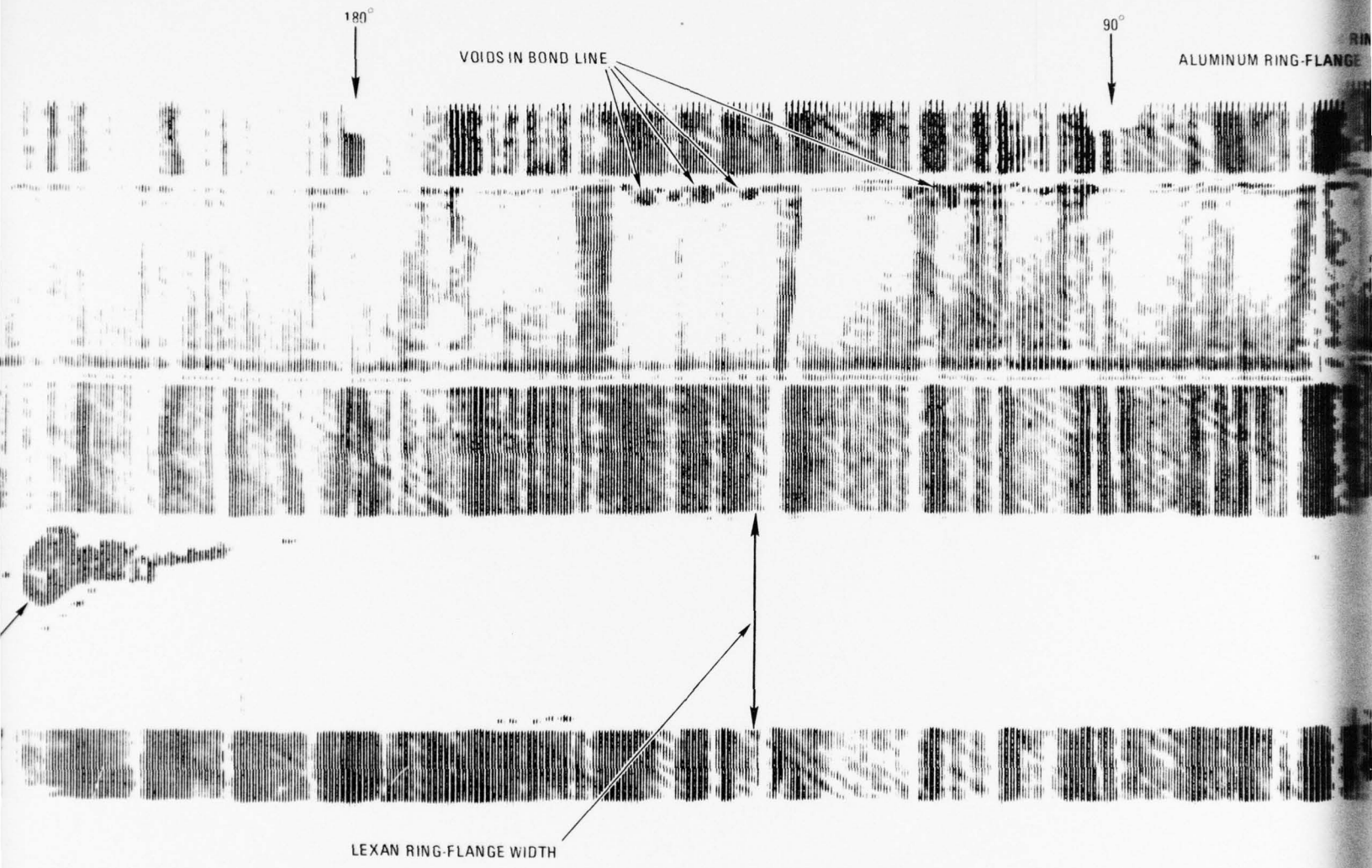

Figure 3.6-4. Cylinder Assembly Ultrasonic Scan (Worst Case)

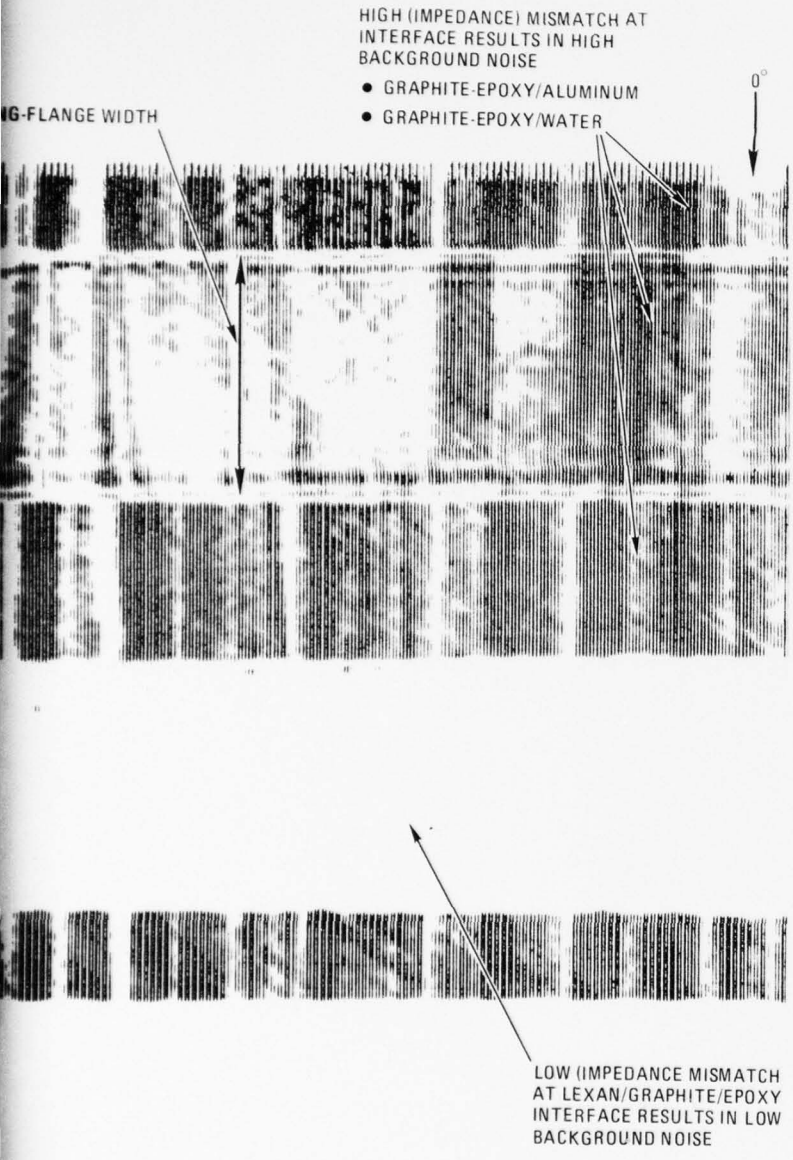
HIGH (IMPEDANCE) MISMATCH AT INTERFACE RESULTS IN HIGH BACKGROUND NOISE
• GRAPHITE-EPOXY/ALUMINUM
• GRAPHITE-EPOXY/WATER
0°
IG-FLANGE WIDTH
LOW (IMPEDANCE MISMATCH AT LEXAN/GRAPHITE/EPOXY INTERFACE RESULTS IN LOW BACKGROUND NOISE

SECTION 4

MANUFACTURING PROCESSES

4.1 INTRODUCTION

The process recommended for fabrication of the conceptual Mark 12A composite Midbay structure was developed at Convair and previously used for making cylinders and cones for the HEAO-B and AMMRC cone frusta programs. The general procedure consists of layup in a female tool made of bulk graphite and having a coefficient of linear thermal expansion of approximately 1.2 microinches/inch F.

4.2 SHELL STRUCTURE

In the case of the shell structure, moduler plies will be layed into the tool one module at a time, with each module split into five gore sections. Butt or overlap joints will be staggered from module to module so that at any meridian there will be no more than one butt joint. Preplying and debulking of the prepreg will be done at certain stages of the layup to minimize the amount of movement and the amount of bleed that occurs during the cure.

4.3 DOUBLER AND PADS

The scalloped doubler section will be laid up in two halves in a separate tool and debulked. These will then be laid into the female tool containing the debulked shell material and located accurately. Bleeder fabric and a silicone rubber overpress will be added. The tool will then be envelope-bagged placed in an autoclave for cure.

4.4 COMPOSITE RING

The composite ring will be fabricated as a 360° section. Each ply will be cut into small gores. The center section of the upstanding leg may either be debulked or cured prior to final layup and cure. Tooling will consist of a split male tool made of bulk graphite. Debulking and use of an overpress will minimize tendencies to wrinkle.

4.5 LAYUP AND CONSOLIDATION OF PREPREG

The prepreg recommended for the conceptual Mark 12A composite Midbay Structure is T300/5208. This is the same material currently being used at Convair for design and manufacturing of ABRV composite structures under contract with AVCO.

The prepreg will be laid up into large flat sheets of generally two plies. The gores for the shell layup will then be cut using aluminum templates. Teflon coated glass cloth or Mylar film will be used as an aid in transferring the gores from the flat into the female tool. Consolidation will be attained at suitable stages of the cycle. Final debulking will be conducted in an autoclave under full vacuum, and will consist of heating at 2° to 5° F/minute to 160° ±5F, applying 50 ±5 psig autoclave pressure, holding 15 to 20 minutes, and cooling under vacuum and pressure to below 100° F.

4.6 CURING

The final cure cycle for T300/5208 consists of applying full vacuum at RT, raising part temperature 2° to 3° F/minute to 205° ±5° F, holding at temperature for 40 ±5 minutes, raise temperature at 1° F/minute to 225° ±5° and hold for 60 minutes ±10 minutes, apply 100 psig autoclave pressure, holding an additional 120 ±5 minutes at temperature and pressure, raise temperature at 1° F/minute to 350° ±5° and hold for 60 minutes, cool slowly (less than 2° F/minute) under pressure to 150° F. There is no postcure required with this system.

4.7 RV SUBSTRUCTURE ASSEMBLY

The crucial requirement in the assembly of the composite mid-body structure is compliance with the stringent dimensional tolerances between the internal rings and the shell. These involve primarily shell surface profile, ring concentricity, and ring perpendicularity tolerances.

Well proven molding techniques will be used to attain the basic shell profile tolerances in the detail stage. The final assembly fixture will feature a series of precision machined and located external formers to accurately locate the shell relative to the center-line of the fixture and to a datum station plane. The fixture will also be equipped with an extractable central mandrel, accurately registered at each end for true position relative to the shell profile formers. This central mandrel will carry a locating device for each of the internal rings in the mid-body structure. Variation in the thickness of the ring/shell bond will be allowed to permit accurate centralization of the rings relative to the shell outer profile. In the case of a typical ring installation, the procedure will be:

1. Extract the central mandrel from the fixture.
2. Prepare the aluminum and graphite-epoxy surfaces for bonding.
3. Install the ring on the locating device on the mandrel.
4. TIR check the ring for concentricity relative to the mandrel.
5. Insert the mandrel into the assembly fixture to trial fit the ring.
6. Measure and record the gap between the ring and the inside of the shell.

7. Extract the mandrel and ring.
8. Meter adhesive onto the ring and onto the shell at the ring location to suit the gap measured in Step 6.
9. Insert the mandrel with attached ring into the assembly fixture.
10. Allow the specified set-up time applicable to the adhesive without disturbing the assembly fixture.
11. Detach the bonded ring from the locating devise and extract the center mandrel.

In combination with the repeatable precision molding technique proposed for the basic shell, this assembly technique will assure the provision of dimensionally accurate mid-body structure at low cost.

SECTION 5

CONCLUSIONS AND RECOMMENDATIONS

5.1 CONCLUSIONS

The recommended configuration described in Paragraph 2.2.1.3 for a composite mid-bay substructure is entirely feasible and producible using proven techniques already demonstrated on production flight hardware. The above conclusion is substantiated by the following findings during the study phase.

1. Change of heat shield backface temperature from 600° F to 400° F results in maximum front face temperature of 260° F for the mid bay composite structure making graphite/epoxy the prime candidate to be used for the current concept and temperature.
2. T300/5208 is the choice fiber/resin because its strength and stiffness combination are the most compatible with the tensile strain allowable of the C/P heatshield.
3. T300/5208 was selected for the recommended configuration on the basis of yielding minimum weight for compatibility with the heat shield strain limitation.
4. Composite materials can significantly reduce the weight of the MK12A Midbay. The recommended configuration indicates a weight savings of 3.7 lbs.
5. Low density materials, beryllium and magnesium, are not suitable for a ring application primarily due to unacceptable high stress concentrations and questionable reliability of anti corrosion treatment of threads, respectively.
6. More fabrication experience and test data are available on graphite/epoxies.
7. Graphite/polyimides are approximately 50% more costly than graphite/epoxies.
8. Current baseline design appears structurally adequate based on analysis performed.
9. Fabrication techniques developed in previous Convair programs are applicable.
10. Bulk graphite female molds, as developed for the HEAO-B program, are best for contour tolerance control.
11. High modulus graphite reinforced addition polyimides microcrack on cooldown after cure and postcure.
12. Consideration for manufacturing and Quality Assurance plans are outlined in Appendix B and C, respectively.

5.2 RECOMMENDATIONS

1. Pursue the application of graphite composites to reentry vehicle structures with the objective of attaining a minimum weight saving of 25%. This value is considered feasible in view of the 19% saving indicated using the conservative approach adopted in this study.

2. Implement material systems and laminate development to obtain improved interlaminar strength for increased resistance to impulsive loadings.

3. Initiate the development of moisture inhibition techniques and investigate the integration of this effort with an approach to satisfying to EMP requirements.

4. Develop high strength bonded joints to minimize the weight of aluminum rings and to improve performance at elevated temperature.

5. Build a prototype graphite-epoxy reentry vehicle structure to demonstrate a 25% weight saving and to demonstrate structural integrity by suitable tests.

SECTION 6

REFERENCES

1. Hertz, J. and Harbison, R. C., "Material Selection Rationale for AGT/UGT Specimens," General Dynamics Convair Division, Memo M-129, 2 September 1976.

2. Hertz, J., "Survey of Available Data on Candidate Graphite Reinforced Addition Polyimide Systems for Mark 12A," General Dynamics Convair Division, Memo M-128, 31 August 1976.

3. Lee, H. and Neville, K.,"Handbook of Epoxy Resins," McGraw-Hill Book Co., 1967.

4. Mahaffey, J. E., "Literature Survey Environmental Degradation of Fiber Glass Reinforced Plastics in Aircraft Applications," North American Aviation, Inc., Report No. NA64-H-941, November 1964.

5. Hertz, J., et.al., "Advanced Composite Applications for Spacecraft and Missiles," General Dynamics Convair Division, AFML Report AFML-TR-71-186, Vol. II, March 1972.

6. General Dynamics, Fort Worth Division, "Boron-Epoxy Composite Characteristics After Exposure to Different Aircraft Environments," WPAFB, Report No. MAA 68-48, 12 July 1968.

7. C. Fisher, General Electrical Letter No. 3735-1169, "Loads Versus Altitude and Heat Shield Back Face Temperature, etc.," dated 16 July 1976.

8. "MK12A Graphite Composite Structure Design Requirements to Support Feasbility Studies," GE-RESD, 7 July 1976, Modified Figure 7 at a meeting between SAMSO, TRW and GD/Convair on 8 September, 1976.

9. General Dynamics/Convair Drawing Number 72CO681, "Thrust Ring -- Concept No. 1, Midbay Composite Structure," J. Prunty, 15 September 1976.

10. "Convair Thermal Analyzer," Computer Program No. 4560, GDC-BTD69-005A, 29 May 1969.

11. "Advanced Composite Missile and Space Design Data," AFML-TR-74-97, June 1974.

12. "Stage IV Thermal Release," D. Huling, General Electric, 1 December 1964.

SECTION 6

REFERENCES (CONT'D)

13. "Thermal Properties of Selected Materials," General Dynamics/Convair Internal Report No. 966-3-CHM-66-002, 18 May 1966.

14. Brooks, A.L., "Graphite Resin Screening Tests," Ktech Corp., Report TR76-09, November 1976.

15. "Graphite Resin Screening Tests," Ktech Corp., Report AFWL-78-30. (Group A)

16. "Graphite Resin Screening Tests," Ktech Corp., Report (Group B and C) (To be determined).

APPENDIX A

STATION 32 AND STATION 42

COMPUTER PROGRAM INPUT LISTINGS

```
TITLE - MAIDA MID BAY, ONE-DIMENSIONAL, UPDATED PROPERTIES  .040 ADHESIVE
    2              -1.   -2.    5.          0.         45.    1
   16   14     2    7     2

MATERIAL BLOCK

    1 91.7  -3.   -4.   -4.   -4. EPON 934 ADHESIVE
    2  97.  -5.   -6.   -6.   -6. GRAPHITE/EPOXY

TABLES

          1          2
          1          9
         0.         1.
        45.         1.
         2          4
         1         10
         0.         5.
        35.         5.
        35.         1.
        45.         1.
         3          3
         2          2
       500.       .315 }
       900.       .315 } SPECIFIC HEAT, EPON 934, BTU/LB-°R
      1100.       .315 }
         4          2
         4          3
       500.       .266 }
      1100.       .266 } THERMAL CONDUCTIVITY, EPON 934, BTU/HR-FT-°R
         5          2
         2          2
       160.       .075 }
       810.       .330 } SPECIFIC HEAT, GRAPHITE/EPOXY, BTU/LB-°R
         6          3
         4          3
       160.       .13  }
       540.       .59  } THERMAL CONDUCTIVITY, GRAPHITE/EPOXY, BTU/HR-FT-°R
       810.       .7   }
         7         12
         1          4
         0.       600. }
        33.       600. }
        34.       610. }
        36.       635. }
        37.       666. } HEAT SHIELD INNER SURFACE TEMPERATURE, °R
        38.       698. }
        39.       734. }
        40.       764. }
        41.       794. }
        42.       818. }
        43.       840. }
      43.8        860. }

NODE BLOCK

         1    2                                  -7.
    1    2    3     1 .005    1.    1. 560.
    1    3    4     1 .005    1.    1. 560.
    1    4    5     1 .020    1.    1. 560.
    1    5    6     1 .005    1.    1. 560.
```

```
1     6     B     1 .005    1.    1. 560.
2     7     B     2 .005    1.    1. 560.
2     8     B     2 .005    1.    1. 560.
2     9     B     2 .005    1.    1. 560.
2     10    B     2 .005    1.    1. 560.
2     11    B     2 .005    1.    1. 560.
2     12    B     2 .005    1.    1. 560.
2     13    B     2 .005    1.    1. 560.
2     14    B     2 .005    1.    1. 560.
2     15    B     2 .005    1.    1. 560.
2     16    B     2 .005    1.    1. 560.

RESISTANCE BLOCK

      2     B     2     3          1
      3     B     3     4
      4     B     4     5
      5     B     5     6
      6     B     6     7
      7     B     7     8
      8     B     8     9
      9     B     9    10
     10     B    10    11
     11     B    11    12
     12     B    12    13
     13     B    13    14
     14     B    14    15
     15     B    15    16
```

```
TITLE - STATION 32 THRUST RING, ALUMINUM
    2              -1.   -2.    5.          0.        45.     1
   82   61     3     8

MATERIAL BLOCK

    1 91.7 .315 .266 .266 .266 EPON 934 ADHESIVE
    2 97.0  -4.  -5.  -6.  -6. GRAPHITE/EPOXY
    3 173.  -7.  -8.  -8.  -8. ALUMINUM

TABLES

         1          2
         1          9
        0.          1.
       45.          1.
         2          4
         1         10
        0.          5.
       35.          5.
       35.          1.
       45.          1.
         3         12
         1          4
        0.        600.
       33.        600.
       34.        610.
       36.        635.
       37.        666.   } HEAT SHIELD INNER SURFACE TEMPERATURE, °R
       38.        698.
       39.        734.
       40.        764.
       41.        794.
       42.        818.
       43.        840.
      43.8        860.
         4          2
         2          2
      160.       .075  } SPECIFIC HEAT, GRAPHITE/EPOXY, BTU/LB-°R
      810.       .330
         5          3
         4          3
      160.        .13  }
      540.        .59  } THERMAL CONDUCTIVITY, GRAPHITE/EPOXY, (THICKNESS DIRECTION), BTU/HR-FT-°R
      810.        .70  }
         6          2
         4          3
      160.        6.5  }
      760.        29.  } THERMAL CONDUCTIVITY, GRAPHITE/EPOXY, (PARALLEL TO GRAPHITE), BTU/HR-FT-°R
         7          2
         2          2
      500.         .2  }
     1000.        .24  } SPECIFIC HEAT, ALUMINUM, BTU/LB-°R
         8          2
         4          3
      500.         67.  }
     1000.        106.  } THERMAL CONDUCTIVITY, ALUMINUM, BTU/HR-FT-°R

NODE BLOCK

         1    2
```

2	8	1	.010	3.	1. 560.
3	8	1	.020	3.	1. 560.
4	8	1	.010	3.	1. 560.
5	3				
6	8	2	.005	3.	1. 560.
7	8	2	.015	3.	1. 560.
8	8	2	.015	3.	1. 560.
9	8	2	.015	3.	1. 560.
10	2				-3.
11	8	1	.010	.5	1. 560.
12	8	1	.020	.5	1. 560.
13	8	1	.010	.5	1. 560.
14	3				
15	8	2	.005	.5	1. 560.
16	8	2	.015	.5	1. 560.
17	8	2	.015	.5	1. 560.
18	8	2	.015	.5	1. 560.
19	8	2	.015	.5	1. 560.
20	8	2	.015	.5	1. 560.
21	8	2	.015	.5	1. 560.
22	8	2	.005	.5	1. 560.
23	2				-3.
24	8	1	.010	1.5	1. 560.
25	8	1	.020	1.5	1. 560.
26	8	1	.010	1.5	1. 560.
27	3				
28	8	2	.005	1.5	1. 560.
29	8	2	.015	1.5	1. 560.
30	8	2	.015	1.5	1. 560.
31	8	2	.015	1.5	1. 560.
32	8	2	.015	1.5	1. 560.
33	8	2	.015	1.5	1. 560.
34	8	2	.015	1.5	1. 560.
35	8	2	.005	1.5	1. 560.
36	3				
37	8	1	.010	1.5	1. 540.
38	8	1	.005	1.5	1. 540.
39	3				
40	8	3	.054	1.5	1. 540.
41	8	3	.300	.26	1. 540.
42	8	3	.500	.15	1. 540.
43	2				-3.
44	8	1	.010	1.5	1. 560.
45	8	1	.020	1.5	1. 560.
46	8	1	.010	1.5	1. 560.
47	3				
48	8	2	.005	1.5	1. 560.
49	8	2	.015	1.5	1. 560.
50	8	2	.015	1.5	1. 560.
51	8	2	.015	1.5	1. 560.
52	8	2	.015	1.5	1. 560.
53	8	2	.015	1.5	1. 560.
54	8	2	.015	1.5	1. 560.
55	8	2	.005	1.5	1. 560.
56	2				-3.
57	8	1	.010	1.	1. 560.
58	8	1	.020	1.	1. 560.
59	8	1	.010	1.	1. 560.
60	3				
61	8	2	.005	1.	1. 560.
62	8	2	.015	1.	1. 560.

```
63    b    2 .015   1.    1. 560.
64    b    2 .115   1.    1. 560.
65    2                      -3.
66    b    1 .010   1.    1. 560.
67    b    1 .020   1.    1. 560.
68    b    1 .010   1.    1. 560.
69    3
70    b    2 .005   1.    1. 560.
71    b    2 .015   1.    1. 560.
72    b    2 .015   1.    1. 560.
73    b    2 .015   1.    1. 560.
74    2                      -3.
75    b    1 .010   1.    1. 560.
76    b    1 .020   1.    1. 560.
77    b    1 .010   1.    1. 560.
78    3
79    b    2 .005   1.    1. 560.
80    b    2 .015   1.    1. 560.
81    b    2 .015   1.    1. 560.
82    b    2 .015   1.    1. 560.
```

RESISTANCE BLOCK

```
B    2    1         3        11
B    3    4                  12
B    4    5                  13
B    6    5         7        15
B    7    8                  16
B    8    9                  17
B   11   10        12        24
B   12   13                  25
B   13   14                  26
B   15   14        16        28
B   16   17                  29
B   17   18                  30
B   18   19                   9      31
B   19   20                          32
B   20   21                          33
B   21   22                          34
B   24   23        25        44
B   25   26                  45
B   26   27                  46
B   28   27        29        48
B   29   30                  49
B   30   31                  50
B   31   32                  51
B   32   33                  52
B   33   34                  53
B   34   35                  54
B   35   36                  55      22
B   37   36        38
B   38   39
B   40   39        41
B   41   42
B   44   43        45        57
B   45   46                  58
B   46   47                  59
B   48   47        49        61
B   49   50                  62
B   50   51                  63
B   51   52                  64
```

```
      52 53
      53 54
      54 55
      57 56                58          66
      58 59                            67
      59 60                            68
      61 60          62                70
      62 63                            71
      63 64                            72
      66 65          67                75
      67 68                            76
      64 69                            77
      70 69          71                79
      71 72                            80
      72 73                            81
      75 74          76
      76 77
      77 78
      79 78          80
      80 81
      81 82                            73
      64 73                            82
```

APPENDIX B

MANUFACTURING PLAN

APPENDIX B

MANUFACTURING PLAN

THE MK12A MID BAY SUBSTRUCTURE MANUFACTURING PLAN WILL BE PREPARED TO THE FOLLOWING OUTLINE AND INCLUDED IN THE FINAL REPORT.

I INTRODUCTION - DEFINITION OF MANUFACTURING TASK

II DESCRIPTION OF PRODUCT- PRODUCT IS DEFINED, SIZE, SHAPE

III GROUND RULES - CUSTOMER/COMPANY AGREEMENTS OF BASIC CRITERIA

IV MAKE OR BUY - DEFINITION OF BUY PRODUCTS

V SUBCONTRACTING - DETAIL LISTING OF OUT-PLANT SERVICES

VI MANUFACTURING FACILITIES -

1. PLANT LAYOUT - PHYSICAL LOCATION WHERE MAJOR TASKS ARE TO BE PERFORMED
2. OPERATION SEQUENCE AND STATION CHART - GRAPHIC DISPLAY OF OPERATION SEQUENCE AND FLOW
3. FACILITIES AND EQUIPMENT - FACILITIES OR EQUIPMENT REQUIRED FOR PROGRAM
4. MANUFACTURING AIDS - MANUFACTURING SUPPORT AIDS

VII MANUFACTURING ANALYSIS - PRODUCT IS BROKEN DOWN INTO ASSEMBLIES AND SUBASSEMBLIES

1. MANUFACTURING SEQUENCE AND FLOW - DIRECTIONAL GUIDE OF TOTAL MANUFACTURING TASK
2. MAJOR COMPONENT BREAKDOWN AND ASSEMBLY SEQUENCE - MAJOR COMPONENT DESCRIPTION
3. MANUFACTURING PRODUCIBILITY - UNIQUE MATERIAL OR PROCESS DESCRIPTION

VIII TOOLING PLAN - TOTAL TOOLING PLAN AND IMPLEMENTATION

1. TOOLING PHILOSOPHY - BASIC TOOLING PHILOSOPHY BASED ON QUANTITIES TO BE PRODUCED
2. MASTER AND CONTROL TOOLS - MASTER AND CONTROL TOOL CONCEPTS
3. MAJOR ASSEMBLY TOOLS - MAJOR ASSEMBLY TOOLS DESCRIPTION
4. DETAIL TOOLS - DETAIL TOOLING POLICY

IX PROGRAM SCHEDULE - MASTER PHASING CHART OF ALL ACTIVITIES

XI QUALITY CONTROL POLICY - METHODS OF CONTROL

XI MANPOWER - MANPOWER SPREAD FOR TOOLING AND MANUFACTURING

APPENDIX C

QUALITY ASSURANCE PLAN

APPENDIX C

MK12A

QUALITY ASSURANCE

PLAN

THE MK12A MID BAY SUBSTRUCTURE QUALITY ASSURANCE PLAN WILL BE PREPARED TO THE FOLLOWING OUTLINE AND INCLUDED IN THE FINAL REPORT.

SCOPE

- GEARED TO SUPPORT PREPRODUCTION YET DELIVER A QUALITY PRODUCT
- IDENTIFY AND DEVELOP PRODUCTION CAPABILITIES

APPROACH

- USE THE PROJECT QA ADMINISTRATOR CONCEPT
- USE THE QA PLAN TO IMPLEMENT EXISTING QA SYSTEMS TO MEET PROGRAM REQUIREMENTS

PROGRAM

- ASSUME MIL-Q-9858A TYPE PROGRAM WITH QA PLAN APPROVED BY CUSTOMER
- ELEMENTS INCLUDE - INSPECTION FLOW PLAN, QAR's, MRB WITH CUSTOMER PARTICIPATION
- DESIGN REVIEW INCLUDING TOOLING - IDENTIFIES INSPECTION AND TEST METHODOLOGY
- PROCUREMENT - P.O. REVIEW AND RECEIVING INSPECTION TASKS PLANNED
- PRODUCTION, PROCESS, AND FAB - SURVEILLANCE AS WELL AS PLANNED DISCRETES
- CERTIFICATION - PERSONNEL AND EQUIPMENT
- TRACEABILITY - MATERIAL, PROCESS AND TEST DATA CORRELATION TO FINISHED DETAIL
- DELIVERY - MATERIAL CERTS, TABULATED QAR DATA, PROCESS & TEST DATA

APPENDIX D

CURE CYCLES

APPENDIX D

Panel cure and postcure cycles were generally those recommended by the respective material suppliers. A summary of those used on this program are given below.

T-300/5230

Cure Cycle: Apply full vacuum (29 in. mercury, minimum) and 8 to 13 psig autoclave pressure at RT. Heat at 2 to 3F/minute to 150F ±5. Raise autoclave pressure to 100 psig ±5 and vent vacuum when pressure reaches 20 psig. Heat to 350F ±5 at 2 to 3F/minute and hold 2 hours at this temperature. Cool to below 150F under pressure at a rate not to exceed 10F/minute. Vent and debag.

Postcure Cycle: Postcure unrestrained in a circulating air oven. Heating rate is approximately 3F/minute. Hold 2 hours at 350F, 2 hours at 400F, 2 hours at 450F, and 4 hours at 500F. Cool at a rate not to exceed 10F/minute.

T-300/F-178

Cure Cycle: Apply 4 to 6 in. Mercury vacuum at RT. Heat at 3 to 5F/minute to 270F ±10. Hold at temperature for 30 minutes ±5. Apply full vacuum (approximately 29 in. mercury) plus 100 psig ±5 autoclave pressure. Raise temperature to 350F ±8 at 3 to 5F/minute and hold 2 hours minimum. Cool to below 150F under vacuum and pressure at a rate not to exceed 10F/minute. Vent and debag.

Postcure Cycle: Postcure unrestrained in a circulating air oven. Heating rate is approximately 3F/minute. Hold 2 hours at 350F, 2 hours at 400F, 2 hours at 450F, 4 hours at 500F and 24 additional hours at 450F. Cool at a rate not to exceed 10F/minute.

HM-S/5230

Cure and postcure cycles are the same as those given for T-300/5230.

HM-S/4397

Precompaction: Apply 29 in. mercury vacuum at RT. Heat at 3 to 5F/minute to 200F ±10 and hold for 30 minutes ±5. Cool to below 100F at a rate not to exceed 10F/minute. Vent and debag.

Cure Cycle: Apply 29 in. mercury vacuum at RT. Heat at 2 to 3F/minute to 275F ±10. Apply 85 psig ±5 autoclave pressure and hold 30 minutes ±5 at temperautre and pressure. Heat at 2 to 3F/minute to 400F ±10 and hold a minimum of 60 minutes. Cool to below 150F under vacuum and pressure. Vent and debag.

Postcure Cycle: Postcure unrestrained in a circulating air oven. Heat at 2 to 3F/minute. Hold 2 hours at 400F, 2 hours at 410F, 2 hours at 420F, 2 hours at 430F, 2 hours at 440F, 40 hours at 450F. Cool slowly.

GY-70/5230

Cure and postcure cycles are the same as those given for T-300/5230.

T-300/934

Cure Cycle: Apply 29 in. mercury vacuum minimum at RT, and hold 30 minutes minimum. Heat at approximately 3F/minute to 250F ±10, and hold at temperature for 45 minutes ±5. Apply 100 psig ±5 autoclave pressure, and hold at temperature and pressure for an additional 45 minutes ±5. Raise temperature to 350F $^{+10}_{-0}$ at above heating rate, and hold temperature for a minimum of 2 hours. Cool to below 175F at a rate not to exceed 10F/minute. Vent and debag.

Postcure Cycle: None

HM-S/934

Cure and postcure same as for T-300/934 except pressure of 8 to 13 psig plus vacuum was applied at start of cycle.

GY-70/934

Cure and postcure same as that for HM-S/934.

T-300/5208

Cure Cycle: Apply 29 in. mercury vacuum minimum plus 8 to 13 psig autoclave pressure at RT. Heat at 1.0 to 1.5F/minute to 255F ±5, and hold at temperature for 60 minutes ±5. Raise autoclave pressure to 85 psig ±5, and hold an additional 60 minutes ±5 at temperature. Heat at 1.0 to 1.5F/minute to 355F ±10, and hold for a minimum of 2 hours at temperature. Cool to below 140F at a rate not to exceed 10F/minute. Vent and debag.

Postcure Cycle: None

A-S/3501

Cure Cycle: Apply 29 in. mercury vacuum minimum at RT. Heat at approximately 3F/minute to 350F $^{+10}_{-0}$ applying 100 psig ±5 autoclave pressure at 275F ±5. Hold a minimum of 2 hours at 350F $^{+10}_{-0}$. Cool under vacuum and pressure to below 150F at a rate not to exceed 10F/minute. Vent and debag.

Postcure Cycle: None

HM-S/948

Cure Cycle: Apply 29 in. mercury minimum and hold 30 minutes ±5 at RT. Heat at 2 to 5F/minute to 175F ±5. Apply 100 psig ±5 autoclave pressure and hold an additional 15 to 20 minutes. Heat at 2 to 5F/minute to 250F $^{+10}_{-0}$. Hold a minimum of 2 hours, and cool under vacuum and pressure to below 175F. Vent and debag.

Postcure Cycle: None

T-300/948

Cure and postcure same as that described for HM-S/948.

APPENDIX E

TEST DATA

Table 1. Tension Test Data on Unidirectional, $[0]_8$, T-300/5230

Panel No.	Ultimate Tensile Strength, ksi			Tensile Modulus msi			Ultimate Tensile Strain, μ-in			Poisson's Ratio	Resin Content	Fiber Volume	Specific Gravity
	RT	350F	600F	RT	350F	600F	RT	350F	600F	RT	Wt.%	%	
-3	207	185	178	20.6	23.6	23.1	10,000	7,840	7,710	0.31	24.47	69.99	1.611
	227	201	186	23.2	24.5	23.0	9,870	8,200	8,090	0.31	24.36	70.02	1.615
	229	207	169	24.9	25.1	22.5	9,200	8,330	7,510	0.28			
-6	198	211	187	23.7	24.3		8,350	8,680			25.64	68.57	1.606
	211	220	179	23.0	22.2		9,170	9,910			31.30	62.28	1.601
	211	217	188	23.4	25.0		9,020	8,680					
N	6	6	6	6	6	3	6	6	3	3	4	4	4
X	214	207	181	23.1	24.1	22.9	9,250	8,610	7,770	0.30	26.44	67.72	1.608
S	12.0	12.7	7.3	1.4	1.1	0.32	586	713	295	0.017	3.29	3.69	0.006
C_v	5.6%	6.1%	4.0%	6.1%	4.5%	1.4%	6.3%	8.3%	3.8%	5.8%	12.4%	5.4%	0.38%

Table 2. Tensile Test Data on Unidirectional, $[0]_8$, T-300/F-178

Panel No.	Ultimate Tensile Strength, ksi			Tensile Modulus msi			Ultimate Tensile Strain, μ-in			Poisson's Ratio	Resin Content	Fiber Volume	Specific Gravity
	RT	350F	600F	RT	350F	600F	RT	350F	600F	RT	Wt.%	%	
-5	165	180	168	21.0	22.5		7,860	8,000		0.31	29.12	64.32	1.596
	180	181	163	21.5	22.2		8,370	8,150		0.35	28.88	64.59	1.596
	169	177	160	21.4	22.2		7,900	7,970		0.32			
-8	183	180	143	21.0	22.1	20.4		8,140	7,010	0.32	29.58	63.81	1.596
	173	179	151	20.4	22.0	22.2		8,140	6,800	0.30	29.71	63.67	1.598
	160	168	168	21.2	21.6	21.1		7,780	7,960	0.30			
N	6	6	6	6	6	3		6	3	6	4	4	4
$\bar{X}$	172	178	159	21.1	22.1	21.2		8,030	7,260	0.32	29.32	64.10	1.597
S	8.8	4.8	10.0	0.39	0.30	0.91		145	618	0.019	0.39	0.43	0.001
C_v	5.1%	2.7%	6.3%	1.9%	1.3%	4.3%		1.8%	8.5%	5.8%	1.3%	0.67%	0.063%

Table 3. Tension Test Data on Unidirectional, $[0]_8$, HMS/4397

Panel No.	Ultimate Tensile Strength, ksi			Tensile Modulus msi			Ultimate Tensile Strain, μ-in			Poisson's Ratio	Resin Content	Fiber Volume	Specific Gravity
	RT	350F	600F	RT	350F	600F	RT	350F	600F	RT	Wt.%	%	
-6	186	169	122	27.0		26.2	6,900		4,690	0.30	27.65	64.71	1.591
	145	194	139	30.9		32.2	4,690		4,320	0.25	27.47	64.95	1.618
	194	236	131	30.7		31.4	6,320		4,170	0.25			
		204											
N	3	4	3	3		3	3		3	3	2	2	2
$\bar{X}$	175	201	131	29.5		29.9	5,970		4,390	0.27	27.56	64.83	1.605
S	26.3	27.7	8.5%	2.2		3.3	1,150		268	0.029	0.13	0.17	0.019
C_v	15.0%	13.8%	6.5%	7.4%		10.9%	19.2		6.1%	10.7%	0.46%	0.26%	1.2%

Table 4. Tensile Test Data on Unidirectional, $[0]_8$, HMS/5230

Panel No.	Ultimate Tensile Strength, ksi			Tensile Modulus msi			Ultimate Tensile Strain, μ-in			Poisson's Ratio	Resin Content	Fiber Volume	Specific Gravity
	RT	350F	600F	RT	350F	600F	RT	350F	600F	RT	Wt.%	%	
-4	155	184	180	35.5	33.3	29.4	4,370	5,530	6,120	0.28	33.46	58.86	1.596
	143	175	172	34.2	34.0	29.4	4,190	5,140	5,850	0.26	33.62	58.69	1.611
	147	204	193	32.6	32.3	30.5	4,510	6,250	6,330	0.25			
-7	143	152	146	29.1	31.6		4,910	4,810			31.42	61.09	1.590
	117	140	168	29.1	32.0		4,020	4,380			30.83	61.75	1.574
	140	157	163	29.1	33.8		4,810	4,640					
N	6	6	6	6	6	3	6	6	3	3	4	4	4
$\bar{X}$	141	169	170	31.6	32.8	29.8	4,470	5,130	6,100	0.26	32.33	60.10	1.593
S	12.8	23.5	15.9	2.9	1.0	0.64	347	681	241	0.015	1.42	1.55	0.015
C_v	9.1%	13.9%	9.3%	9.1%	3.1%	2.1%	7.8%	13.3%	3.9%	5.9%	4.4%	2.6%	0.96%

Table 5. Tension Test Data on Unidirectional, $[0]_8$, GY-70/5230

Panel No.	Ultimate Tensile Strength, ksi			Tensile Modulus msi			Ultimate Tensile Strain, μ-in			Poisson's Ratio	Resin Content	Fiber Volume	Specific Gravity
	RT	350F	600F	RT	350F	600F	RT	350F	600F	RT	Wt.%	%	
-6	127	132	126	47.8	44.9	48.0	2,660	2,940	2,630	0.35	24.97	66.70	1.744
	109	115	108	50.5	39.0	49.7	2,160	2,950	2,170	0.36	25.37	66.23	1.740
	118	122		49.1	39.0		2,400	2,130		0.37			
-10	110	111	126	42.6			2,580				26.11	65.36	1.664
	112	100	132	41.2			2,720				26.32	65.11	1.662
	106	118	140	42.3			2,510						
N	6	6	5	6	3	2	6	3	2	3	4	4	4
$\bar{X}$	114	116	126	45.6	41.0	48.9	2,510	3,010	2,400	0.36	25.69	65.85	1.703
S	7.7	10.7	11.8	4.0	3.4	1.2	203	107	325	0.010	0.63	0.74	0.046
C_v	6.7%	9.3%	9.4%	8.8%	8.3%	2.5%	8.1%	3.6%	13.6%	2.8%	2.5%	1.1%	2.7%

Table 6. Compression Test Data on Unidirectional, $[0]_{24}$, T-300/5230

Panel No.	Ultimate Compression Strength, ksi			Compression Modulus msi			Ultimate Compression Strain, μ-in			Poisson's Ratio	Resin Content	Fiber Volume	Specific Gravity
	RT	350F	600F	RT	350F	600F	RT	350F	600F	RT	Wt.%	%	
-5	152*	119	98.9*	21.3	25.2	23.7	7,570	4,320	4,170	0.30	23.33	71.20	1.612
	154	155	84.1*	20.1	23.8	23.0	6,880	6,400	3,660	0.26	22.93	71.66	1.611
	155*		89.7*	21.8	24.0	22.0	7,100		4,080	0.30			
-8	199	168									29.46	64.30	1.606
	179	174									24.48	69.89	1.607
	140	161											
N	6	5	6	3	3	3	3	2	3	3	4	4	4
$\bar{X}$	163	155	90.9	21.1	24.3	22.9	7,180	5,360	3,970	0.29	25.05	69.26	1.609
S	21.7	21.6	7.5	0.87	0.76	0.85	352	1,470	272	0.012	3.01	3.39	0.003
C_v	13.3%	13.9%	8.2%	4.1%	3.1%	3.7%	4.9%	27.4%	6.9%	4.0%	12.0%	4.9%	0.18%

*Doubler failures

Table 7. Compression Test Data on Unidirectional, $[0]_{24}$, T-300/F-178

Panel No.	Ultimate Compression Strength, ksi			Compression Modulus msi			Ultimate Compression Strain, μ-in			Poisson's Ratio	Resin Content	Fiber Volume	Specific Gravity
	RT	350F	600F	RT	350F	600F	RT	350F	600F	RT	Wt.%	%	
-7	127	148	85.2*	20.5	19.3	18.4*	6,720	8,090	4,630	0.43	31.62	61.57	1.596
	141	152	59.7*	19.5	21.3	17.7*	7,690	7,500	3,370	0.37	30.31	63.01	1.596
	145	153	79.3*	20.5	20.0	19.0*	8,310	7,990	4,170	0.45			
-10	141	152		17.2	20.0		8,290	7,780		0.35	28.36	65.17	1.590
	149	143		17.9	20.8		8,670	7,090		0.32	28.92	64.55	1.597
	149	155		18.2	20.5		8,680	9,020		0.34			
N	6	6	3	6	6	3	6	6	3	6	4	4	4
$\overline{X}$	142	151	74.7	19.0	20.3	18.4	8,060	7,910	4,000	0.38	29.80	63.58	1.595
S	8.2	4.3	13.3	1.4	0.70	0.65	749	652	891	0.052	1.46	1.62	0.003
C_v	5.8%	2.9%	17.9%	7.4%	3.5%	3.5%	9.3%	8.2%	22.3%	13.7%	4.9%	2.5%	0.20%

*Doubler failures

Table 8. Compression Test Data on Unidirectional, $[0]_{24}$, HM-S/4397

Panel No.	Ultimate Compression Strength, ksi			Compression Modulus msi			Ultimate Compression Strain, μ-in			Poisson's Ratio	Resin Content	Fiber Volume	Specific Gravity
	RT	350F	600F	RT	350F	600F	RT	350F	600F	RF	Wt.%	%	
-5	109	96.2*	**	26.2	29.0	**	4,660	3,470	**	0.41	29.06	63.14	1.589
	100	88.8*		27.1	38.6		3,990	1,730		0.40	31.81	60.06	1.584
	110	102.9		30.8	28.0		4,230	3,010		0.45			
N	3	3		3	3		3	3		3	2	2	2
$\bar{X}$	106	96.0		28.0	31.9		4,290	2,740		0.42	30.44	61.60	1.587
S	5.5	7.1		2.4	5.9		339	902		0.026	1.94	2.18	0.0035
C_v	5.2%	7.3%		8.7%	18.3%		7.9%	32.9%		6.3%	6.4%	3.5%	0.22%

*Doubler failures

**Early doubler failure; insufficient material to run additional tests

Table 9. Compression Test Data on Unidirectional, $[0]_{24}$, HM-S/5230

Panel No.	Ultimate Compression Strength, ksi			Compression Modulus msi			Ultimate Compression Strain, μ-in			Poisson's Ratio	Resin Content	Fiber Volume	Specific Gravity
	RT	350F	600F	RT	350F	600F	RT	350F	600F	RT	Wt.%	%	
-3	97.5	112	49.2*	26.4	26.4	19.0	3,780	4,310	2,590	0.55	31.58	60.92	1.616
	82.0	100	24.6*	25.5	28.0	25.2	3,280	3,290	980	0.48	31.55	60.95	1.618
	98.5	120	73.8*	25.3	25.5	22.8	3,970	4,640	3,240	0.30			
-6	102	72.8	61.3								29.73	62.97	1.615
	84.8	76.4	64.8*								29.49	63.24	1.623
	66.6	77.3	69.0*										
N	6	6	6	3	3	3	3	3	3	3	4	4	4
X	88.6	93.1	57.1	25.7	26.6	22.3	3,680	4,080	2,270	0.44	30.59	62.02	1.618
S	13.4	20.3	18.0	0.58	1.3	3.1	356	704	1,160	0.13	1.13	1.26	0.004
C_v	15.1%	21.8%	31.5%	2.3%	4.8%	14.0%	9.7%	17.2%	51.3%	29.3%	3.7%	2.0%	2.2%

*Doubler failures

Table 10. Compression Test Data on Unidirectional, $[0]_{24}$, GY-70/5230

Panel No.	Ultimate Compression Strength, ksi			Compression Modulus msi			Ultimate Compression Strain, μ-in			Poisson's Ratio	Resin Content	Fiber Volume	Specific Gravity
	RT	350F	600F	RT	350F	600F	RT	350F	600F	RT	Wt.%	%	
-8	57.1	59.5	67.4*	41.8	45.5	42.0	1,290	1,340	1,610	0.45	22.28	69.93	1.727
	75.0	83.1	64.1*	45.2	46.0	40.6	1,700	1,880	1,580	0.53	22.62	69.52	1.723
	70.7	81.1		52.9	44.0		1,630	1,940		0.40			
-9	75.1	58.6									23.78	68.12	1.675
	83.6	68.3									22.96	69.11	1.710
	89.2	83.2											
	77.9	78.8											
N	7	7	2	3	3	2	3	3	2	3	4	4	4
$\bar{X}$	75.5	73.2	65.8	46.6	45.2	41.3	1,540	1,720	1,600	0.46	22.91	69.17	1.709
S	10.2	10.9	2.3	5.7	1.0	0.99	219	330	21.2	0.066	0.64	0.78	0.024
C_v	13.5%	14.9%	3.5%	12.2%	2.3%	2.4%	14.2%	19.2%	1.3%	14.3%	2.8%	1.1%	1.4%

*Doubler failures

APPENDIX F

TEST PLAN

646-0-76TD-009
18 October 1976
Rev. A 10/21/76
Rev. B 11/8/76
Rev. C 11/16/76

MK12A

GRAPHITE MID-BODY SHELL

FEASIBILITY STUDY

Contract DAAG-46-76-C-0073

TEST PLAN

Prepared by: Hugh McCutchen, Jr.

Approved: R. C. Harbison
R. C. Harbison

1. INTRODUCTION

This test plan describes the testing to be conducted during the second phase of Contract DAAG-46-76-C-0073. The primary objective of this contract is to determine the weight saving attainable by the application of composite materials in lieu of aluminum on the midbay structure of the MK12A. During the original conceptual design phase which culiminated in the First Design Review, 7 October 1976, a feasible concept was developed. This employed graphite/epoxy composite and demonstrated a significant weight saving. Data on above ground tests presented at this review, however, led to a redirection of the study involving a continuation of conceptual design, reconsideration of material selection, and revision to the proposed test program. The following section presents the rationale for the revised approach to the study and the associated test efforts.

2. RATIONALE FOR THE EXTENDED CONCEPTUAL DESIGN STUDY AND THE ASSOCIATED TEST PROGRAM

During the original conceptual design phase of the program, three graphite/epoxy and five graphite/polyimide systems were studied for applicability to the MK12A Midbay program. These were:

	Graphite/Epoxy	Graphite/Polyimide
Ultra-high Modulus Fiber	GY-70/934	GY-70/5230
High Modulus Fiber	HM-S/934	HMS/5230 & HMS/4397
High Strength Fiber	T-300/5208	T300/5230 & T300/F178

Early in the program the heat shield backface peak temperature was changed from 600F to 400F (reference G. E. Letter 3735-1207). Analysis based on this revision demonstrated that the peak temperature of the midbay skin would be 257F. This permitted the selection of a graphite/epoxy for the baseline design. The specific graphite/epoxy, HM-S/934, was selected after structural analysis indicated that this material system gave minimum weight for compatibility with the heat shield strain criteria. A recommended design based on this material showed a weight saving of 4.21 pounds compared with the all aluminum midbay weight.

During the first design review the results of the plate slap tests on the candidate materials were presented by AFML. These results showed that for this criterion T-300 is the best fiber for application to the MK12A. Convair was then directed to use it in a continued conceptual study for the remainder of the current program.

In comparison with the HM-S fiber used in the recommended baseline design, since T-300 has a lower modulus, it carries a lower stress at the strain limit imposed by the heat shield. This results in an increase in skin thickness to carry the loads in the shell of the midbay. The change in the fiber therefore results in a reduction in the weight savings attainable by the use of composites on the MK12A.

In view of this situation, a possible candidate for future consideration is a concept in which the heat shield is cured directly on the midbay structure with a resultant weight saving from the elimination of the bond. Thermal analysis shows that in this case the structural temperature will increase significantly, a change that will probably necessitate the use of graphite/polyimide for the skin. Furthermore, at the first design review it was noted that polyimide and epoxy systems may react differently to nuclear explosion environments. Hence, it is necessary to obtain data on polyimide materials.

Based on the above considerations, the following approach will be adopted for the remainder of the program with respect to material systems and the associated test program. T-300/5208 is selected as the most suitable graphite/epoxy system for the recommended baseline design. T-300/5230 graphite/polyimide is selected as the best system for possible higher temperature applications such as may occur if the heat shield bond was eventually deleted or if other changes resulted in higher structural heating. The two particular resin systems were selected as the most prevalently used high temperature epoxy and addition polyimide system. They also have the significant advantage of giving high fiber volumes which results in relatively high modulus values for a high strength composite and thereby increases potential weight saving.

In the test area the overall objective will be to evaluate both candidate materials with respect to critical design features of the MK12A midbody, such as bonded attachments, quantify weight impacting parameters, such as notch factors, and seek improved interlaminar strength for higher resistance to plate slap tests. Specific objectives for each test are given preceding the test in the following sections.

This test plan does not include any elevated temperature testing of the basic G/E or G/PI material and only a token amount of joint testing at elevated temperature. Since the resin is the only thing which is degrading due to temperature, tests are included of a bonded joint which depends totally on the adhesive for strength. Hysol data on the selected adhesive, EA934, shows that it has 58% of its room temperature strength at 200F. Hysol data on the alternate adhesive EA9309 shows 25% of room temperature strength at 100F. Elevated temperature conditions are not expected to drive the design of the MK12A midbody, since the percent strength retention of both adhesives is significantly greater than the corresponding percent of room temperature loads. Therefore, very limited elevated temperature testing is planned.

3. GENERAL REQUIREMENTS

A. All testing will be done at room temperature except as specified.

B. Record at failure: Ultimate Load
Ultimate Stress
Failure Mode

C. All dimensions are in inches.

D. All bonding will be done at room temperature and will simulate the bonding proposed for the MK12A. Bondline thicknesses will be mechanically controlled.

E. Unless otherwise noted, all specimens shall have standard load introduction tabs bonded on both sides of all graphite parts.

F. A representative of Department 642-2 (Structural Analysis) shall review each test setup and shall witness at least the first test of each series.

4. LAP SHEAR TESTS

Objective: A series of bonded joint tests will be run to determine adhesive-adherend strength characteristics. The primary bonded joints in the midbody are between graphite and 7000 series aluminum. The graphite layups are biased towards longitudinal and include some ± 45 and 90 degree plies.

Two currently used and highly efficient epoxy adhesive systems have been selected for the joint evaluation phase. The baseline system is Hysol's EA934, which has excellent shear strength from cryogenic temperatures to approximately 350F. It is the adhesive currently used on Mark 12 for bonding the heat shield to the aluminum substructure. Convair has used it extensively in bonding large graphite/epoxy composite structures.

The second selected adhesive, Hysol EA9309, has much higher shear and peel strengths than the EA934. It maintains good strengths from cryogenic temperatures to 180F, and has an upper temperature limit of approximately 250F for very short exposures. It has a lower viscosity than the EA934 and is more difficult to use in thick bond lines, although it maintains its strength over a large range of bond line thicknesses. The EA9309 is a newer system which has had limited service life. Convair's experience with this system is on the current production of the Nimbus-G antenna and on the Army's cone frusta program.

Convair believes that it would be adequate to run a comparison of the adhesives with only one combination of adherends, since the properties of the graphite/polyimide and graphite/epoxy are so similar.

The largest loads occur at or near room temperature. In the MK12A midbody concept the structural bonds will be toleranced in the range of 0.005 to 0.030 inches in thickness. Hence, the following test series will be run to obtain data for use in design. The joints will be subjected to finite element analysis to verify the procedure for joint strength prediction with varying joint configurations.

Materials:

Al = 7075-T6 Aluminum
Ad = EA934 Adhesive and EA9309 Adhesive
G/E = T300/5208 Graphite/Epoxy
G/PI = T300/XXXX Graphite/Polyimide
0.070 layups are $[0/45/0/-45/0/90/0]_s$
0.140 layups are $[0/45/0/-45/0/90/0]_{s2}$
0° is in the load direction
All widths are 1.0

Test: All tests shall be run in tension at 1200 to 1400 lbs/min.

Test Matrix:

Test	Overlap	Bond	Figure	Repetitions G/E	Repetitions G/Pi *
Single Lap Shear	0.5	0.005	1	3	3
Single Lap Shear	1.0	0.005	2	3	3
Double Lap Shear	0.5	0.005	3	3	3
Double Lap Shear	0.5	0.010	3		3
Double Lap Shear	0.5	0.015	3		3
Double Lap Shear	0.5	0.020	3		3
Double Lap Shear	0.5	0.025	3		3
Double Lap Shear	0.5	0.030	3	3	3
Double Lap Shear	1.0	0.005	4		3
Single Scarf	2.8	0.005	5	3	3

*3 each of EA934 and A9309 Adhesive

5. STATION 32.18 SIMULATED RING TEST

Objectives: Station 32.18 is the most highly loaded bonded joint in the midbody. A series of tests will be run to verify the configuration proposed at the first design review. Since the program cannot afford a full cylinder or conical test specimens, a straight simulation has been designed. The laminate has been thickened to simulate the longitudinal flexural rigidity of the heat shield-bond-graphite combination. A honeycomb

DATE 10-12-76
PREPARED BY H. McCutcheon
CHECKED BY
REVISED DATE

MODEL MK 12A

REPORT NO.

FIGURE 1. ½" Single Lap Shear Specimen

Specimen 1.00 wide, drawn twice size.

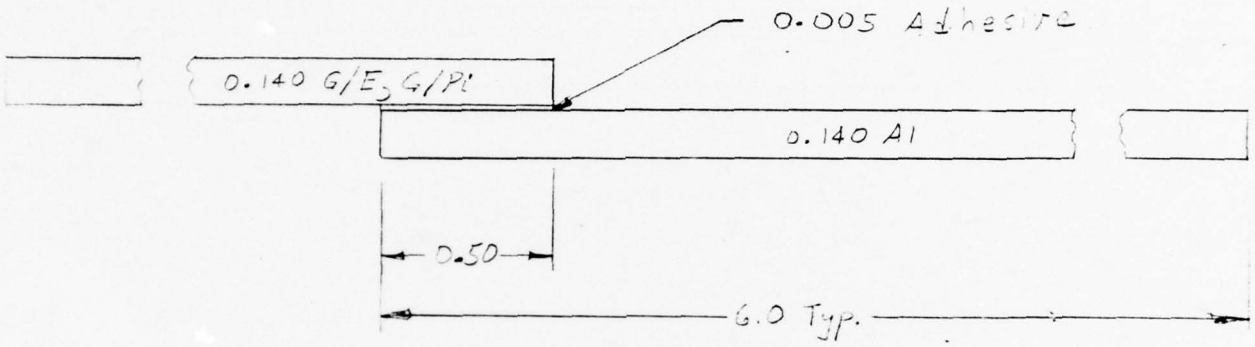

FIGURE 2. 1.0" Single La[illegible] Shear [illegible]

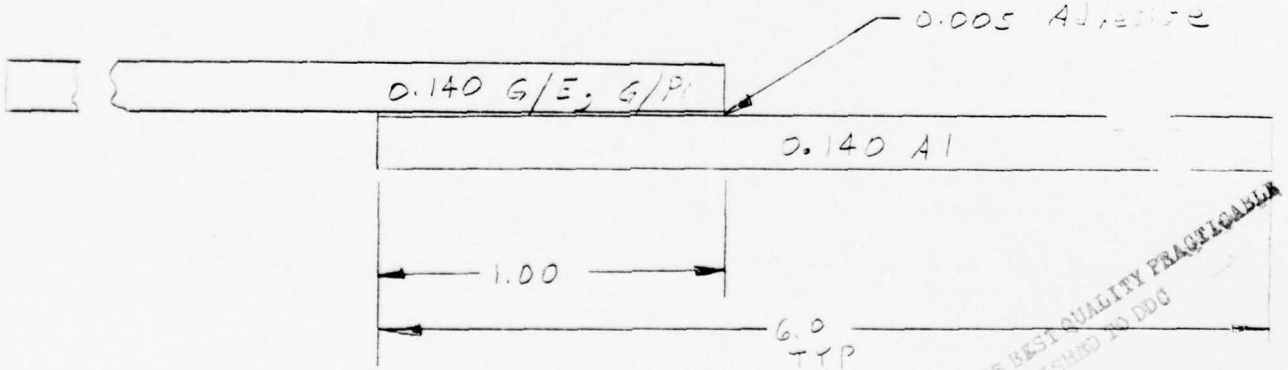

Joint [illegible]

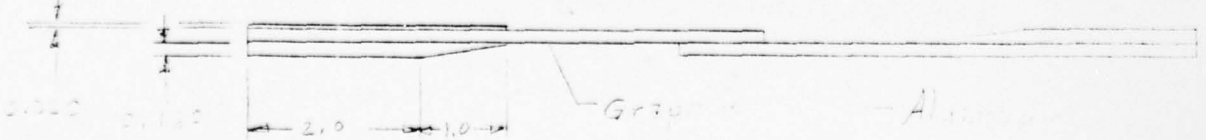

1277 (2-68)

DATE 10-12-76
PREPARED BY H. McCutcheon
CHECKED BY
REVISED DATE

PAGE [TEMP | PERM]

MODEL MK12A

REPORT NO.

FIGURE 3. 0.5 DOUBLE LAP SHEAR, BOND THICKNESS With Varying Bond Thickness

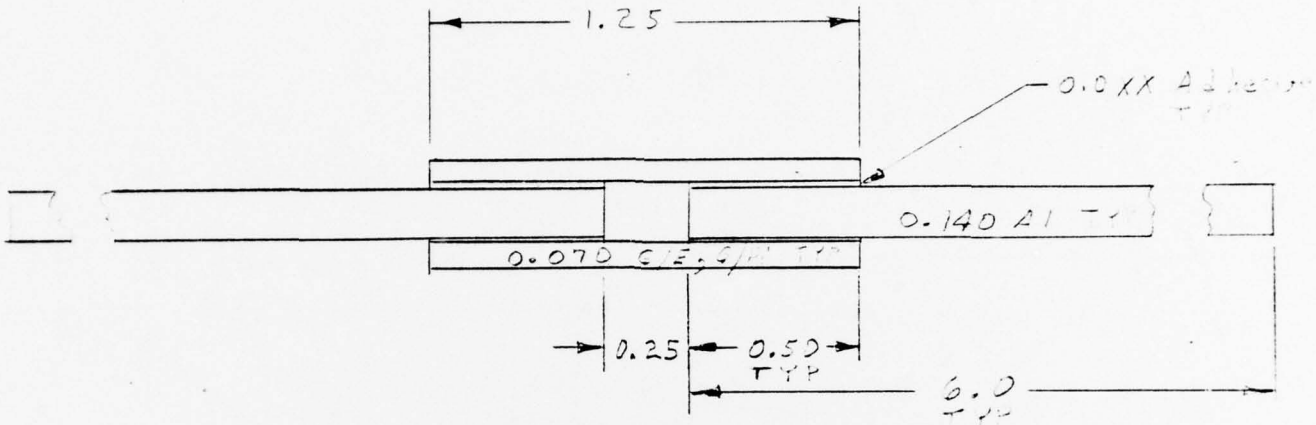

Adhesive Thicknesses (3 specimens each):

0.0XX = 0.005, 0.010, 0.015, 0.020, 0.025, 0.030

FIGURE 4. 1.0 DOUBLE LAP SHEAR SPECIMEN

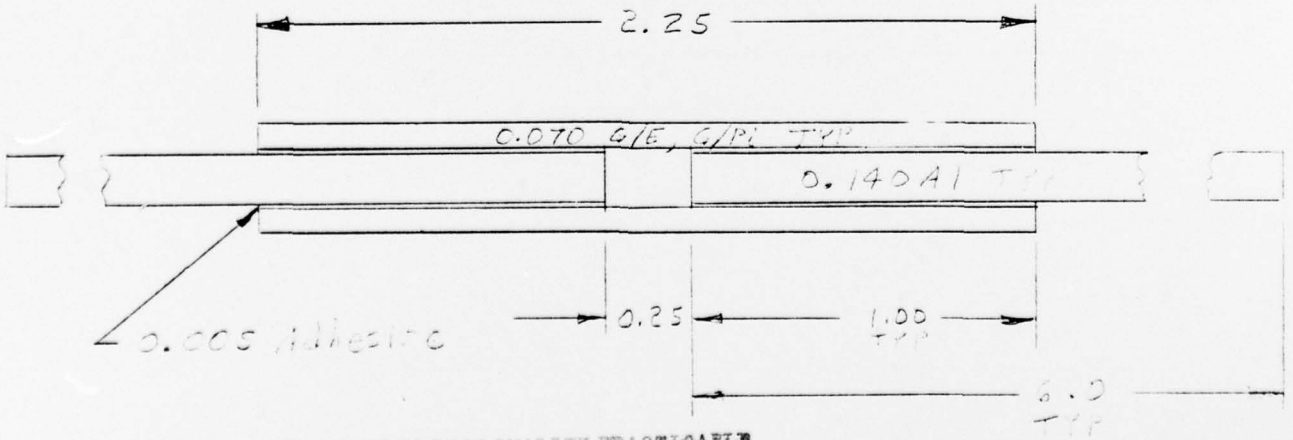

1277 (2-68)

FIGURE 5. SCARF JOINT SPECIMEN

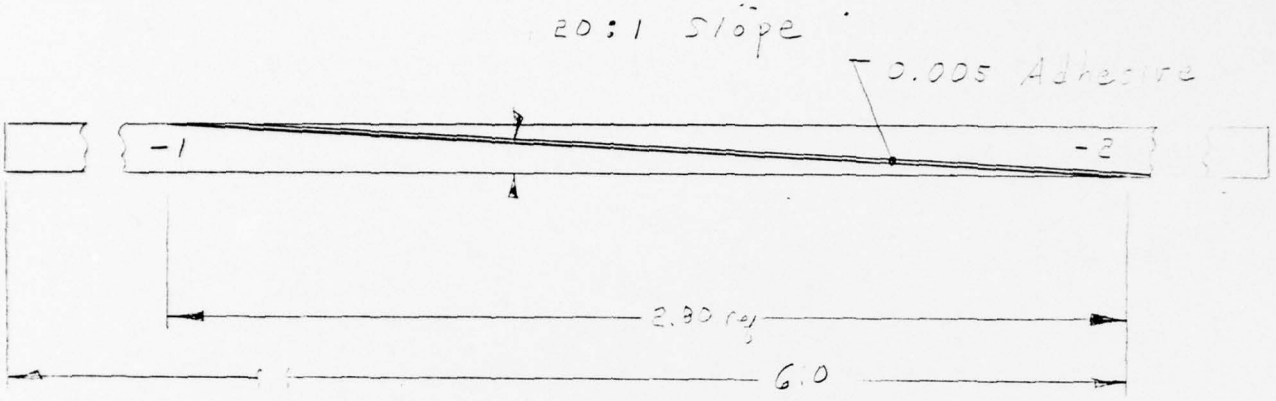

-1 0.140 Aluminum
-2 0.140 G/E, G/Pi

Use standard doubler TDC on G/Pi end.

elastic foundation has been selected to represent the hoop elastic restraint offered by the midbody and to shear out the load in a manner similar to air drag. A finite element analysis of the test specimen has confirmed that the specimen is reasonable. The graphite/epoxy specimens and graphite/polyimide specimens are tested at room temperature since that is near the maximum load condition. The graphite/polyimide specimens are tested at the maximum temperature anticipated in a modified design which would require the use of polyimides. Examination of the load versus time curves and temperature versus time curves of G. E. letter No. 3735-1169, dated 16 July 1976, show that loads decrease dramatically before bond line temperatures rise significantly. Only modest reductions in bond strength are anticipated at the peak temperatures and hence only 3 elevated temperature tests are performed at the maximum temperature to demonstrate that there is no problem in the bonds at elevated temperature.

Materials:

-1 7075-T651 Aluminum - 2" straight ring segment per 72C0685

-2 7075-T651 Aluminum - $1/2 \times 2 \times 15$ loading bar

-3 7075-T651 Aluminum $2.5 \times 6 \times 17$ support

-4 HRH-10-1/8-4.0 Honeycomb $0.75 \times 2 \times 15$

-5 T300/5208 $[0_4/45/0_4/90/0_4/-45/0_2]_S$ 2×15 and T300/Polyimide, same layup

Bond -1 to -5 using EA 934 0.020 thick RT cure

Bond -5 to -4 to -3 using EA 934

Align loading bar vertically in test machine and insure that it is uniformly bearing on ring and test machine head. The bar should be adjacent to the tangency point in the ring.

Test Matrix: Number of repetitions

	Temperature		
	RT	130	195
Graphite/Epoxy	3	3	-
Graphite/Polyimide	3	-	3

Load at 2000 lbs/min to failure. See Figure 6 for test specimen configuration.

DATE 10-16-76
PREPARED BY HUGH MCCUTCHEN JR
CHECKED BY
REVISED DATE

PAGE TEMP PERM

MODEL MK12A

REPORT NO.

FIGURE 6.
STATION 32.18 SIMULATED RING TEST

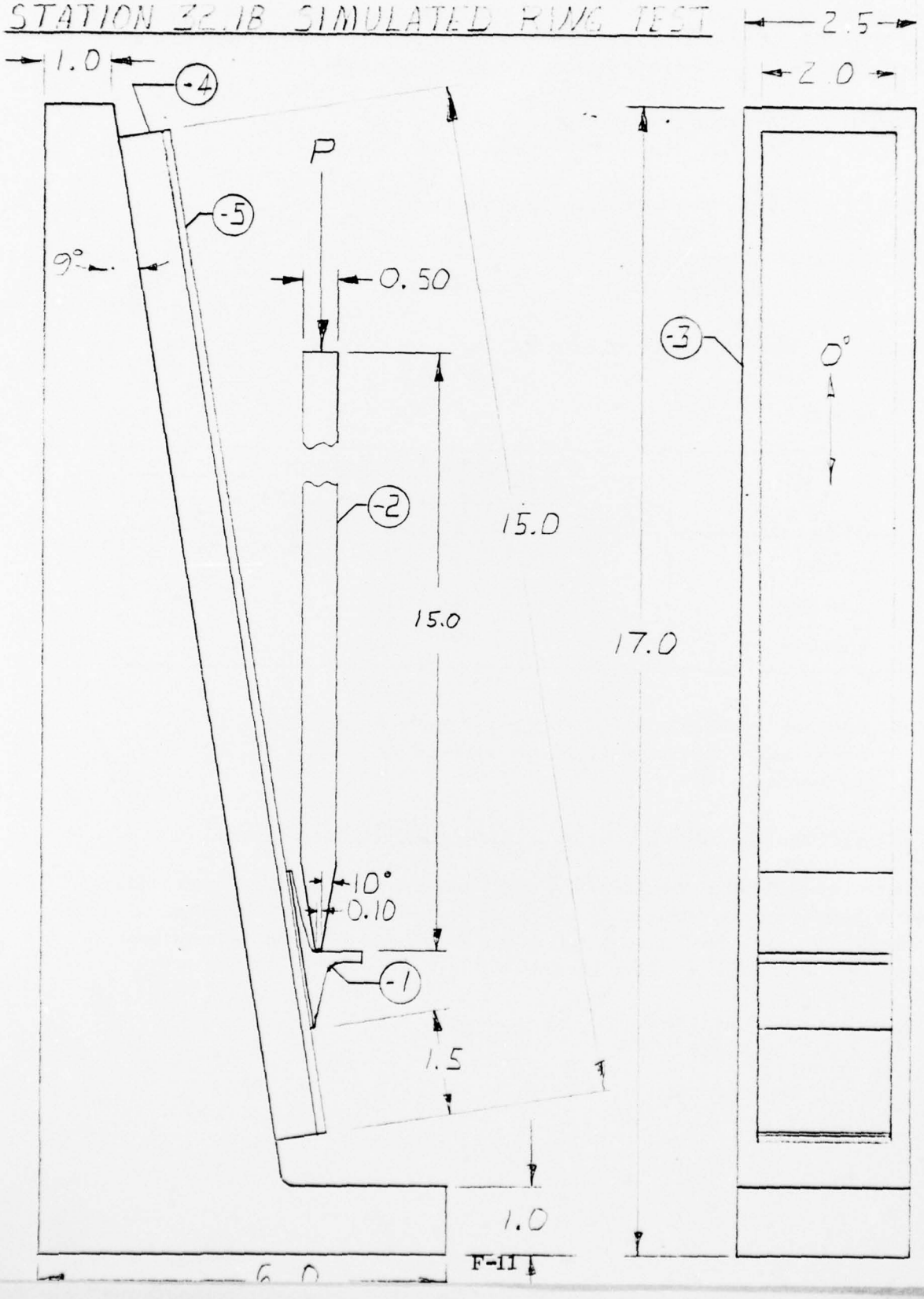

1277 (2-68)

6. GORE STRESS CONCENTRATION TESTS

A series of tension and compression tests will be run to evaluate the stress concentration associated with transmitting load across cut plies as are found at gore edges. The test laminate is near pseudoisotropic since portions of the mid body have extra longitudinal plies and other portions have extra hoop plies.

Material: T300/5208 Graphite/Epoxy
T300/5230 Graphite/Polyimide

Layup: $[90/45/90/0/-45/90]_S$ See Figure 7.

Test Specimens: Tension - 1.0 × 9.0
Compression - 0.25 × 5.5 celanese

Test: Head travel of 0.05 in/min.

Test Matrix:

Test	Number of Repetitions			
	G/E		G Pi	
	Tension	Comp	Tension	Comp
Control	4	4	4	4
0.08 Gap	4	4	4	4
0.20 Overlap	4	4	4	4

Note: Bond two layers of test panel together to make compression specimens. Center half of the compression specimens on ply 12 splice and half on ply 6 splice.

7. LONGITUDINAL PLY TERMINATION STRESS CONCENTRATION

The mid body requires longitudinal strength forward and hoop stiffness aft. Plies must therefore transition from 0° to 90° and some 0° plies must terminate. A series of tension and compression tests will be run to evaluate the stress concentration associated with these ply discontinuities.

Materials: T300/5208 G/E
T300/5230 G/Pi

Layup: See Figure 8

DATE 10-18-76
PREPARED BY MCCUTCHEN
CHECKED BY
REVISED DATE

PAGE TEMP PERM

MODEL MK12A

REPORT NO.

FIGURE 7. GORE CONCENTRATION PANEL

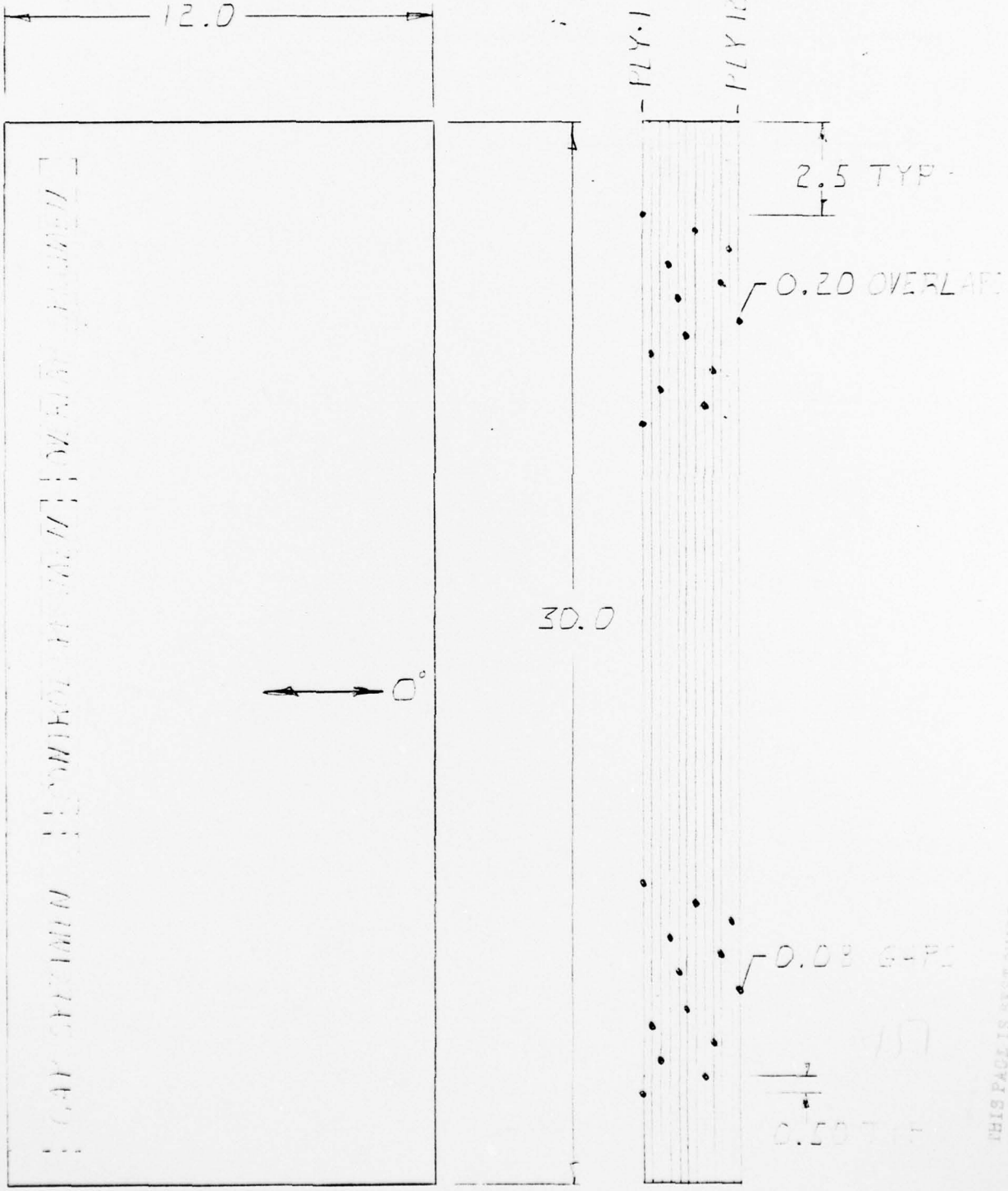

1277 (2-68)

DATE 10-17-76
PREPARED BY MCCUTCHEN
CHECKED BY
REVISED DATE

PAGE TEMP PERM

MODEL MK12A

REPORT NO.

FIGURE 8. PLY DISCONTINUITY PANEL

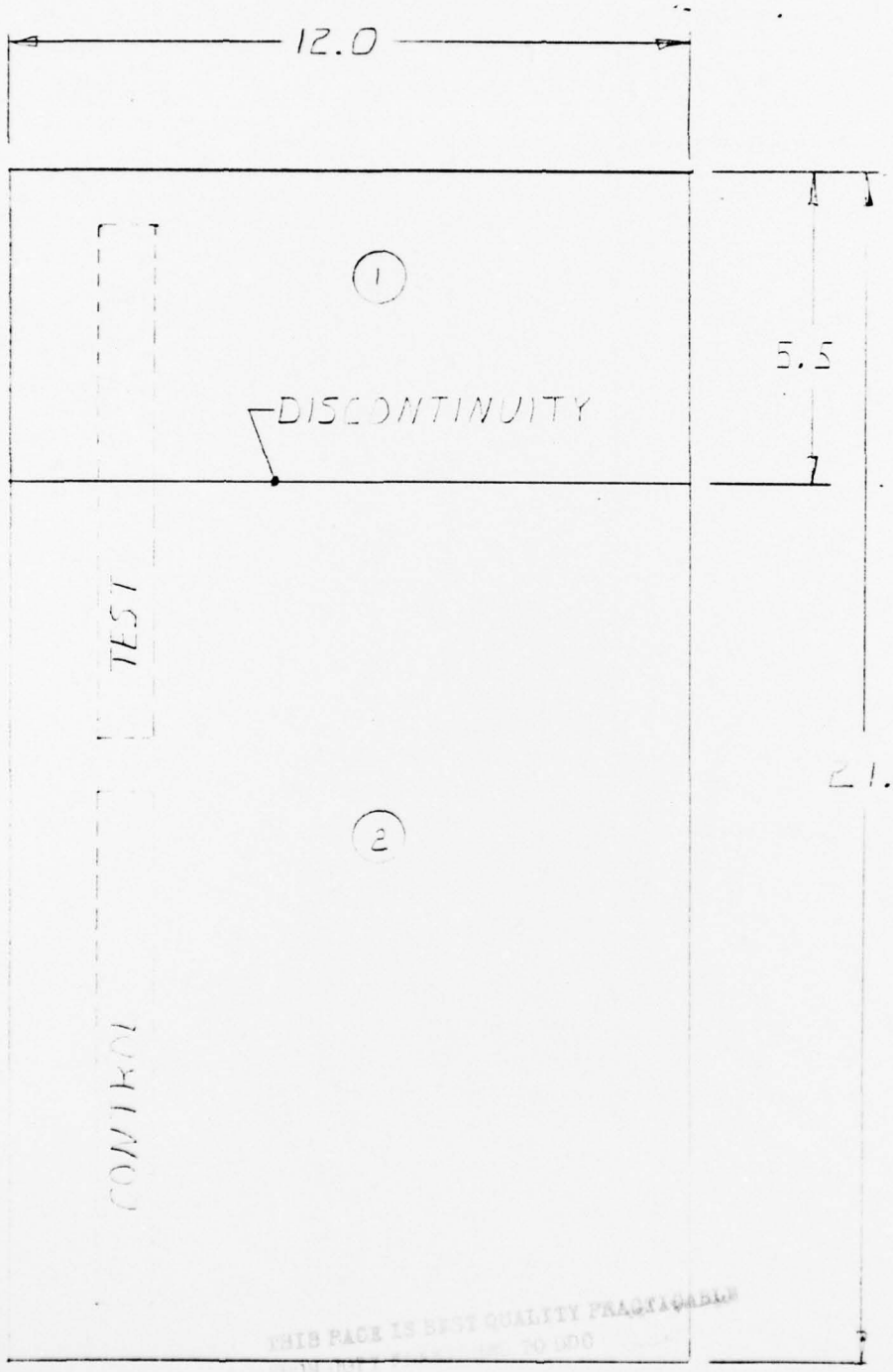

1277 (2-68)

Test Specimens: Tension 1 × 9
Compression 0.25 × 5.5 celanese

Test: Head travel of 0.05 in/min

Test Matrix:

Test	Number of Repetitions			
	G/E		G/Pi	
	Tension	Comp.	Tension	Comp
Control	4	4	4	4
Discontinuity	4	4	4	4

8. FLEXURE AT DOUBLER TERMINATIONS TESTS

The mid body has discontinuous, cocured doublers in the vicinity of Station 40. There are significant flexural moments which are transmitted across these doublers. A series of flexural tests will be run to evaluate stress concentrations and peel effects at doubler terminations.

Materials: T300/5208 G/E
T300/5230 G/Pi

Layup: See Figure 9

Test Specimens: 1.0 × 6.0 flexural

Test: Standard four point flexure fixture.
Head travel of 0.10 in/min.

Test Matrix:

Test	Number of Repetitions	
	G/E	G/Pi
Control	4	4
Step in Tension	4	4
Step in Comp.	4	4

DATE 10-17-76
PREPARED BY MCCUTCHEN
CHECKED BY
REVISED DATE

PAGE TEMP PERM

MODEL MK12A

REPORT NO.

FIGURE 9. DOUBLER TERMINATION PANEL

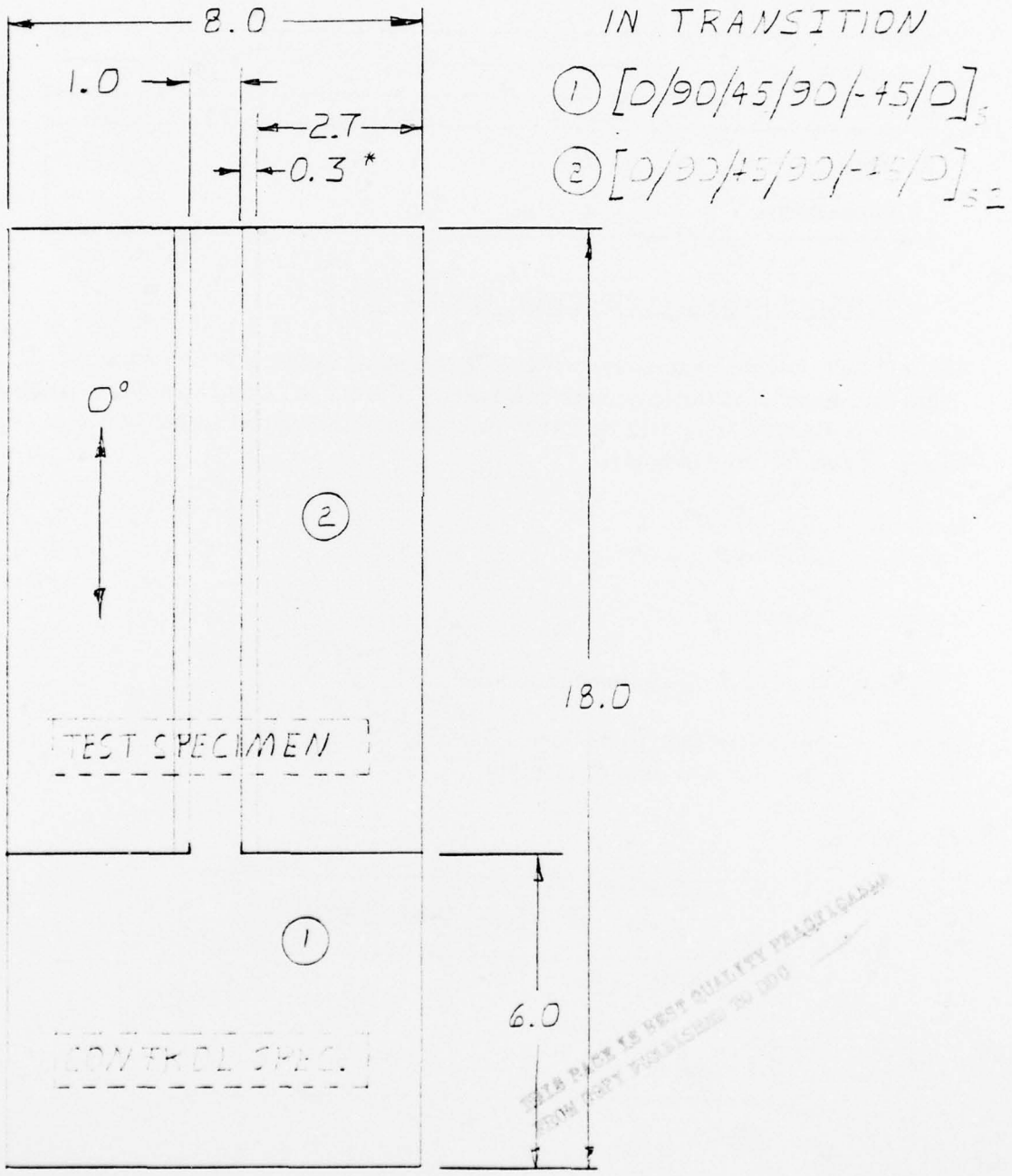

1277 (2-68)

SYM

9. INTERLAMINAR TENSION IMPROVEMENT TESTS

Convair will conduct a brief screening test program on high strength graphite reinforced resin matrix systems to determine parameters which influence interlaminar tension strength. Materials to be evaluated include T-300/epoxy, T-300/polyimide and A-S/epoxy. T-300 shall be evaluated both as tape and woven fabric. The effect of fiber volume will also be evaluated. Crossplied laminates, $[0/\pm 60]_{2S}$, shall be used for the screening program. Both short beam shear and interlaminar tension tests will be conducted, and the laminates will also be characterized for specific gravity, resin content, and fiber volume.

Short beam shear testing will utilize standard 0.6 by 0.25-inch specimens. The span-to-depth ratio will be 4 to 1. Loading head and supports will be 1/16-inch radius rods. A head travel speed of 0.05 in./min. will be used. A minimum of three specimens from each laminate will be tested.

Interlaminar tension testing will be conducted by bonding 0.75-inch diameter discs of composite between two 0.75-inch diameter threaded steel rods. The adhesive will be Hysol's EA9309, and all bonding will utilize a RT cure cycle. The specimens will be tested at a head travel rate of 0.05 in./min. A minimum of three specimens from each laminate will be tested.

DISTRIBUTION LIST FOR FINAL REPORT
CONTRACT DAAG46-76-C-0073

	No. of Copies
AFML/LTN ATTN: Mr. H. Materne Wright-Patterson Air Force Base, OH 45433	1
AFFDL/FBC ATTN: Mr. J. Woods Mr. D. Roselius Capt. Eller Wright-Patterson Air Force Base, OH 45433	1 1 1
Air Force Office of Scientific Research ATTN: LTC J. Morgan Bolling Air Force Base, Bldg. 410 Washington, DC 20332	1
AFWL/DYV ATTN: K. Smith Kirtland Air Force Base, NM 87117	1
HQ, SAC/XPQM ATTN: Cpt. Vankuren Offutt Air Force Base, NB 68113	1
SAMSO/MNNR ATTN: Capt. Graham Norton Air Force Base, CA 92409	1
SAMSO ATTN: YAPC, LTC Staubs RSSE, Capt. Bohlen RSMA, Lt Higgins P. O. Box 92960 Worldway Postal Center Los Angeles, CA 90009	1 1 1
Director BMD Advanced Technology Center ATTN: D. Harmon J. Papadopoulos P. O. Box 1500 Huntsville, AL 35807	1 1

No. of Copies

AVCO Corporation
ATTN: Mr. S. Fesenden 1
201 Lowell Street
Wilmington, MA 01887

General Dynamics Corporation
Convair Division
ATTN: W. Garcia 1
5001 Kearny Villa Road
San Diego, CA 92138

General Electric Company/RESD
ATTN: Mr. J. Casanto 1
3198 Chestnut Street
Philadelphia, PA 19101

Lockheed Missiles & Space Co.
ATTN: Mr. A. D. McDonald 1
P. O. Box 504
Sunnyvale, CA 94088

McDonnell Douglas Astronautics Company
ATTN: Mr. G. Fitzgerald 1
Mr. H. Parachenian 1
5301 Bolsa Avenue
Huntington Beach, CA 92646

TRW Defense & Space Systems
ATTN: L. Berger 1
P. O. Box 1310
San Bernadino, CA 92402

Defense Documentation Center 2
Cameron Station, Bldg. 5
5010 Duke Station
Alexandria, VA 22314

Director
Army Materials & Mechanics Research Center
ATTN: DRXMR-H, J. F. Dignam 1
DRXMR-H, L. R. Aronin 1
DRXMR-AP 1
DRXMR-PL 2
DRXMR-PR 1
Watertown, MA 02172

Army Materials and Mechanics Research Center
Watertown, Massachusetts 02172
COMPOSITE MATERIAL APPLICATION TO THE MK12A
RV MIDBODY SUBSTRUCTURE
W Garcia, J Hertz, J Prunty and H McCutchen,
General Dynamics Convair Division

AD ______
UNCLASSIFIED
UNLIMITED DISTRIBUTION

Technical Report AMMRC TR79-51 July 1978
152 pp — illus — tables, Contract DAAG46-76-C-0073
D/A Project 1W162113A661,
AMCMS Code 612113.11.07000
Final Report, October 1976 to July 1978

Key Words
Composite materials
Composite structures
Fiber composites
Graphite composites
Missile airframes

The work reported herein represents a feasibility study to reduce weight of the MK12A reentry vehicle midbay structure by replacing the aluminum structure with graphite composite materials. Following conceptual design of the MK12A midbay structure utilizing advanced composite materials, the effort was redirected to the Advanced Ballistic Reentry Vehicle (ABRV). Specimens and subcomponent elements representative of the ABRV configuration were provided for nuclear vulnerability and hardness testing at the Air Force Weapons Laboratory.

Army Materials and Mechanics Research Center
Watertown, Massachusetts 02172
COMPOSITE MATERIAL APPLICATION TO THE MK12A
RV MIDBODY SUBSTRUCTURE
W Garcia, J Hertz, J Prunty and H McCutchen,
General Dynamics Convair Division

AD ______
UNCLASSIFIED
UNLIMITED DISTRIBUTION

Technical Report AMMRC TR79-51 July 1978
152 pp — illus — tables, Contract DAAG46-76-C-0073
D/A Project 1W162113A661,
AMCMS Code 612113.11.07000
Final Report, October 1976 to July 1978

Key Words
Composite materials
Composite structures
Fiber composites
Graphite composites
Missile airframes

The work reported herein represents a feasibility study to reduce weight of the MK12A reentry vehicle midbay structure by replacing the aluminum structure with graphite composite materials. Following conceptual design of the MK12A midbay structure utilizing advanced composite materials, the effort was redirected to the Advanced Ballistic Reentry Vehicle (ABRV). Specimens and subcomponent elements representative of the ABRV configuration were provided for nuclear vulnerability and hardness testing at the Air Force Weapons Laboratory.

Army Materials and Mechanics Research Center
Watertown, Massachusetts 02172
COMPOSITE MATERIAL APPLICATION TO THE MK12A
RV MIDBODY SUBSTRUCTURE
W Garcia, J Hertz, J Prunty and H McCutchen,
General Dynamics Convair Division

AD ______
UNCLASSIFIED
UNLIMITED DISTRIBUTION

Technical Report AMMRC TR79-51 July 1978
152 pp — illus — tables, Contract DAAG46-76-C-0073
D/A Project 1W162113A661,
AMCMS Code 612113.11.07000
Final Report, October 1976 to July 1978

Key Words
Composite materials
Composite structures
Fiber composites
Graphite composites
Missile airframes

The work reported herein represents a feasibility study to reduce weight of the MK12A reentry vehicle midbay structure by replacing the aluminum structure with graphite composite materials. Following conceptual design of the MK12A midbay structure utilizing advanced composite materials, the effort was redirected to the Advanced Ballistic Reentry Vehicle (ABRV). Specimens and subcomponent elements representative of the ABRV configuration were provided for nuclear vulnerability and hardness testing at the Air Force Weapons Laboratory.

Army Materials and Mechanics Research Center
Watertown, Massachusetts 02172
COMPOSITE MATERIAL APPLICATION TO THE MK12A
RV MIDBODY SUBSTRUCTURE
W Garcia, J Hertz, J Prunty and H McCutchen,
General Dynamics Convair Division

AD ______
UNCLASSIFIED
UNLIMITED DISTRIBUTION

Technical Report AMMRC TR79-51 July 1978
152 pp — illus — tables, Contract DAAG46-76-C-0073
D/A Project 1W162113A661,
AMCMS Code 612113.11.07000
Final Report, October 1976 to July 1978

Key Words
Composite materials
Composite structures
Fiber composites
Graphite composites
Missile airframes

The work reported herein represents a feasibility study to reduce weight of the MK12A reentry vehicle midbay structure by replacing the aluminum structure with graphite composite materials. Following conceptual design of the MK12A midbay structure utilizing advanced composite materials, the effort was redirected to the Advanced Ballistic Reentry Vehicle (ABRV). Specimens and subcomponent elements representative of the ABRV configuration were provided for nuclear vulnerability and hardness testing at the Air Force Weapons Laboratory.

Army Materials and Mechanics Research Center
Watertown, Massachusetts 02172
COMPOSITE MATERIAL APPLICATION TO THE MK12A
RV MIDBODY SUBSTRUCTURE
W. Garcia, J. Hertz, J. Prunty and H. McCutchen,
General Dynamics Convair Division

Technical Report AMMRC TR79-51 July 1978
152 pp — illus — tables, Contract DAAG46-76-C-0073
D/A Project 1W162113A661,
AMCMS Code 612113.11.07000
Final Report, October 1976 to July 1978

AD ________

UNCLASSIFIED
UNLIMITED DISTRIBUTION

Key Words

Composite materials
Composite structures
Fiber composites
Graphite composites
Missile airframes

The work reported herein represents a feasibility study to reduce weight of the MK12A reentry vehicle midbay structure by replacing the aluminum structure with graphite composite materials. Following conceptual design of the MK12A midbay structure utilizing advanced composite materials, the effort was redirected to the Advanced Ballistic Reentry Vehicle (ABRV). Specimens and subcomponent elements representative of the ABRV configuration were provided for nuclear vulnerability and hardness testing at the Air Force Weapons Laboratory.

Army Materials and Mechanics Research Center
Watertown, Massachusetts 02172
COMPOSITE MATERIAL APPLICATION TO THE MK12A
RV MIDBODY SUBSTRUCTURE
W. Garcia, J. Hertz, J. Prunty and H. McCutchen,
General Dynamics Convair Division

Technical Report AMMRC TR79-51 July 1978
152 pp — illus — tables, Contract DAAG46-76-C-0073
D/A Project 1W162113A661,
AMCMS Code 612113.11.07000
Final Report, October 1976 to July 1978

AD ________

UNCLASSIFIED
UNLIMITED DISTRIBUTION

Key Words

Composite materials
Composite structures
Fiber composites
Graphite composites
Missile airframes

The work reported herein represents a feasibility study to reduce weight of the MK12A reentry vehicle midbay structure by replacing the aluminum structure with graphite composite materials. Following conceptual design of the MK12A midbay structure utilizing advanced composite materials, the effort was redirected to the Advanced Ballistic Reentry Vehicle (ABRV). Specimens and subcomponent elements representative of the ABRV configuration were provided for nuclear vulnerability and hardness testing at the Air Force Weapons Laboratory.

Army Materials and Mechanics Research Center
Watertown, Massachusetts 02172
COMPOSITE MATERIAL APPLICATION TO THE MK12A
RV MIDBODY SUBSTRUCTURE
W. Garcia, J. Hertz, J. Prunty and H. McCutchen,
General Dynamics Convair Division

Technical Report AMMRC TR79-51 July 1978
152 pp — illus — tables, Contract DAAG46-76-C-0073
D/A Project 1W162113A661,
AMCMS Code 612113.11.07000
Final Report, October 1976 to July 1978

AD ________

UNCLASSIFIED
UNLIMITED DISTRIBUTION

Key Words

Composite materials
Composite structures
Fiber composites
Graphite composites
Missile airframes

The work reported herein represents a feasibility study to reduce weight of the MK12A reentry vehicle midbay structure by replacing the aluminum structure with graphite composite materials. Following conceptual design of the MK12A midbay structure utilizing advanced composite materials, the effort was redirected to the Advanced Ballistic Reentry Vehicle (ABRV). Specimens and subcomponent elements representative of the ABRV configuration were provided for nuclear vulnerability and hardness testing at the Air Force Weapons Laboratory.

Army Materials and Mechanics Research Center
Watertown, Massachusetts 02172
COMPOSITE MATERIAL APPLICATION TO THE MK12A
RV MIDBODY SUBSTRUCTURE
W. Garcia, J. Hertz, J. Prunty and H. McCutchen,
General Dynamics Convair Division

Technical Report AMMRC TR79-51 July 1978
152 pp — illus — tables, Contract DAAG46-76-C-0073
D/A Project 1W162113A661,
AMCMS Code 612113.11.07000
Final Report, October 1976 to July 1978

AD ________

UNCLASSIFIED
UNLIMITED DISTRIBUTION

Key Words

Composite materials
Composite structures
Fiber composites
Graphite composites
Missile airframes

The work reported herein represents a feasibility study to reduce weight of the MK12A reentry vehicle midbay structure by replacing the aluminum structure with graphite composite materials. Following conceptual design of the MK12A midbay structure utilizing advanced composite materials, the effort was redirected to the Advanced Ballistic Reentry Vehicle (ABRV). Specimens and subcomponent elements representative of the ABRV configuration were provided for nuclear vulnerability and hardness testing at the Air Force Weapons Laboratory.